Order Number 9510698

Formation and stability of perflubron in saline emulsions for biomedical applications: An interfacial approach

Oleksiak, Christian Bernard, Ph.D.

City University of New York, 1994

U·M·I
300 N. Zeeb Rd.
Ann Arbor, MI 48106

A

FORMATION AND STABILITY OF PERFLUBRON IN SALINE EMULSIONS FOR BIOMEDICAL APPLICATIONS: AN INTERFACIAL APPROACH

by

CHRISTIAN B. OLEKSIAK

A dissertation submitted to the Graduate Faculty in Chemistry in partial fulfillment of the requirements for the degree of Doctor of Philosophy, The City University of New York.

1994

This manuscript has been read and accepted for the Graduate Faculty in Chemistry in satisfaction of the dissertation requirements for the degree of Doctor of Philosophy.

May 5, 1994
Date

Chair of Examining Committee

May 10, 1994
Date

Executive Officer

Supervisory Committee

The City University of New York

Abstract

FORMATION AND STABILITY OF PERFLUBRON IN SALINE EMULSIONS FOR BIOMEDICAL APPLICATIONS: AN INTERFACIAL APPROACH

by

Christian B. Oleksiak

Advisor: Professor Henri L. Rosano

Perflubron, a hydrophobic fluid with a high capacity for dissolving respiratory gases, can be used as an injectable temporary oxygen delivery system provided that it is emulsified, using a biocompatible emulsifier, in an aqueous solution isotonic to blood. A concentrated formulation developed by Alliance Pharmaceutical Corp. consists of perflubron droplets stabilized by a monolayer of egg yolk phospholipids (EYP), ca. 250 nm in diameter, and perflubron-free EYP vesicles. The emulsion, prepared under nitrogen atmosphere (EYP are oxidation-sensitive) and sterilized in a static autoclave for 15 minutes at 121°C and 20 psi, is stable for years at positive temperatures. This uncommon stability with respect to flocculation and coalescence was studied taking a simpler, non-oxidation-sensitive, hydrogenated phospholipid (PL90H) as a model for the very complex, oxidizable, and varied EYP. It was concluded that stability for the perflubron/PL90H/saline emulsion could be achieved provided that the interfacial film is doped with a negatively charged surfactant and/or with a

highly hydrated surfactant, either of which would prevent the droplets from approaching one another. These results were extended to EYP, which naturally contain both major ingredients giving rise to a very structured film at the perflubron/saline interface (phosphatidylcholine, phosphatidylethanolamine, cholesterol) and charged and/or hydrated minor ingredients that prevent flocculation and coalescence (phosphatidylserine, phosphatidylglycerol, phosphatidylinositol, etc.). Injection trials showed that the droplets were recognized as invaders by the human immune system, which resulted in too rapid a clearance from the blood stream. It is suggested that an additive with a long hydrated moiety (ethoxylated cholesterol, CnEO) be anchored at the interface, on the assumption that the highly hydrated ethoxylated chains will wrap the droplets in a thick layer of water, making them invisible to the immune system. Perflubron/EYP-CnEO/saline emulsions are under injection trials. The theoretical importance of the interface in the formation of micro- and fine emulsions was studied concomitantly and a new mathematical model was developed emphasizing two measurable physical properties of the interface: its rigidity and the interfacial free energy.

Acknowledgements

My first thanks go to Professor Henri L. Rosano, my mentor, who provided me with the essentials: financial support, confidence, knowledge, and a perennially exciting research topic. I feel particularly lucky to have grown with a scientist whose mission is "to make the link between basic and applied research." His approach to chemistry will continue to influence my career.

There are no superlatives high enough to express the extent of my gratitude to Stéphane Habif. First, he opened the doors of Professor Rosano's labs to "non-Chimie-Paris" students, and second, his enthusiasm, energy, optimism, professionalism and help in producing this work made my graduate school days fly by. I am confident that we will collaborate again. On a more personal level, I deeply value his trustworthy friendship (and that goes for his growing family as well).

I would like to thank the members of the City University of New York for their guidance, financial and technical support: Professor Richard Pizer (Executive Officer, Ph.D. Program in Chemistry), Professor Michael Green (Chairman, City College Chemistry Department), Scott Berlant, and Hugo Shimatz. I would also like to thank the members of my thesis committee -- Professors Henri Rosano, John Arents, and David Locke, the City University of New York; Dr. Fouad Saleeb, Kraft General Foods, Tarrytown, NY; Dr. David Chang, L & F Products Technical Center, Montvale, NJ; and Dr. Hank Graham, Alliance Pharmaceutical Corp., San Diego, CA -- for their help and support.

I feel the deepest gratitude for the financial and technical support provided by Alliance Pharmaceutical Corp. Particularly, I would like to thank Duane Roth (President and CEO), Ernie Schutt, Tim Pelura, Leo Trevino, and Jeff Weers, for making my work more efficient. Similarly, I would like to acknowledge the financial and technical support of Kraft General Foods. There, Charles Canti, Fouad Saleeb, John Cavallo, David Ikenberry, and Jim Bay Loh provided me with great encouragement and assistance.

Part of this research would not have been possible without the access to various pieces of equipment, as well as technical assistance, provided by Penkem, Inc., Bedford Hills, NY; Unilever Research U.S., Edgewater, NJ; and The Liposome Company, Princeton, NJ.

I would like Pascal Normand, Laurent Bonel, and Stéphane Fouris to know how much I appreciated their help. Aside from his professional assistance, I would like to thank Stéphane Fouris for making life in Room 1128 so enjoyable (Motown songs will never sound the same again!).

I owe a lot to Martha Browne for her painstaking editorial help. (I am sure that we will soon laugh about the "pains" involved.) I will always carry with me her sense of perfection and her respect for *le mot juste*. I hope she will continue to enlighten me and give me clippings.

Last but not least, my love and gratitude go to my parents, who always trusted my decisions, supported me, and let me be who I am today. And to all those who gave me understanding and comfort regardless of my ups and downs during these four years (especially Joe Wolin): your patience will not be forgotten.

Table of Contents

List of Tables and Figures

CHAPTER II

CHAPTER III

CHAPTER IV

CHAPTER V

CHAPTER I

INTRODUCTION / OBJECTIVE

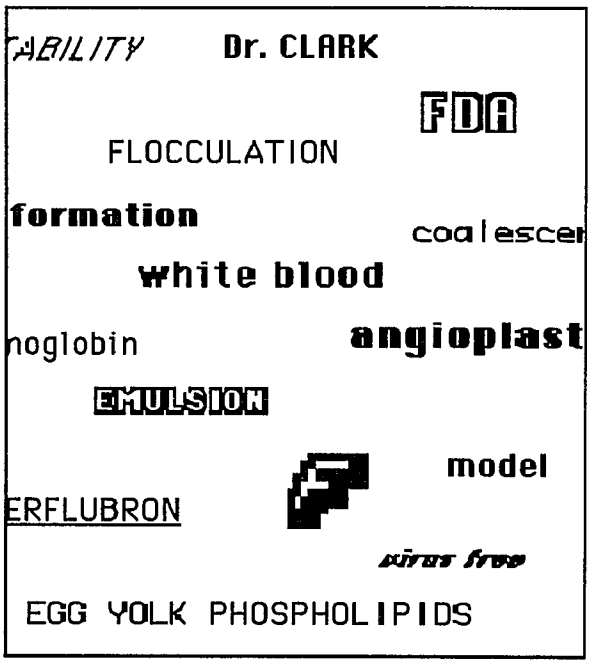

I. INTRODUCTION / OBJECTIVE

The story of "white bloods," or, more accurately, artificial respiratory gas carriers, began in 1966 when Clark and Gollan [1] demonstrated in a now famous experiment that perfluorocarbons (PFCs) have a high capacity for dissolving oxygen. They showed that a mouse could survive for several hours while immersed in oxygenated PFC and, more important, that it could live through the experiment. At a time when transfused blood could be tainted with, among other things, lethal viruses (e.g., the hepatitis C virus) and parasites (e.g., the parasite responsible for malaria) and when worldwide shortage of blood supplies (especially for rare blood types) was already becoming a major public health concern (not to mention an economic concern), the prospect of a sterile respiratory gas carrier free from blood type antigens and available in unlimited quantities was a very exciting one. The discovery of a new deadly virus responsible for the acquired immunodeficiency syndrome (AIDS) in the early 1980s made the search for a virus-free oxygen-carrying solution a top priority. Unfortunately, since PFCs are not soluble in water, they cannot be injected alone (the injection of pure PFC into the blood stream would cause a lethal oil embolus) and must therefore be emulsifed in a solution compatible with human blood. The emulsification process consists of the reduction of the PFC into small droplets (small enough to pass through the capillaries of the circulatory system) and the coating of these droplets with a biocompatible surfactant that will prevent the droplets from coalescing (that will stabilize the emulsion, in other words).

Sloviter and Kamimoto did the groundbreaking work on the use of PFCs as a potential respiratory gas carrier in 1967 when they successfully

used an emulsion of PFC to oxygenate an isolated rat brain [2]. In vivo use of a PFC emulsion was reported in 1973 by Geyer, who substituted the entire blood volume of a rat with an emulsion of PFC [3]. In 1978, a Japanese group (Green Cross Corp., Osaka, Japan) developed a product (Fluosol-DA) for commercial use that, after numerous successful trials on human patients [4], was approved by the United States Food and Drug Administration (FDA) in 1989 for use in percutaneous transluminal coronary angioplasty (PTCA). These "first generation products," even if imperfect (low PFC concentration, instability of the emulsions, low circulation times, and undesirably high half-life values for certain components of the emulsions) and with limited applications, opened the road for the improved "second generation emulsions."

Distinct from the "white bloods" are the so-called "red bloods." These all use or mimic hemoglobin (Hb), the actual active ingredient of the red blood cells (RBCs). It was proven very early (in 1868 [5]) that hemoglobin was extremely toxic when injected directly after extraction from the RBCs. Even trace amounts of certain RBC membrane components can cause serious side effects, ranging from vasoconstriction and perturbation of lung and kidney functions to cardiac arrest [6]. Furthermore, pure Hb solutions (stroma-free Hb solution, SFHS) have a short circulation time (2 to 3 hours [7]) and an affinity for oxygen too high for them to be truly efficient (the oxygen is not totally unloaded at the tissue level [7]). Finally, naked Hb is very unstable [8]. The stability, the efficacy, and the safety of Hb have been major sources of concern. One way of addressing these issues is through modifications of the Hb proteinic complex, such as intrachain crosslinking, polymerization, and conjugation with dextran or PEG [9]. Another way to protect the patient from the

toxic effects of Hb and to protect the unstable Hb is to encapsulate it into phospholipidic liposomes [10], very much as nature originally intended it. The problem with the encapsulated Hb approach is that the circulation time of the artificial "red blood" in the circulatory system is too short, and the membrane of the liposomes must be modified accordingly [11]. Furthermore, the primary source of Hb is outdated stocks of donated human blood, but these do not represent a quantity large enough to solve the existing blood shortage problem. Extracting Hb from non-human sources (bovine Hb, or Hb produced by genetically altered bacteria) adds an immunogenic problem to all the other problems mentioned above [12]. The latest approach addresses the problem of Hb availability through the synthesis of a "purely artificial Hb molecule." The synthetic heme is embedded into a modified phospholipidic bilayer. If the idea is interesting, the efficacy and the safety of the product are still to be proven [13].

Ironically, the chief advantage of PFCs over the seemingly more natural hemoglobin is safety. PFCs do not interact with any chemicals in the body and can be manufactured in near-perfect sterility.

The subject of this dissertation is one of the second generation PFC emulsions. Initially formulated by Long in the mid-1980s, it was developed by Alliance Pharmaceutical Corp. (San Diego, CA). The highly concentrated system consists of perflubron (a PFC with a half-life of four days) emulsified in a saline solution (90 to 100% w/v of perflubron in saline) using egg yolk phospholipids (EYP) as an emulsifier (EYP are commonly used in injectable emulsions for total parenteral nutrition). The emulsion is stable for years at positive temperatures. Another interesting aspect of perflubron and emulsions of perflubron is their wide array of

potential biomedical applications, in such areas as respiratory gas carriers, imaging solutions, adjuncts in cancer therapy, perfusion of organs before transplant, and lung distress syndrome therapy [14], among others still under development. When I arrived at CUNY in 1990, the perflubron/EYP/saline emulsion was still in the exciting stage of characterization and formulation improvement. In particular, the interface, EYP, seemed to play a crucial part in the stability of the resulting systems. My objective was dual: both a practical and a theoretical understanding of the part played by this interface.

On a practical level, the problem was that not all batches of egg yolk phospholipids would yield stable emulsions. The question, then, was, What ingredient(s), naturally present in egg yolk phospholipids, stabilize(s) or destabilize(s) the emulsion? A study of the interfacial film of EYP through surface isotherm measurements, coupled with a composition analysis, revealed that, due to their complexity and sensitivity to oxidation, EYP were very difficult to investigate. Other authors had concluded that it would be very difficult to predict emulsion stability on the basis of EYP analysis alone [15]. Accordingly, we decided to study a simpler model for EYP, one less sensitive to oxidation, namely a hydrogenated phosphatidylcholine (PL90H). The stability of perflubron/PL90H/saline emulsions was investigated and the results were extended to EYP and the part played by the different constituents. Recently, the residence time of the emulsions in the circulatory system, and thus their efficiency, became a problem: injections of the perflubron/EYP/saline emulsions in human patients resulted (after five to six hours) in a rapid increase of the spleen and liver density due to storage of the perflubron-filled droplets in these organs (the density of perflubron is 1.93 g/ml). It is believed that the

droplets are recognized by the immune system as invaders and stored in the spleen and the liver where they are destroyed by macrophages. Modifying the interface appears to be the most promising approach towards making the droplets invisible to the immune system. The resulting systems are under injection trials to test their innocuousness and their residence time in the circulatory system.

On a theoretical level, an alternative mathematical model for the formation of micro- and fine emulsions was developed. This model places the emphasis on the interface of the droplets of the emulsion. The interface is seen not as a virtual line but rather as a three-dimensional structure whose physical properties are the key parameters in the formation of the emulsions. The rigidity of the interface and the interfacial free energy of the system -- both measurable physical entities -- are found to be of particular importance.

The body of this dissertation is divided into four parts: Chapter Two, after a brief presentation of emulsions in general, introduces the perflubron/EYP/saline emulsions that are the subject of this research; Chapter Three concentrates on the stability of the emulsions and on the hydrogenated phospholipidic model for EYP (PL90H) used for studying them; Chapter Four is concerned with ways of increasing the residence time of the emulsions in the circulatory system; and Chapter Five looks at the interface in a more theoretical way. New perspectives afforded by this work are given in the conclusion, Chapter Six.

CHAPTER II

PERFLUBRON / EGG YOLK PHOSPHOLIPIDS (EYP) / SALINE EMULSIONS

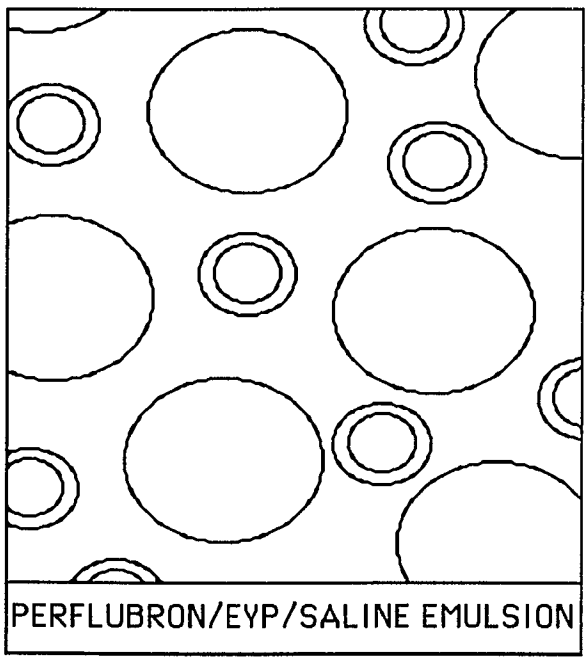

II. PERFLUBRON / EGG YOLK PHOSPHOLIPIDS (EYP) / SALINE EMULSIONS

II.1. WHAT IS AN EMULSION?

II.1.a. Definitions

To give a very broad definition, an emulsion is the system that results from the mixing of two partially miscible fluids. Visually, emulsions vary according to the size of the dispersed phase droplets, from a milky-white opaque solution (the droplets, larger than 0.3 μm, scatter the incident visible light) through a gray translucent solution (having diameters between 0.1 and 0.3 μm, the droplets cannot scatter the entire spectrum of visible light) and finally to a transparent solution, also known as a microemulsion (the droplets, smaller than 0.1 μm in diameter, are too small to scatter any component of the visible light). In most cases, one of the fluids is aqueous in nature, and thus a terminology has been adopted to name the two possible kinds of emulsions. By convention, the aqueous fluid is called "water" and the non-aqueous (i.e., water-insoluble) fluid is called an "oil." We then have an "oil-in-water" (O/W) emulsion when the continuous phase is water and the dispersed phase the oil, and a "water-in-oil" (W/O) emulsion in the opposite case. The subject of emulsions is of very great importance in industry and was studied empirically well before fundamental research clarified the theoretical issues. In particular, it was understood early on that the addition of an "emulsifier" not only made the emulsification process (i.e., the mixing of the water phase and the oil phase) easier, but also yielded more stable emulsions (i.e., emulsions that would not separate so readily into the water and oil phases). It is well known today that the emulsification process is very costly from an energy

point of view, as it requires a tremendous increase in the water/oil interfacial area. Moreover, this undesirable situation, in which a large total surface of oil is directly in contact with water, is avoided by a rapid merging (coalescence) of the dispersed droplets (a droplet of volume 2V has surface area smaller than twice the surface area of a droplet of volume V), eventually yielding phase separation (this process is even more rapid when, as is often the case, the difference in density between the two fluids is large, as the droplets are pushed against one another during their migration to the surface or to the bottom of the emulsion). The emulsifier partially solves these two problems. First, because of their nature (one part of the molecule is water-soluble, while the other is oil-soluble), the emulsifier molecules concentrate at the interface (the most energetically favorable situation) and reduce the interfacial free energy, thus reducing the work needed to increase the interface (i.e., facilitating the emulsification process). Second, because the emulsifier molecules surround each dispersed phase droplet, they can prevent the coalescence of the droplets (the nature of the the emulsifier itself makes it more or less capable of preventing coalescence). After this very broad presentation of concepts and definitions, it is necessary to describe in greater detail the most complex component of the emulsion: the emulsifier.

II.1.b. The emulsifier

As mentioned above, the emulsifier lowers the interfacial free energy between the continuous phase and the dispersed phase because of its dual characteristics: one part of the molecule is water-soluble -- or hydrophilic -- while another part of the same molecule is oil-soluble -- or

lipophilic. This fact gave rise to an empirical, but nonetheless very useful, system of classification: emulsifiers are classified according to their hydrophile-lipophile balance (HLB) or, in other words, according to the ratio of the hydrophilic character of the molecule to its lipophilic character. This classification is of great importance as it allows one to predict whether the use of a particular emulsifier will yield an O/W or a W/O emulsion, according to Bancroft's rule [1], which states that the phase in which the emulsifier is more soluble tends to be the continuous phase. Griffin first developed an experimentally based scale [2, 3], and a number of different formulae have been developed to predict the HLB of a molecule from the contribution of its different parts (the polar and the nonpolar parts) [4]. It is important to note that the HLB is an additive property. As a result, it is easy to calculate the HLB of a mixture of emulsifiers. As a rough approximation, one can predict that an emulsifier with a low HLB (below 6) is mostly liposoluble and therefore will yield a W/O emulsion, and that an emulsifier with a high HLB (above 8) will yield an O/W emulsion. In reality, however, certain aspects of the emulsion are not reflected in the HLB classification. In particular, (a) things are more complicated when the emulsifier is charged, (b) the volume of the dispersed phase plays an important part in the nature of the emulsion (although it is possible to prepare an emulsion with 90% (v/v) of dispersed phase [5], in most cases, the higher the phase volume, the more likely that phase will be the continuous phase of the emulsion), (c) the shape of the molecule, in addition to its HLB, determines the way it will adsorb at the interface (for example, two emulsifiers with the same HLB might yield emulsions with different degrees of stability; in particular, a mixture of emulsifiers often yields more stable emulsions than a single emulsifier with

the same HLB), and finally, (d) no mention of the effect of temperature on the nature of the emulsion is made in the HLB classification, and it is well known that heating an emulsion above the so-called phase inversion temperature (PIT) can lead to an inversion of phases (e.g., if the hydrated part of the emulsifier dehydrates and becomes less hydrophilic) [6, 7].

The stability of emulsions in general, and of perflubron/EYP/saline emulsions in particular, will be the subject of Chapter III.

II.1.c. Perflubron/EYP/saline emulsions

Perflubron/EYP/saline emulsions, the subject of this dissertation, are classical emulsions, in the sense that an oil phase (perflubron) is dispersed in a water phase (the saline) while EYP play the part of the surfactant and stabilize the resulting system. Upon closer examination, however, these emulsions are not so classical: first, perflubron is an oil only in the very broad sense of the definition (i.e, it is not water-soluble), and its special characteristics (e.g., fluorinated nature, high density) raise specific difficulties, which I will discuss later; second, the surfactant (EYP) is, unusually, soluble neither in the oil phase nor in the water phase, and this, as we will see, must be taken into consideration both during the preparation of the emulsion and when we seek to explain the uncommonly long stability of the system.

The next subchapters will cover the three components of the perflubron/EYP/saline emulsions (II.2); the preparation of these emulsions (II.3); and their physico-chemical characterization (II.4).

II.2. THE THREE COMPONENTS OF THE PERFLUBRON / EYP / SALINE EMULSION

II.2.a. Perflubron

Perflubron is the active ingredient in the perflubron/EYP/saline emulsion.

Physico-chemical properties

Perflubron (or perfluorooctylbromide, PFOB, $C_8F_{17}Br$, Figure II-1) is a member of a very large family, the perfluorochemicals (PFCs). PFCs are cyclic or straight-chain hydrocarbons in which hydrogen atoms have been replaced with fluorine [8]. According to some authors, they are to be called "fluorocarbon" or "perfluorocarbon" only when they contain neither any hetero atoms (such as oxygen, nitrogen, or sulfur) nor any other halogen or hydrogen atoms [8]. Some other authors, less restrictive, use the term "fluorocarbon" or "perfluorocarbon" for any PFCs that contain no other halogen or hydrogen atoms [9]. Perflubron contains a bromine atom and is therefore a perfluorochemical, which we may define broadly as a “highly fluorinated organic material” [10].

Perflubron is synthesized by the oligomerization method, whereby tetrafluoroethylene molecules are combined [11]. This method yields pure perflubron in a reproducible manner, in contrast to the substitution

method, which is somewhat unselective and can produce mixtures of products [10].

Perflubron is a dense (1.93 g/ml at 20°C), colorless, odorless, and hydrophobic liquid. Some of its physico-chemical properties are listed in Table II-I. Most of these properties differ greatly from the properties of n-octane (a hydrocarbon with an equal chain length) due (a) to the very strong (ca. 116 kcal/mol [8]) and short (1.36 Å) carbon-fluorine bonds, which lead to low interaction dispersive forces between the perflubron molecules [12], and (b) to the intrinsic properties of the fluorine and bromine atoms. Some of these properties, which make perflubron a good candidate for biomedical applications, are listed below.

Chemical inertness of perflubron: the very strong C-F bond is not reactive and the large fluorine atoms offer steric protection to the carbon group [8].

A high capacity for dissolving gases: it is believed that the low interaction forces between perflubron molecules lead to cavities that are filled by gases such as oxygen, carbon dioxide, and nitrogen [8, 10].

A low sound velocity: the cavities within the fluid slow down the propagation of sounds [8].

An acceptable vapor pressure value: even though there seems to be a direct relationship between the molecular weight and the excretion rate of PFCs, perflubron (with a relatively high molecular weight (499) [13]) shows a short half-retention time in the organs (two to four days) that makes it safe to inject. The limiting values here are a half-retention time less than two weeks (a longer half-retention time is not considered suitable for injection) and a vapor pressure less than 20 mmHg at 37°C (a larger value leads to emphysema of the lung [10]).

A high density: the substitution of all the hydrogen atoms by halogen atoms leads to a high density fluid. Consequently, even though perflubron has a high absolute viscosity, it will pour like water (the kinematic viscosity is the ratio of the absolute viscosity to the density) [14].

Applications:

The different properties listed above give rise to many potential biomedical applications for perflubron and emulsions of perflubron.

Their capacity for dissolving respiratory gases and the fact that, in contrast to what occurs with hemoglobin, there is no chemical fixation between the gas and the PFC (so that the extraction of oxygen by the tissues, for example, is easier and faster -- a linear rather than a sigmoidal oxygen loading curve) [10, 15], combined with low kinematic viscosities, make them very attractive for use in providing microvascular support in ischaemic tissues (e.g., angioplasty, blood substitute) [8, 10, 15], for perfusing isolated organs before reimplantation [16, 17, 18], for increasing tumor oxygenation and thus increasing tumors' sensitivity to either radiation or chemotherapy (adjunct to cancer therapy [19]), and for regulating gas supply in cell culture systems [20, 21].

Perflubron can also be used as a contrast agent for imaging the lungs, gastrointestinal tract, and reticuloendothelial tissues (because of the radio-opacity of the bromine atom) and for imaging various tissues in ^{19}F magnetic resonance [22, 23]. The low velocity of sound in perflubron makes it usable in sonography as well [22].

The list above is not exhaustive, and new applications are currently under investigation. A more detailed review of current interest in PCFs for biomedical applications can be found in Habif's thesis [24.a].

For certain applications (e.g., respiratory gas carrier, or blood substitute), perflubron must be injected in the circulatory system. As mentioned above, perflubron is a hydrophobic liquid that will cause an oil embolus if injected alone. Therefore, it must be emulsified in a solution (the saline) compatible with the human blood, using an injectable surfactant (the EYP) prior to injection.

II.2.b. Egg Yolk Phospholipids (EYP)

Definitions

The story of the discovery of phospholipids (lipids containing phosphoric acid residue) dates to the beginning of the nineteenth century. In 1811, L. N. Vauquelin reported the presence of organically bound phosphorus in fat-containing preparations obtained from brain matter. In 1846, Gobley isolated from egg yolk an orange-colored sticky substance with emulsifying properties, which he named lecithin after λεκιθος (lekithos), the Greek word for egg yolk. In a remarkably short time, the structure of lecithin was identified, and the presence of phospholipids was demonstrated (by Töpler, in 1861) in plant seeds as well. It would soon be acknowledged that phospholipids were the major elements in biological membranes [25].

Phospholipids are polar lipids (lipids insoluble in acetone) that contain phosphorus. They are divided into two main classes, the glycerophospholipids and the sphingophospholipids. (I will not discuss the sphingophospholipid class, which is of little interest for perflubron in saline emulsions.) As shown in Figure II-2, in the case of

glycerophospholipids, the phosphate and the lipid chains are esterified to a glycerol molecule. The different glycerophospholipid types vary according to the X group with which the phosphate is esterified. Table II-II lists the most commonly occurring glycerophospholipids. Another level of variety lies in the nature of the acyl residues R_1 and R_2 (chain length and degree of saturation) [26].

Phospholipids have been studied in depth, and for decades, because they are the major structural elements of biological membranes. This fact arises from their ability, a result of their amphiphilic structures, to form bilayered vesicles spontaneously when dispersed into water: the phospholipid molecule consists of two non-polar hydrocarbon chains attached to a phosphate-containing polar head group (Figure II-3). When the phospholipid is dispersed into water, hydrophobic effects yield lipid aggregates with the polar head groups in contact with the water and inward-facing hydrocarbon chains. Due to geometric factors (phosphatidylcholine is truncated cone-shaped), the bilayer (flexible) is the favored structure (Figure II-4). When dispersed into systems consisting of oil and water, phospholipids will concentrate at the interface to minimize the energy of the system. Down to a certain limit, the radius of curvature of the system depends on the volume of the dispersed phase, the shape and concentration of the amphiphilic molecule, and the mechanical work provided to the system to reduce the dispersed phase into small droplets and to bring the amphiphilic molecule to the interface (Figure II-5).

Extraction

There exist several methods to extract phospholipids from egg yolk [27, 28, 29, 30]. Habif [24.b] developed two methods: in the first one,

inspired by the Wells and Hanahan extraction method, the lipids are first extracted from the egg yolk using a chloroform:methanol (2:1) solution and the phospholipids subsequently precipitated in cold acetone; in the alternative method, inspired by the Ramesh extraction method, the lipoprotein complexes are denaturated with methanol in a first step, after which the phospholipids are extracted with chloroform, and the chloroform fraction washed with a saline solution. In both cases, some non-polar compounds are trapped within the phospholipid crystals, and a purification step is necessary. The residue is dissolved in chloroform (and a minimal amount of methanol) with salicylic acid, onto which the polar compounds adsorb. The salicylic acid-phospholipid fraction is separated and cleaned from the non-polar phase, and finally the purified phospholipids are eluted using methanol. Table II-III gives the average composition of egg yolk phospholipids (EYP) and their fatty acid contents.

It is very important to note that EYP contain many natural minor ingredients such as cholesterol, lysophospholipids, pigments, etc.

Physico-chemical properties

Chemical properties

Because of the complexity of the phospholipid molecules, many modifications are possible (Table II-IV, Figure II-6) [31]. Although the modifications displayed in Table II-IV and Figure II-6 are usually carried out deliberately, to obtain phospholipids with specific properties, attention should also be paid to the unintentional and undesired modifications of phospholipids. These include:

hydrolysis of the acyl residues, which can proceed under very mild conditions in both acidic and basic media, yielding lysophospholipids (lysogenic at high doses) and free fatty acids that can form insoluble soaps and destabilize the membranes. Hydrolysis is a function of pH and temperature. Precautions should be taken during the emulsion preparation.

oxidation of the double bond(s) of the acyl chains, which results in the formation of various residues such as hydroperoxides, aldehydes, and ketones of various length (all toxic when injected). The minor ingredients naturally present in EYP can be sensitive to oxidation as well (in particular the pigments). It should be kept in mind during emulsion preparation that oxidation is a function of the oxygen level, the degree of saturation of the acyl residues, the presence of antioxidants (e.g., vitamin E), and the exposure to light (photo-oxidation).

Phase behavior of phospholipids:

One of the most important features of phospholipid bilayers, when fully hydrated (which is the case in the systems under our consideration) and composed of a single phospholipid species, is a well-defined sharp thermotropic phase transition, often called the gel to liquid crystal phase transition [26, 32]. The fluid phase is conventionally called L_α and the gel phase L_β. For certain phospholipids, an intermediate phase $L_{\beta'}$ characterized by a rippled bilayer is found in the gel phase. It is hardly necessary to note that the liquid crystal phase is very important in biological systems, where life processes require molecular disorder and mobility, with constant orientation of the fundamental groups involved [33, 34, 35, 36, 37, 38]. Extensive theoretical work has been done in the attempt to comprehend the meaning of the phase transition temperature

(PTT) [32, 39]. Tardieu et al. showed that the main factor influencing the value of PTT was the nature of the acyl chains, and concluded that the phase transition in lipid bilayers resulted from "melting" or disordering of the hydrocarbon tails of lipids [40]. This theory was further refined by Chapman et al. [41], who recognized that, in contrast to hydrocarbon melts, phospholipid melts were anisotropic, due to the anchoring of the chains to the head group, itself anchored at the water interface; the disordering is thus less important than in the case of hydrocarbon melts. Raman spectroscopy studies yielded additional refinements (namely that the two hydrocarbon chains in each lipid were not identical) [42], and Cevc found that the polar surface of the membrane regulated the melting point of the chains as well [43]. Despite all the refinements brought to the theory, the phase transition can be simply, and fairly accurately, understood as follows:

below PTT: gel phase: the hydrocarbon chains are parallel and in all trans conformation (except for the CH_2-CH_3 group of R_1),

above PTT: liquid crystal phase: the chains are disordered by trans to gauche rotation of some of the C-C bonds.

As mentioned before, the term "EYP" refers to a very complex system: not only are different species present, varying among themselves in hydrocarbon chain length and degree of saturation, but some non-phospholipid minor ingredients (e.g., cholesterol, pigments) are present as well. As a result, the main transition temperature is no longer clearcut (it ranges from -10 to +5°C), and the binary phase diagram for EYP and water as a function of temperature becomes very complex [33,44].

The surface properties of EYP will be developed in Chapter II.4.a.

Because they are the main constituents of biological membranes and are extracted from an animal source, the phospholipids described above are injectable. Provided they can adsorb at the perflubron/saline interface (see Chapter II.4.a), they can be used as an emulsifier to disperse perflubron in a saline solution compatible with human blood.

II.2.c. Saline

Perflubron, the active ingredient of the perflubron/EYP/saline emulsions, is not water-soluble. As a consequence, it is not directly injectable in the human circulatory system. It is for this reason that perflubron must be emulsified (using EYP as an emulsifier) in an aqueous solution (i.e., the saline) compatible with human blood. The composition of the saline is as follows:

NaCl	5.1 g/l
diNaEDTA	0.6 g/l
Na_2HPO_4	3.2 g/l
NaH_2PO_4	1.8 g/l

A phosphate buffer was used to adjust the pH of the saline to 6.8, at which the hydrolysis of phospholipids was found to be minimal [45]. EDTA was used to bind the divalent metal cations that can be responsible for droplet flocculation [46, 47]. The osmolarity of the saline was adjusted to 290 mOsm/l to be compatible with human blood osmolarity (275 - 295 mOsm/l) [15].

Now that the three components of the emulsion have been presented, the next step is actually to make the emulsion. This will be the subject of the next subchapter.

II.3. EMULSION PREPARATION

An optimum concentration range of perflubron in saline was found to be 43 to 52% (v/v). If the EYP-to-perflubron ratio is too low, there will be too few EYP molecules to yield an emulsion with small particle size (for a given volume of dispersed phase, the smaller the droplets, the larger the total interfacial area, and thus the larger the number of amphiphilic molecules required to cover the interface), and if the EYP-to-perflubron ratio is too large, the excess EYP will be present as perflubron-free vesicles that (a) may be detrimental to the emulsion stability [48], (b) are not acceptable from biomedical and cost-efficiency points of view [49], and (c) have detrimental effects on cholesterol metabolism [49, 50]. The optimum EYP-to-perflubron ratio, then, was found to be 9.5% (w/v), which corresponds to 4% (w/v) and 5% (w/v) for the extrema concentrations of perflubron in saline (43 and 52%).

In the experiments described in the present dissertation, the concentrations of dispersed phase and continuous phase are kept constant, 43% v/v and 53% v/v respectively, as is the emulsifier concentration, 50mM.

Figure II-7 shows a scheme for the preparation of perflubron/EYP/saline emulsions. The emulsifier (EYP) is first dispersed in the aqueous phase (saline) by magnetic stirring, at room temperature and under nitrogen atmosphere (to prevent oxidation), until a milky dispersion

is obtained. To be water-dispersible the emulsifier should be in its liquid crystalline phase--i.e., above its critical transition temperature--and the emulsification must therefore also be performed above this temperature. Then the mixture is submitted to mechanical work (3min./13,500rpm) in an Ultra-Turrax (UT) T25 (IKA Works, Inc., Cincinnati, OH) fitted with a dispersing tool S25 KG-25 F. The oil (perflubron) is added and the system is mixed (5min./13,500rpm) until it yields a homogeneous pre-emulsion; this pre-emulsion is fed into a microfluidizer (MF) M110-T (Microfluidics Corp., Newton, MA) (69MPa(10,000psi)/5-7 passes), and the resulting emulsion, contained in glass vials with rubber stoppers and crimped aluminum seals, is sterilized in a static autoclave (AMSCO) (121°C/140kPa(20psi)/15 min.). The total volume of each emulsion sample is 300 ml.

As we have seen before, emulsions in general are very complex and varied systems, and their properties cannot be predicted on theoretical considerations alone. Substantial empirical investigation is therefore necessary to characterize the perflubron/EYP/saline emulsions. Particular attention will be paid to the EYP interfacial film, the structure of the emulsions (population distribution, structure of the droplets, and particle size), and their rheological properties.

II.4. EMULSION CHARACTERIZATION

II.4.a. Surface properties of phospholipids

As discussed in II.1, an emulsifier has two roles:

1. to lower the interfacial free energy between the hydrophilic and the hydrophobic phases (and thus to decrease the work of formation of the interface), and

2. to surround the dispersed phase droplets with a film capable of ensuring emulsion stability.

EYP lowers the water/perflubron interfacial free energy.

The drop-volume method [51.a] was used to measure the interfacial free energy between perflubron and the saline with and without the phospholipid interfacial film [60]. Dipalmitoylphosphatidylcholine (DPPC) was used as a simpler model for EYP (DPPC is a single species phospholipid and a saturated -- non-oxidation-sensitive -- compound). The results showed that the interfacial free energy was drastically reduced, from 50 mN/m for the bare interface to less than 1 mN/m in the presence of DDPC at the interface. Furthermore, the DPPC-coated droplets do not coalesce readily with the perflubron phase, as the sodium dodecyl sulfate (SDS, an emulsifier used for the calibration of the apparatus)-coated droplets do, but instead stay at the surface of the perflubron phase for hours. So the film not only reduces the interfacial free energy between the saline and the perflubron but seems to provide the droplets with a strongly adsorbed film that yields stability (by preventing coalescence).

Surface properties of monolayers as determined by surface isotherm measurements.

Even though phospholipids are amphiphilic molecules, they are virtually insoluble in aqueous phase (the Critical Micellar Concentration (CMC) of phospholipids is 10^{-4} to 10^{-5} mM) and can be studied by the monolayer technique [52].

History

That hydrophobic substances can be spread on water has been known for a long time (Plutarch, in Natural Phenomenon XII of the Moralia, speculates on causes for the well-known calming effect of oil on a rough sea [53]), but the first recorded scientific experiment was carried out by Benjamin Franklin, who showed in 1774 that oil could not be spread thinner than 25Å (molecular dimensions) [54]. (Franklin (1706-1790), one need hardly point out, would not have expressed his result in angstroms, having died well before the birth of Anders Angstrom in 1814; the first attested use of the word in English was in 1897.) It was only a century later, after the ground-breaking works of Young, Laplace, Plateau, and Gibbs, that monolayer experimentation was developed, mainly thanks to the ingenious method developed by Pockels (1891) for manipulating oil films on water (she used moving barriers at the top of a water-filled trough) [55]. On a molecular level, Rayleigh [56] showed, 10 years later, that the film spread at the surface of the trough was one molecule thick; and Hardy suggested in 1913 that the amphiphilic molecules were oriented at the surface of the water, the hydrophilic part buried in the water and the hydrophobic part above the surface [57]. Finally, in 1916-17, Langmuir, using the now well-known Langmuir trough, demonstrated the orientation

of fatty acid molecules at the surface, and showed that, regardless of the chain length of the fatty acid, the films always compress to the same limiting area [58]. The monolayer technique as we know it today was born--and it is still in wide use, as it can give a direct understanding of the origin and magnitude of molecular interactions within a single layer of complex molecules. Parameters commonly studied through this technique are the surface pressure, the surface potential, and the surface viscosity as a function of surface area per molecule. I will concentrate on the surface pressure and the surface potential, since the rheological parameters were investigated through another technique (see II.4.c).

Surface pressure

Surface tension (better, surface free energy (γ_0)) can be defined as the work required to increase the area of a surface isothermally and reversibly per unit amount. Work is needed to fight the tendency that molecules have to leave the surface of the fluid (where they experience energetically unfavorable unbalanced attractive forces) to join the bulk of the fluid (where they are, on average, subjected to equal forces of attraction in all directions), giving rise to a spontaneous contraction of the surface (Figure II-8). When spread at the surface, the insoluble amphiphilic molecules will apply a two-dimensional osmotic pressure: there is a repulsion in the plane of the surface that reduces its tendency to contract. In other words, the amphiphilic film reduces the surface free energy of the fluid. This lowering is called the surface pressure, Π (Figure II-9).

(1) $$\Pi = \gamma_0 - \gamma$$

where γ_0 = surface free energy of the bare surface

γ = surface free energy of the film-covered surface

An entirely analogous expression is used for the surface free energy at the liquid-liquid interface. This case is studied using the so-called "duplex film method" [59, 60]. A duplex film is a film that is thick enough for the two interfaces (i.e., liquid-film and film-air) to be independent and for each to possess its own surface tension (Figure II-10). Let us consider the effect of increasing the interface isothermally and reversibly. As defined above, the surface pressure at the interface Π_i is:

(2) $$\Pi_i = \gamma_{O/W} - \gamma_i$$

where $\gamma_{O/W}$ = interfacial free energy of the bare oil/water interface

γ_i = interfacial free energy of the film-covered interface

The surface pressure of the film Π_D is:

(3) $$\Pi_D = \gamma_{W/A} - \gamma_D$$

where $\gamma_{W/A}$ = surface free energy at the bare water/air interface

γ_D = surface free energy at the duplex film-covered surface

The work required to expand the duplex film (γ_D) is equal to the work to expand both interfaces (oil/air, $\gamma_{O/A}$, and oil/water, $\gamma_{O/W}$) reduced by the surface pressure at the virtual oil/water interface (Π_i):

(4) $$\gamma_D = \gamma_{O/A} + \gamma_{O/W} - \Pi_i$$

From Equation 2 it follows that

(5) $$\gamma_D = \gamma_{O/A} + \gamma_i$$

The surface pressure of the duplex film is then:

(6) $$\Pi_D = \gamma_{W/A} - \gamma_{O/A} - \gamma_i$$

In the case of phospholipids, the hydrocarbon chains that constitute the oil phase are on average 16 to 18 carbons long. Therefore, $\gamma_{O/A}$ and $\gamma_{W/A}$ are approximately equal to 29 mN/m and 72 mN/m, respectively, at 25°C. Then:

(7) $$\Pi_D = 72 - 29 - \gamma_i$$
$$\Pi_D = 43 - \gamma_i$$

Therefore, if the surface pressure of the duplex film exceeds 43 mN/m, negative interfacial free energy occurs. This is the condition for spontaneous emulsification [51.b] and is a good indicator of a well-organized film that can sustain high lateral pressures without breaking into a three-dimensional structure (i.e., without collapsing).

The film can exhibit different physical states according to (a) the nature of the film itself, (b) the nature of the subphase, (c) the temperature of the film, and (d) the pressure applied to it. Monolayers can be roughly classified as condensed, expanded, or gaseous films.

In condensed films, the cohesion is very strong and causes islands to form at areas greater than the limiting area A_0 (examples of such films can be found with palmitic or stearic acid and higher straight-chain fatty acids). As a result, no pressure develops at large film surface area, but as soon as the islands are packed together, the pressure rises very steeply (Figure II-11(1)).

In expanded films, the film is still coherent but occupies a larger area than in the condensed state (Figure II-11(2)). This results from a strong cohesion between the chains and from the absence of electrical repulsion. The equation of state for these films is:

(13) $$(\Pi - \Pi_S)(A - A_0) = kT$$

where Π_S = cohesive pressure within the film (e.g., for a straight-chain derivative, $\Pi_S = 400m/A^{3/2}$, where m is the number of CH_2 groups)

A_0 = area actually occupied by the molecules in the surface (limiting area)

In gaseous films, the molecules are separated and move about the surface independently. The surface pressure approaches zero asymptotically as the area available to the film is increased (molecules

bearing an electrical charge usually form gaseous films, due to the repulsion of the polar groups) (Figure II-11(3)). For these films, a very simple two-dimensional gas state equation can be derived. Neglecting the solute-solute interaction (very dilute surfactant solution, which is the case with the insoluble phospholipids), the lowering of the surface free energy with concentration is approximately linear:

(8) $$\gamma = \gamma_0 - \gamma = bc$$

where c = surfactant concentration at the surface
b = constant

Then,

(9) $$\Pi = \gamma_0 - \gamma = bc$$

and

(10) $$d\gamma/dc = -b$$

Substituting in the Gibbs equation:

(11) $$1/A = (-c/kT)(d\gamma/dc)$$

where k = Boltzmann constant
A = area per molecule
T = temperature

one finds:

(12) $$1/A = \Pi/kT$$
$$\Pi A = kT$$

A given film can go through different physical states as it is compressed, and the transitions observed will depend on the precision of the measurement technique (Figures II-12 and II-13). Another parameter that should not be neglected is the temperature: above phase transition temperature (PTT), the film will remain in the gaseous state until it collapses.

Surface potential

At the interface between a polar liquid (e.g., water) and some other phase (e.g., air), the molecules will have a tendency to orient themselves. Since the molecules possess a dipole moment, their orientation at the surface will yield an asymmetry in the electric field. If the interface is further disturbed by a layer of insoluble molecules that possess a dipole moment of their own and can even be ionized, the nature of the electric field can be dramatically changed. The object of surface potential measurements is to measure the changes in electric field as a monolayer is spread and compressed, isothermally and reversibly, at the surface of the subphase, as a way of obtaining information concerning the orientation of the molecules at the water/air (or oil) interface, which in turn will yield information about the interactions between molecules, between molecules

and the subphase (e.g., ions, water molecules, solutes), and between molecules and the phase above the monolayer (e.g., another oil spread at the surface of the film--as in the duplex film method). The potential of a point is classically defined as the energy required to bring one unit charge from infinity to that point. Considering this definition, one can easily understand the meaning of the potential difference between two points. When the two points in question are in two different phases separated by an interface, the potential difference is called the Galvani potential. Unfortunately, the Galvani potential is impossible to measure: the unit charge is an imaginary one that forces the experimentalist to work with a model (e.g., electron, ion), and this model, going from one phase to the other, will have to adjust to the new environment. But then the work measured is not purely electrostatic but rather involves a non-negligible chemical part (e.g., van der Waals forces). Another alternative is to measure the potential difference between two phases, which is defined as the difference of Volta potential (the work to bring one unit charge from infinity just up to, but not into, the phase, i.e., ca. 10^{-3} mm away) between two phases. According to this definition, the charge does not pass from one phase to the other, and therefore no chemical work is involved; the Volta potential difference is measurable (see below, under Experimental). It is often called the surface potential, but in the present dissertation the term surface potential will be strictly used to describe the change in Volta potential difference produced when a monolayer is spread at an initially cleaned surface [61].

The complexity of the interfacial region in motion (the surface potential is measured while the monolayer is being compressed) makes the quantitative analysis of the surface potential very difficult. One commonly

accepted analogy compares the monolayer with an ordinary plate condenser [62], for which the potential difference between two plates of surface charge density ε, separated by a distance d, in a medium of dielectric constant D, is

(13) $$\Delta V = 4\Pi\varepsilon d/D$$

Schulman and Rideal [63, 64] pushed the analogy further, saying that the effective vertical dipole moments of the molecules in the monolayer can be thought of as the surface charges and spacing of the plates of the condenser. Taking the dielectric constant as unity, the surface potential is then:

(14) $$\Delta V = 4\Pi n\mu\cos\theta$$

where n = number of monolayer molecules per square centimeter
μ = intrinsic moment of the molecule
θ = angle that the intrinsic moment makes with the vertical

This model is actually very imperfect. The reorientation of the subphase molecules just below the film is not taken into consideration, and knowing the value of the dielectric constant would allow the actual measurements performed to coincide more closely with the model (measured μ is typically one-third to one-tenth the actual dipole moment of the molecule). Nonetheless, the concept of "surface dipole moment" is still being used, due probably to its simplicity and to the convenience of the vectorial analogy when it comes to describing the orientation of the molecules in the monolayer. When the film is ionized one must also consider the potential

difference between the surface and the bulk of the subphase due to the ionic double layer (ψ_{AB}) [65]. The surface potential is then:

(15) $$\Delta V = 4\Pi n\mu\cos\theta + \psi_{AB}$$

Experimental

The monolayer technique used to produce the results discussed here was first developed by Schulman [66] and subsequently refined by Christodoulou [67]. The experimental apparatus used for measuring surface pressure and surface potential isotherms is shown in Figure II-14. All the experiments were conducted within a Faraday box. The molecules forming the film to be investigated were dissolved in n-hexane (and a minimal amount of absolute ethanol, if necessary), and the solution was deposited onto the clean aqueous surface with an "Alga" micrometer syringe (Burroughs Wellcome and Co., London). The surface was cleaned by dusting it with calcinated talcum powder, which was removed with the aid of a glass tip connected to an aspirator. The substrate and the film were retained in a fused silica trough and Teflon tape (10.7 x 2.5 x31 cm) of 1.3 liter capacity. Temperature of the substrate was regulated by circulating water from a constant-temperature bath through a glass cooling coil submerged in the substrate. Unless otherwise specified, the aqueous substrate was the saline whose composition was given in II.2.b.

Surface pressures were determined from surface tension measurements made by suspending a sandblasted platinum blade from a transducer-amplifier (Model 311A, The Sanborn Co., Waltham, MA). The transducer output was recorded continuously on a recorder (Sargent,

Model DSR6, E.H. Sargent and Co., Springfield, NJ). The surface tensions were reproducible within ca. 0.2 mN/m.

Surface potentials were measured with an air-ionizing electrode (a Radium-226 source, U.S. Radium Corp., Morristown, NJ) placed 1 to 2 mm above the surface of the liquid substrate and connected to a precision potentiometer, a high-input resistance electrometer (Model 610A, Keithley Instruments, Inc., Cleveland, OH), and a trough electrode (Ag/AgCl) dipped into the bulk of the aqueous substrate. The radioactive electrode was connected to the input terminal of the electrometer with Amphenol low-noise graphitized shielded cable and connectors. The entire circuit was grounded. The e.m.f. of the cell composed of the radioactive electrode, trough electrode, potentiometer, and electrometer, all connected in series, was measured immediately after cleaning the surface of the aqueous substrate (Vo), and compared with the e.m.f. obtained after spreading a film on the surface (V). The difference between the two e.m.f.'s (V - Vo) is the surface potential. The potentiometer opposed a convenient fraction of the cell e.m.f., and the electrometer output was recorded continuously on a recorder (Sargent Model SR). Sensitivity of the surface potential measurements was about $\pm$ 1 mV, and reproducibility of the data was within about 5 mV.

An automatic barrier drive with variable speed control permitted the determination of an optimum compression rate and reproducible Π-A and ΔV-A isotherms. A compression rate of 0.15 to 0.3 percent decrease in area per second was found to be optimal for this study.

All glassware was cleaned with freshly prepared sulfochromic mixture and rinsed thoroughly with distilled water. The substrates were cleared from any surface active ingredient by foaming with nitrogen (the

foam was removed several times by sweeping the surface). The substrates gave adequately stable baseline readings for both the surface pressure and the surface potential measurements.

EYP surface properties

Figure II-15a shows the surface pressure isotherms and the surface potential isotherm of a commercial sample of EYP. Different features of these isotherms must be emphasized, as they will be used to compare the qualities of the different films investigated.

- The film exhibits high collapse pressure (ca. 45 mN/m), which is an indication of a well-organized, well-structured film. It is easy to understand that irregularities or weaknesses in the film will yield a structure that would be unable to withstand high lateral pressures.

- The well-organized, well-structured nature of the film is further evidenced by the large magnitude of the surface potential (380 mV for a surface area of ca. 45 $Å^2$ per molecule). As explained above, the surface potential can be related to the dipole moment of the molecules in the film. It is important to note that we measure the contribution of the average vertical dipole moment directly under the air-ionizing electrode (there can be as many as 10^{+14} molecules under the electrode). As a consequence, if the molecules are randomly distributed in space at the surface of the subphase, the average dipole moment approaches zero. In other words, the higher the surface potential, the more aligned the molecules (the more organized the film).

- As mentioned before, the phase transition temperature of EYP is -5 to +10°C, so the EYP were in the gel phase during the surface isotherm measurement. But EYP are a complex mixture, so some of the minor

components might not be in the gel state at room temperature. This would explain why the film is not in the strictly gaseous state throughout the compression but rather in a liquid expanded state (the film is very expanded).

- Another very important characteristic of the film is its ability to undergo isothermal compression without losing its integrity (e.g., through formation of new irreversible bonds between the molecules, expulsion of some molecules from the film, or damage to the structure of the molecules). This characteristic is evidenced by a reversible compression (no or little hysteresis in the compression/decompression isotherms; see Figure II-15b).

In conclusion, EYP are an excellent candidate for emulsification. Not only are EYP capable of forming a well-organized film at the perflubron/saline interface (by decreasing the interfacial free energy), but the film formed is capable of taking stress without losing its integrity (a very important property when the emulsion will be handled, e.g., during shipping, and injected into the blood stream, where it will be subjected to high levels of shearing).

II.4.b. Perflubron-filled droplets and perflubron-free vesicles

We have seen in Chapter II.3 that not all the vesicles formed during the dispersion of EYP turn into perflubron-filled droplets upon addition of perflubron and homogenization. This subchapter is concerned with the relative percentage of EYP that is turned into perflubron-filled droplets, the average particle size of the droplets, and their lamellarity.

Relative percentage of EYP in perflubron-filled droplets and in vesicles

Perflubron/EYP/saline emulsions were investigated by sedimentation field flow fractionation (SFFF) [68]. A Colloid/Particle Fractionator, Model S101 SedFFF (FFFractionation Inc., Salt Lake City, UT), attached to a Spectra-Physics IsoChrom LC Pump (Spectra-Physics, San Jose, CA) and a Linear UVis 200 Spectrophotometer (Linear Instrument Corp., Reno, NV), was used to generate the data. In this technique, a stream of carrier liquid is introduced into a ribbonlike channel of 0.4 to 1 meter in length and 0.02 cm in diameter, fitted inside a centrifuge basket. The largest particles in the sample cloud, since they are driven by the strongest sedimentation forces, are compressed closest to the wall of the channel. The sample particles are then displaced downstream by the carrier liquid flow. The flow between the walls is parabolic in form, however: fast in the center and slow near the walls. Consequently, particles relatively far from the wall are carried downstream more rapidly than those closer to the wall. The separated sample particles, entrained by the carrier liquid, are eventually eluted from the instrument for detection by an appropriate mechanism. Figure II-16, which shows a fractogram obtained for a perflubron/saline/EYP emulsion, exhibits two peaks. The smaller peak (corresponding to 33% of the total EYP fraction, as calculated by Tarara et al. [69]) represents the empty phospholipid vesicles and the larger peak (67% of the total EYP fraction) represents the perflubron-filled droplets.

Particle size

Particle size was studied through both Transmission Electron Microscopy (TEM) and Photon Correlation Spectroscopy (PCS).

TEM: The emulsion was subjected to rapid freezing in liquid propane, then fractured and coated (platinum replica at 45° angle) for TEM (Figure II-17).

PCS: measurements were carried out on a ZetaSizer 3 (ZS3) particle electrophoresis and multiangle particle size analyzer (Malvern) equipped with a 5mW He-Ne laser of wavelength 633 nm. The emulsion samples were diluted 500-2000 times prior to measurements, which were carried out in the AZ4 cell (4 mm in diameter) at 25°C at a fixed angle of 90°.

Figure II-17 confirms the results obtained by SFFF: both big hemispheres (assumed to be the perflubron-filled droplets) and small hemispheres (assumed to be the smaller vesicles) are visible on the TEM picture. Measurement of the average size of the big hemispheres correlates with the average particle size determined by PCS: the perflubron-filled droplets average 250 nm in diameter.

Lamellarity

Given that 67% of the EYP is adsorbed at the perflubron/saline interface and that the average particle size of the perflubron-filled droplets is 250 nm in diameter, and knowing from surface pressure isotherms the cross-sectional area of a phospholipid (ca. 45 $Å^2$/molecule), we can calculate that there is a single monolayer of EYP adsorbed at the interface.

The emulsion is thus composed of (a) perflubron droplets stabilized by a phospholipid monolayer adsorbed at the interface and (b) small empty (perflubron-free) phospholipid vesicles.

II.4.c. Rheology of the emulsion

Rheology is the science of the deformation and flow of matter. The two extreme rheological behaviors are encountered in Newtonian viscous fluids, on the one hand, and in Hookean elastic solids, on the other. The viscosity of a liquid is a measure of the internal resistance offered to the relative motion of different parts of the liquid [70.a]. In a Newtonian fluid, the shearing force per unit area, τ, between two parallel planes of liquid in relative motion is proportional to the velocity gradient dv/dx between the planes (η is the coefficient of viscosity):

(1) $$\tau = \eta \, dv/dx$$

These Newtonian fluids show no recovery when the stress is removed, the energy involved having been dissipated as heat in overcoming the internal frictional resistance. Such is not the case for elastic solids, which, when stressed, immediately deform by an amount directly proportional to the applied stress and maintain a constant deformation as long as the stress remains constant. When the stress is removed, the elastic energy stored in the solid (various parts of the system were deformed into new non-equilibrium positions relative to one another) is released and the solid immediately recovers its original shape. Most materials, especially colloidal systems, exhibit rheological behaviors that are intermediate

between these two extremes and show both viscous and elastic characteristics. Such materials are termed viscoelastic.

While an Oswald or a Couette viscometer can be used to measure the viscous part of the viscoelasticity (provided the dispersed particles are not too asymmetric), the elastic part (the stored energy) is not measured but released in the system when the experiment is stopped. Creep measurement is used to measure both the viscous and the elastic parts of a viscoelastic fluid (Figure II-18). A constant stress is applied to the sample and the deformation of the sample is observed as a function of time. The observation continues after the stress has been stopped and until no further change can be observed (i.e., until release of the stored energy is complete). The difficulty lies in the time scale of the experiment: the stored energy is released very quickly. One way of solving the problem is by applying a sinusoidal varying stress to the sample and measuring its reponse dynamically. A phase difference, which depends on the viscoelasticity of the fluid, is set up between the stress and the strain: for a purely elastic solid, the stress and the strain are in phase, whereas for a Newtonian fluid, the stress and the strain are 90° out of phase (the strain is behind the applied stress). Various techniques have been designed to measure both the viscosity and the elasticity of a system (plastometers, penetrometers, extensiometers, etc.), but only a few techniques meet the criteria for acceptability: that the information obtained from the measurement be independent of the apparatus, and that the applied stress and the resulting deformation be uniform throughout the sample. Among the acceptable techniques are the torsion pendulum technique (an oscillating torsion resonator is used to achieve the sinusoidal varying stress) [71], the nickel tube resonator technique (the tube is forced into an oscillating

torsional motion by a magnetized excitation coil) [71], and the oscillatory flow in rigid circular tube technique [72]. I will expand on the third technique, which I chose because it requires only readily available apparatus.

Theory of oscillation of a viscoelastic fluid in a circular tube

The theory, developed by Thurston in 1960 [73], gives the acoustical properties of an incompressible fluid confined in a rigid tube of infinite length and circular cross-section and subjected to an axial oscillation. These properties are described by a complex coefficient of viscosity (ratio of the shearing stress to the shearing strain rate), and the velocity profiles for the system and the properties of the acoustic impedance per unit length of tube are determined. The theory is then adapted to the actual measurement constraints (for a tube with finite dimensions) [72, 74].

When a fluid of density ρ fills a rigid tube of radius a and is subjected to a laminar flow, the pressure decrease per unit length, P, the shearing stress at the wall, τ_w, and the volume flow through the tube, U_T, are related by:

$$P\pi a^2 - \tau_w 2\pi a = \rho \frac{\delta U_T}{\delta t} \tag{2}$$

When the flow is pulsatile, U_T, P, and τ_w can be separated into a non-time-varying part (U_S, P_S, and $\tau_{w,S}$) and a time-varying part ($\tilde{U}$, $\tilde{P}$, and $\tilde{\tau}_w$). Equation 2 can then be divided into its time- and non-time-varying parts:

(3) $$P_s \pi a^2 - \tau_{w,s} 2\pi a = 0$$

and

(4) $$\tilde{P}\pi a^2 - \tilde{\tau}_w 2\pi a = \rho \frac{\delta \tilde{U}}{\delta t}$$

Now, if the flow is sinusoidal, the time-varying parts are sinusoidal as well and must be described in complex forms

$$\tilde{U} = U_M e^{(i\omega t)}$$
$$\tilde{\tau} = \tau_w^* e^{(i\omega t)}$$
$$\tilde{P} = P^* e^{(i\omega t)}$$

and Equation 4 thus becomes:

(5) $$P^* - \tau_w^* \left(\frac{2}{a}\right) = \left(\frac{i\omega\rho}{\pi a^2}\right) U_M$$

where P^* and τ_w^* are complex quantities:

$$P^* = P'_M + iP''_M$$
$$\tau_w^* = \tau'_{w,M} - \tau''_{w,M}$$

After we separate the real and the imaginary parts, Equation 5 becomes:

(6)
$$P_w^{'} = \frac{2}{a}\tau_{w,M}^{'}$$
$$P_w^{''} = \frac{2}{a}\left(\frac{\rho\omega}{2\pi a}U_M - \tau_{w,M}^{''}\right)$$

Equations 6 show that $P_w^{'}$ is directly proportional to the stress at the wall of the tube, as opposed to $P_w^{''}$, which is proportional both to a term that depends on the stress at the wall and to an inertial part dependent on the fluid density as well. $P_w^{'}$ is directly proportional to the energy dissipated, while $P_w^{''}$ is proportional to the energy stored but recovered. The apparatus, which will be described below, measures U_M and P^* (both the real and the imaginary parts), but further assumptions are necessary to permit measurement of the viscous and elastic components of the viscoelasticity of the system.

If we assume that the system is homogeneous, the complex coefficient of the viscosity is:

(7)
$$\eta^* = \frac{\tau^*}{G^*} = \eta^{'} - i\eta^{''}$$

where G* is the complex shearing strain rate

η' is the specific viscosity

η'' is the elasticity

The character of the flow (viscous, elastic, or anywhere in between) has been shown to be determined by a parameter $\left(a\sqrt{\left(\rho\omega / \left|\eta^*\right|\right)}\right)$ that, if less than one (which is always the case for the systems under consideration) leads to a simple pressure-to-flow relationship [73, 75]:

$$P'_M = \left(8\eta' / \pi a^4\right) U_M$$
$$P''_M = \left[\left(4\rho\omega / 3\pi a^2\right) - \left(8\eta'' / \pi a^4\right)\right] U_M \quad (8)$$

Comparing Equations 8 to Equations 6, one can obtain the relationship between the complex stress at the wall of the tube and the complex viscosity:

$$\tau'_{w,M} = \left(4\eta' / \pi a^3\right) U_M$$
$$\tau''_{w,M} = \left[\left(4\eta'' / \pi a^3\right) - \left(\rho\omega / 6\pi a\right)\right] U_M \quad (9)$$

Or, in terms of shearing strain rate at the wall of the tube ($G^*_{w,M}$):

$$G^*_{w,M} = \left(4U_M / \pi a^3\right)\left[1 - \left(\rho\omega a^2 / 24\eta^*\right)\right] \quad (10)$$

From Equations 7, 9, and 10 it follows that, if we call the part of the shear stress that is in phase with the shearing strain rate the viscous stress (τ_V) and the part of the shear stress that is 90° out of phase with the shearing strain rate the elastic stress (τ_E), we have:

$$\eta' = \tau_V / G^*$$
$$\eta'' = \tau_E / G^* \quad (11)$$

Rheologists prefer to measure the viscous modulus and the elastic modulus (G" and G', respectively) as a function of increasing (or decreasing) shear strain ($\gamma = G^*/2\Pi f$), and not to measure the viscosity and the elasticity, since these can be confused with results from other

techniques where viscosity and elasticity have other meanings. We then have:

$$G' = \tau_E/\gamma$$
$$G'' = \tau_V/\gamma$$

Experimental

Figure II-19 shows a "Vilastic 3" apparatus (Vilastic Scientific, Inc., "Vilastic 3" Viscoelasticity Analyzer) that was used to determine both the viscous modulus and the elastic modulus of the emulsions. Each system to be tested fills a precision cylindrical tube (tube radius = a; tube length = L) and is subjected to an oscillatory flow (frequency f = 2 Hz). The pressure gradient along, and the volume flow through, the tube (P and U_T, respectively) are measured while the shear strain is increased. The viscous modulus and the elastic modulus are computed according to the theory developed above.

Unless otherwise mentioned, all systems were investigated at room temperature.

Performance characteristics vary with the diameter of the measurement tube and with the material under test. Data below the noise level are automatically discarded.

Viscoelasticity of the perflubron/EYP/saline emulsion

Thurston, who developed the theory set out above and designed the Vilastic 3 apparatus, applied this technique to the study of the viscoelasticity of blood; in particular, he studied the coagulation of red blood cells (or flocculation; see Chapter III.1.b) and the effect of aging and plasma composition on the deformability of red blood cells [76, 77, 78, 79,

80, 81, 82, 83]. My interpretation of the results relative to the perflubron emulsion systems is inspired by the results obtained by Thurston, as our systems are in some respects analogous to blood (both the membrane of the red blood cells and the monolayer of the perflubron-filled droplets are composed mainly of phospholipids, both systems are concentrated, and red blood cells can be spherical when the plasma is made hypotonic to the interior of the red blood cell). In particular, I used the same frequency as Thurston (2 Hz), since it is approximately the frequency experienced in the blood vessels (a crucial point, since the emulsions of perflubron must be injectable).

Figure II-20 shows the viscous and elastic moduli versus shear strain curves for the perflubron/EYP/saline system. The curves must be analyzed on two levels: the order of magnitude of both the viscous and the elastic moduli and the shape of the curves must both be commented upon. The emulsion under consideration exhibits a viscous modulus compatible with that of blood and a low elastic modulus. If we consider the size of the droplets (about 250 nm in diameter) we realize that, unlike the red blood cells (about 7 μm for the largest diameter), they will hardly deform under the pressures applied. So it is not surprising to observe that the viscous modulus versus shear strain curve is almost flat: the slight decrease in viscosity is due to an alignment of the droplets and of the vesicles to the flow, and possibly to a slight deflocculation (we will see later on how flocculation can greatly affect the characteristics of the curves). The same conclusions can be reached from the elastic modulus versus shear strain curve: a colloidal system can only store energy in its structure, whether in chemical bonds (e.g., the low energy bonds that hold the droplets together when the system flocculates) or in the deformation of the existing

structure. The magnitude of G' is low and decreases slightly as the shear strain increases, which is additional evidence that the system is composed of droplets and vesicles that are slightly deformable and/or that slightly flocculate (the G' versus γ curve quickly reaches a plateau when no more bonds can be broken -- i.e., when all the flocs have been broken -- and when the droplets and vesicles have attained their maximum deformation and alignment to the flow). It is important to notice that the flocculation (if there is flocculation) is so moderate that it is not noticed by direct visual observation (see Chapter III.2.a) or by particle size measurements (measuring the particle size in different diluting mediums where the flocs are preserved or broken down can show the occurrence of flocculation; see Chapter III.2.b)

In conclusion, perflubron/EYP/saline emulsions show viscoelastic characteristics compatible with intravenous injection.

II.5. WHY ARE PERFLUBRON/EYP/SALINE EMULSIONS STABLE?

A macroemulsion, unlike a microemulsion, is not a thermodynamically stable system: it is bound to experience physical and/or chemical changes eventually, and the time within which these changes will occur is directly related to the nature of the components of the emulsion and to the treatment to which the emulsion is subjected. In the case of perflubron/EYP/saline emulsions, if the perflubron and the saline solution can be considered stable (perflubron is an inert molecule; see Chapter II.2.a), EYP are very complex and sensitive (see Chapter II.2.c). If we add

to that a drastic thermal treatment (the sterilization step brings the temperature of the emulsions to 121°C for 15 minutes), it becomes very surprising that the emulsions should be stable for several years.

So, the question is "Why are the perflubron/EYP/saline emulsions stable?"

Before we attempt to answer this question, it is necessary to situate the term "stable" within the context of physical chemistry and of emulsion technology in particular.

Table II-I: physico-chemical properties of perflubron

Molecular formula	$C_8F_{17}Br$
Molecular weight	499
Boiling point (°C)	141
Vapor pressure at 37°C (mmg Hg)	14.0
Solubility of O_2 (ml/dl per atmosphere at 37°C)	50 (2.5 for water)
Solubility of CO_2 (ml/dl per atmosphere at 37°C)	213 (65 for water)
Density (g/ml at 20°C)	1.928
Boiling point (°C at 760 mm Hg)	141
Surface tension (mN/m at 25°C)	18.2
Acoustic velocity (m/s)	600

Table II-II: most commonly occurring phospholipids in biological membranes

X	systematic nomenclature	semi-synthetic nomenclature
H	1,2-diacyl-sn-glycerol-3-phosphoric acid	Phosphatidic acid (PA)
$CH_2-CH_2-NH_2$	1,2-diacyl-sn-glycerol-3-phosphoryl-ethanolamine	Phosphatidyl-ethanolamine (PE)
$CH_2-CH_2-N(CH_3)_3$	1,2-diacyl-sn-glycerol-3-phosphorylcholine	Phosphatidylcholine (PC)
$CH_2-CH(+NH_3)-COO^-$	1,2-diacyl-sn-glycerol-3-phosphorylserine	Phosphatidylserine (PS)
$CH_2-CHOH-CH_2OH$	1,2-diacyl-sn-glycerol-3-phosphorylglycerol	Phosphatidylglycerol (PG)

Table II-II: most commonly occurring phospholipids in biological membranes (continued)

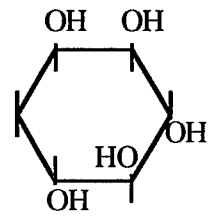	1,2-diacyl-sn-glycerol-3-phosphorylinositol	Phosphatidylinositol (PI)
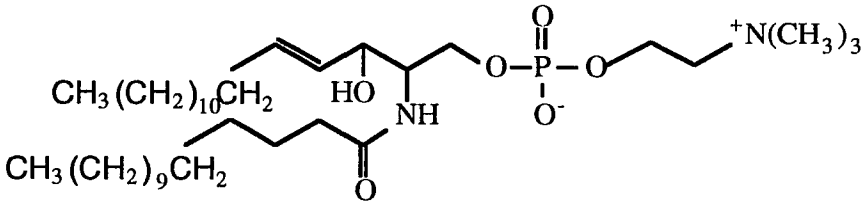		Sphingomyelin (SM)

Table II-III: normalized EYP composition [84]
and EYP fatty acid content [85]

Phosphatidylcholine	70 ±1.5 %
Phosphatidylethanolamine	18 ± 1.0 %
Lysophosphatidylcholine	6 ± 2.1 %
Sphingomyelin	3 ± 0.2 %
Cholesterol	3.± 0.1 %
PS, PG, PI, pigments, etc.	minor components
Palmitic acid (C16:0)	37.7 %
Stearic acid (C18:0)	9.2 %
Oleic acid (C18:)	32.9 %
Linoeic acid (C18:2)	17.0 %
Arachidonic acid (C20:4)	4 - 6 %

Table II-IV: possible modifications of phospholipids

on the phosphoric acid ester	**on the glyceride moiety**
- acylation of the free amino group of phosphatidylethanolamine [86]	- enzymatic or chemical hydrolysis of one fatty acid yielding lysophospholipids [87]
- methylation of the free amino group of phosphatidylethanolamine [86]	- hydroxylation of fatty acids [88]
- enzymatic hydrolysis of the alcohol component from the ester group [86]	- hydrogenation of fatty acids [89]
- enzymatic transesterification [86]	- transesterification [90]
	- addition of halogens [91]

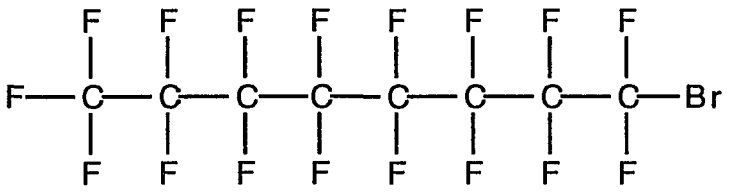

Figure II-1: perflubron structure

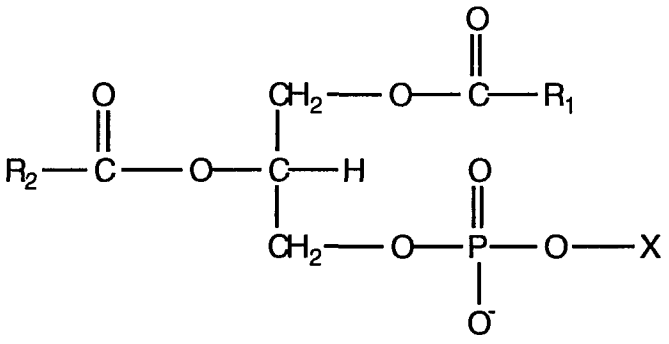

Figure II-2: glycerophospholipid structure

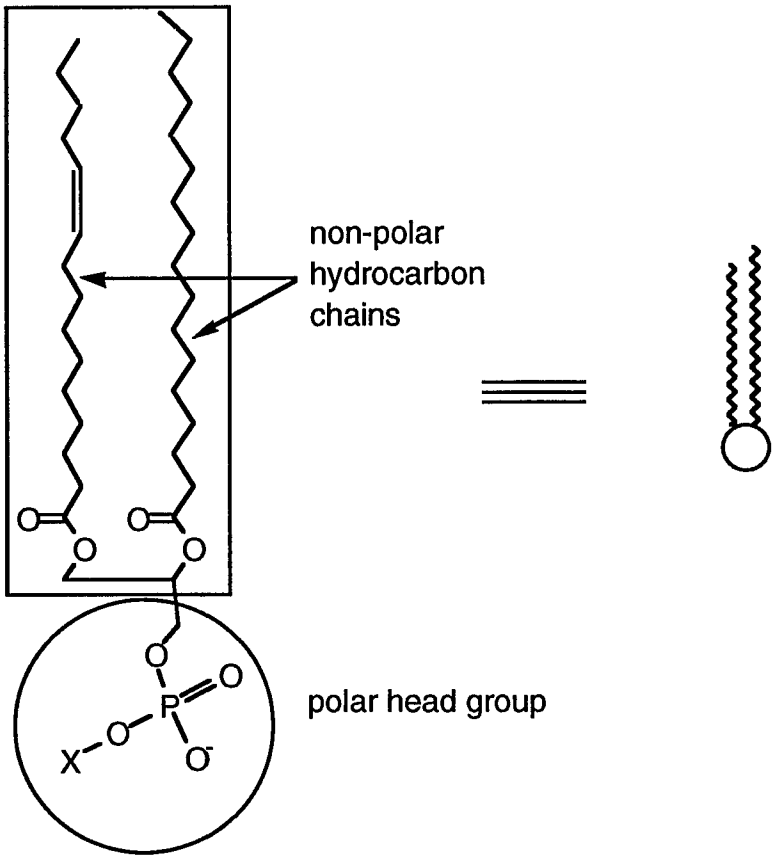

Figure II-3: the amphiphilic nature of phospholipids

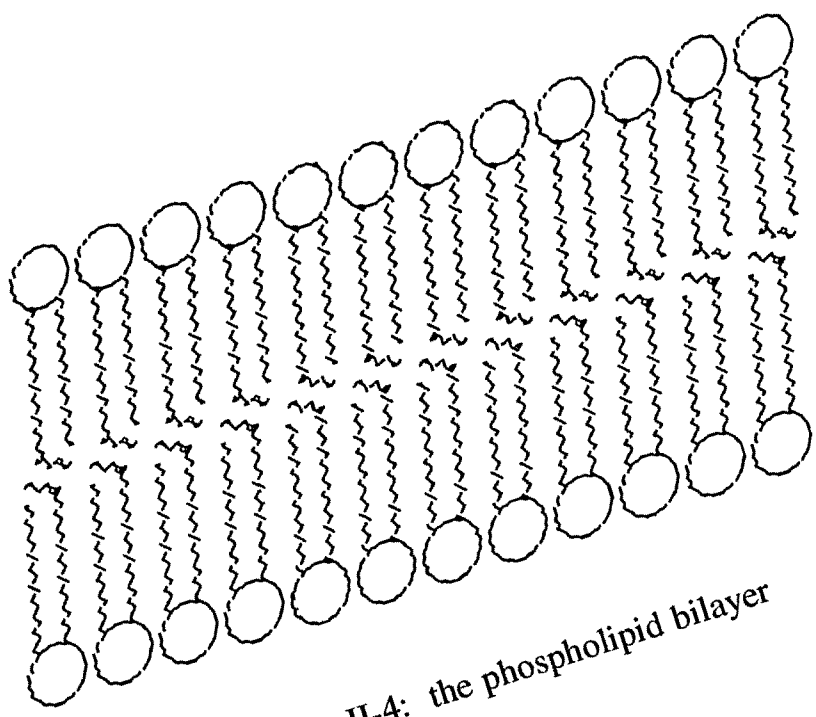

Figure II-4: the phospholipid bilayer

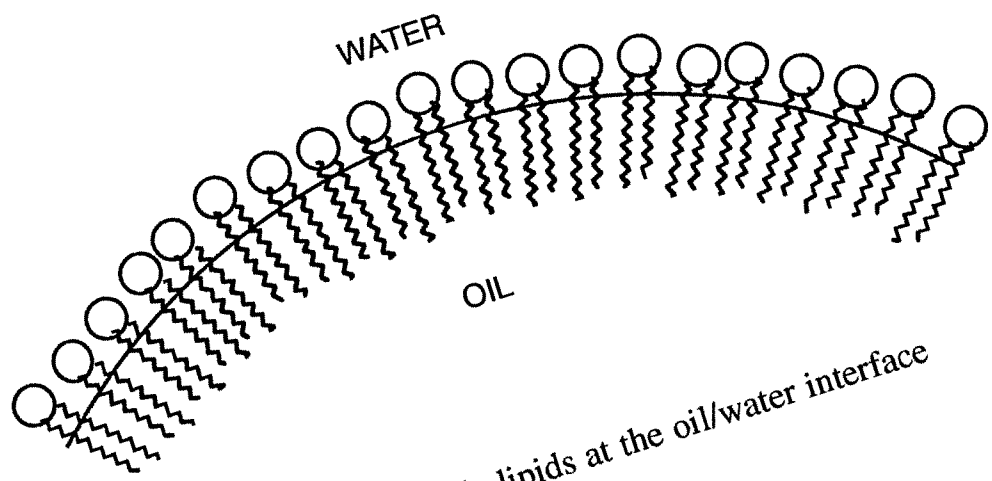

Figure II-5: phospholipids at the oil/water interface

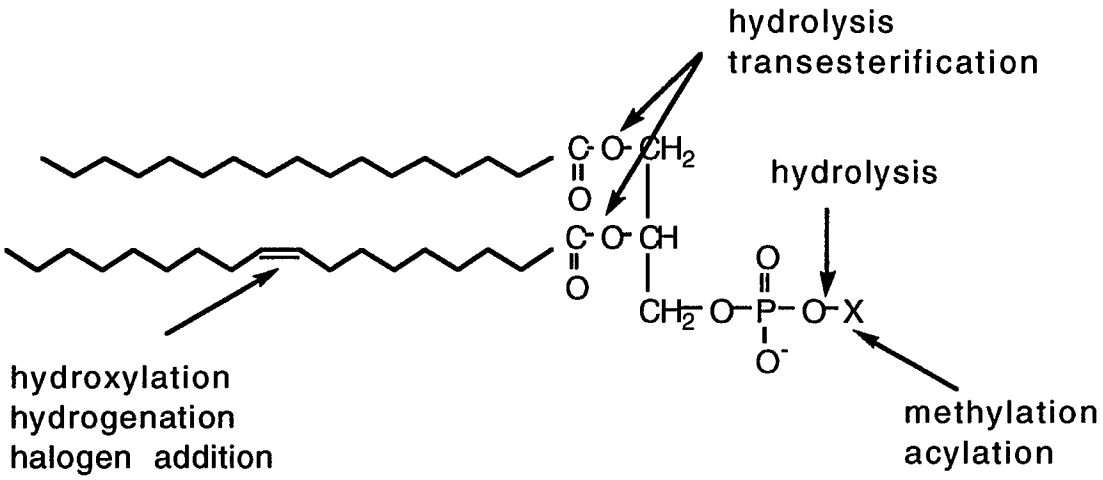

Figure II-6: phospholipid modification possibilities

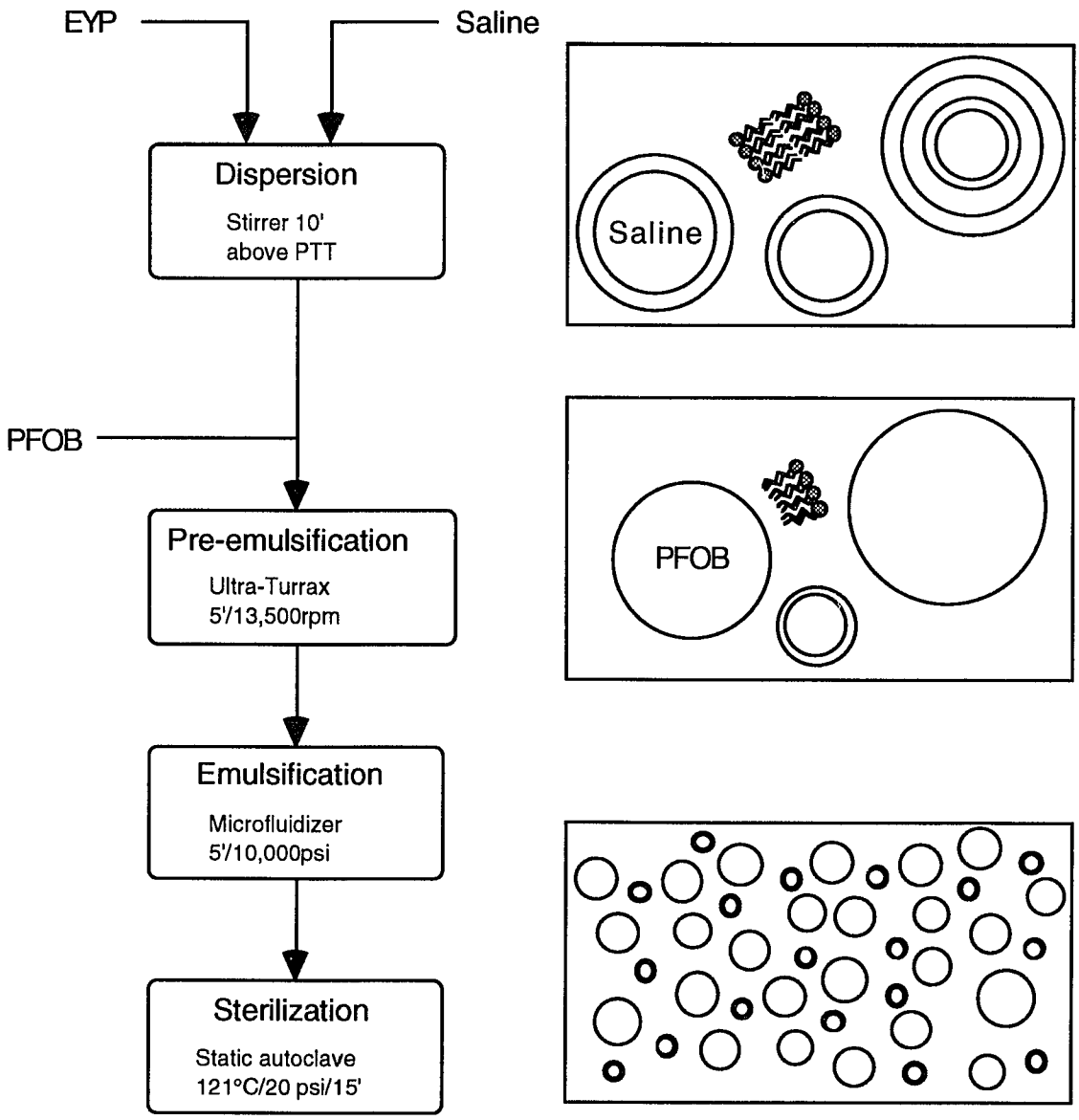

Figure II-7: emulsion preparation

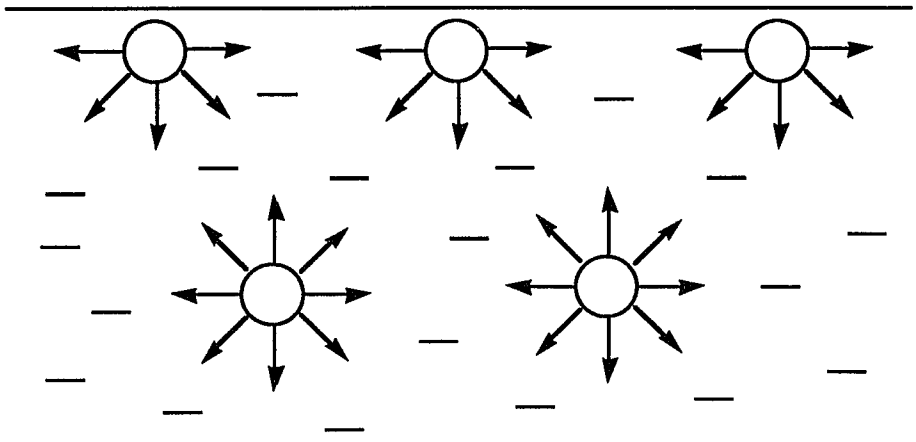

Figure II-8: attractive forces between molecules at the surface and in the interior of a liquid [70.b]

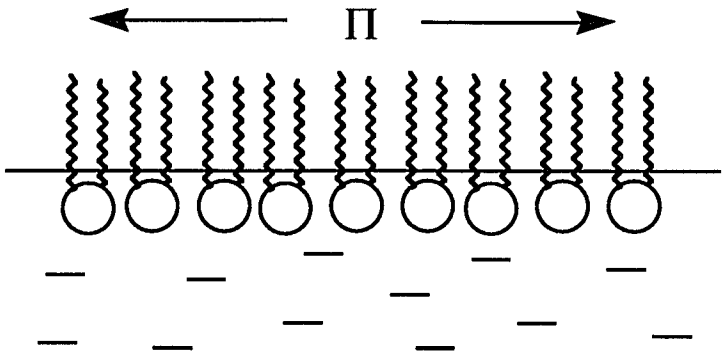

Figure II-9: surface pressure

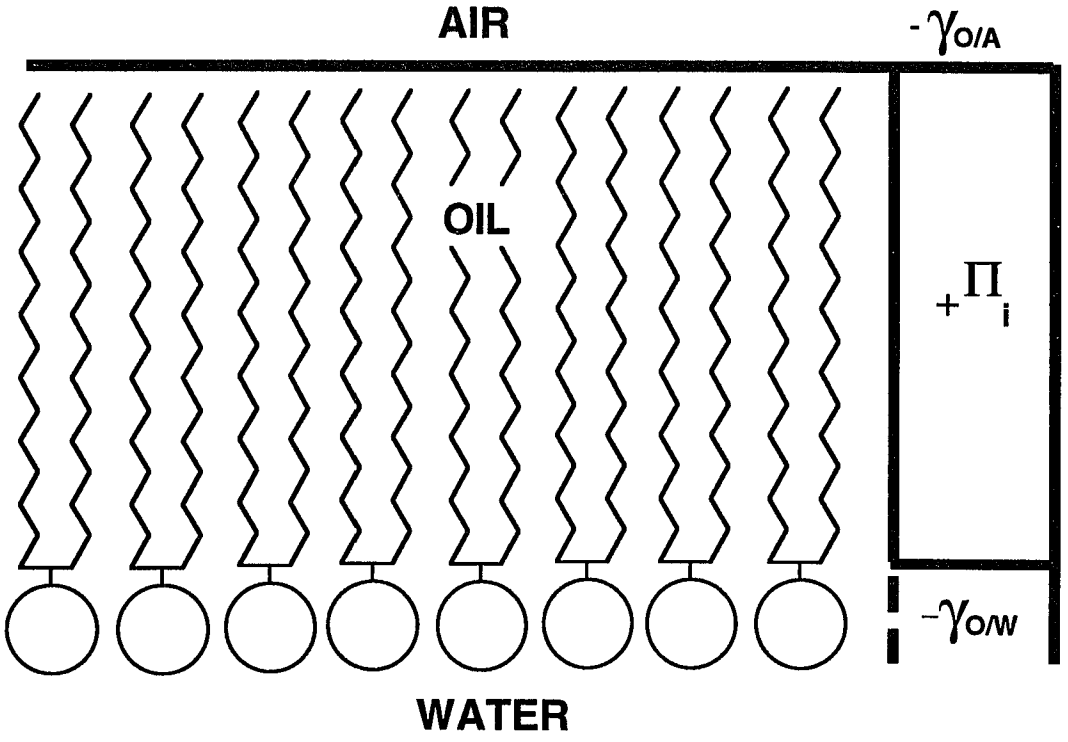

Figure II-10: the duplex film

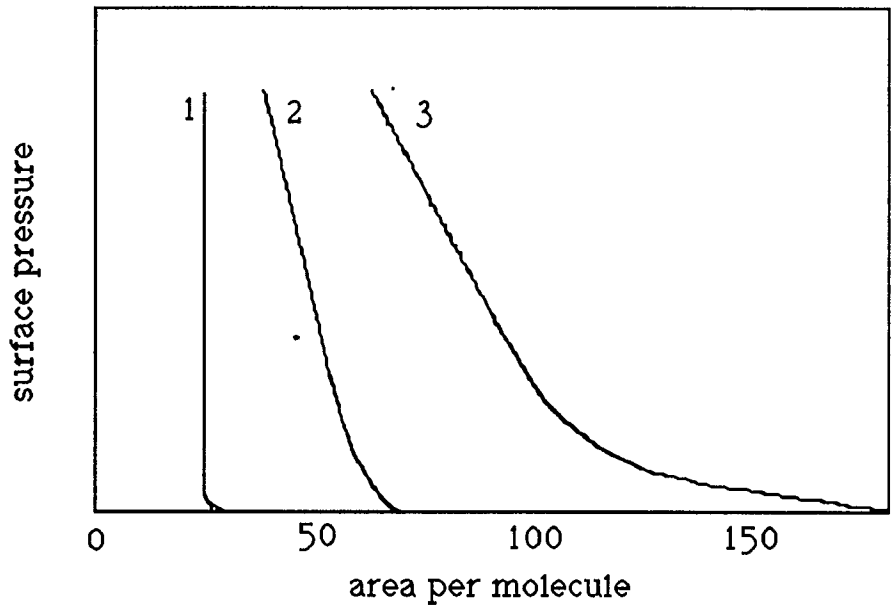

(1: condensed state; 2: expanded state; and 3: gaseous state)

Figure II-11: physical states of monomolecular films

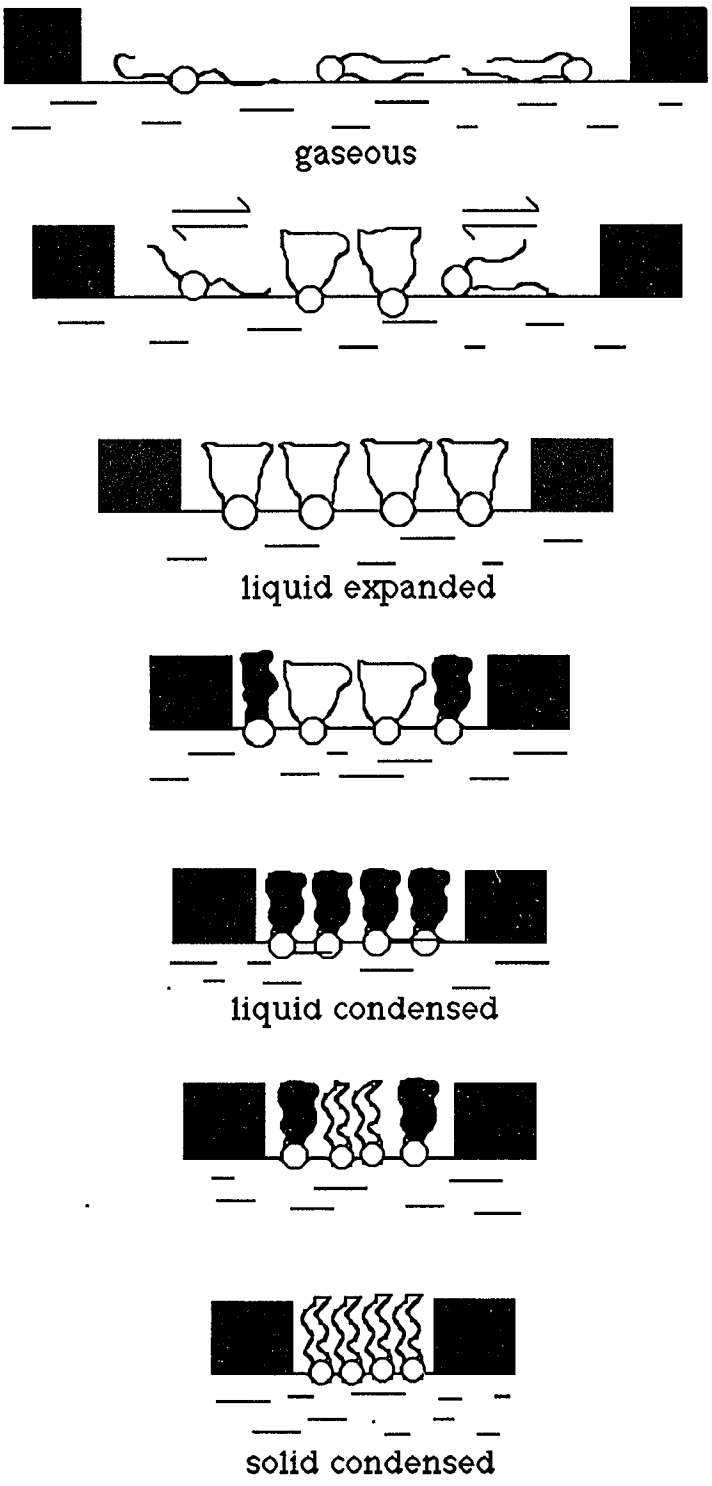

Figure II-12: physical states of monomolecular films [92]

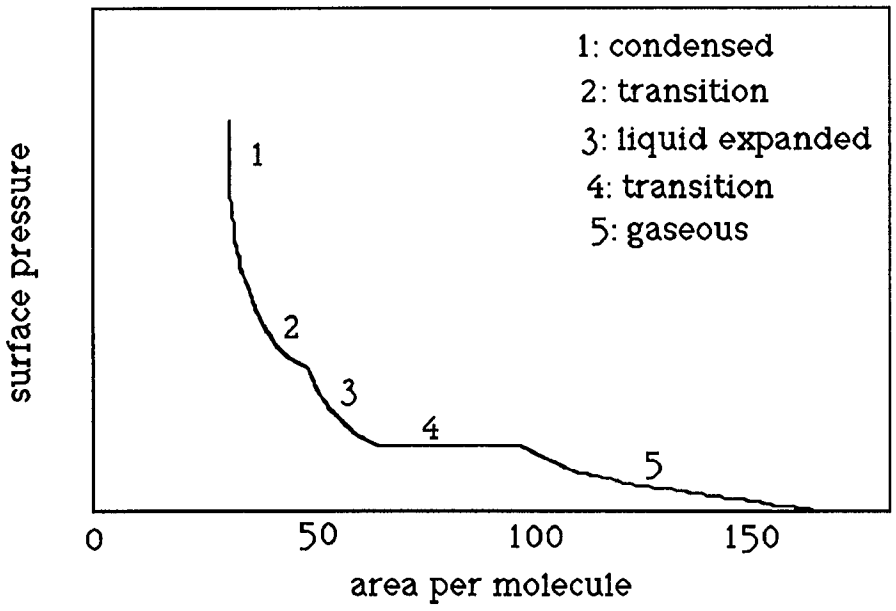

Figure II-13: schematic representation of a Π-A curve

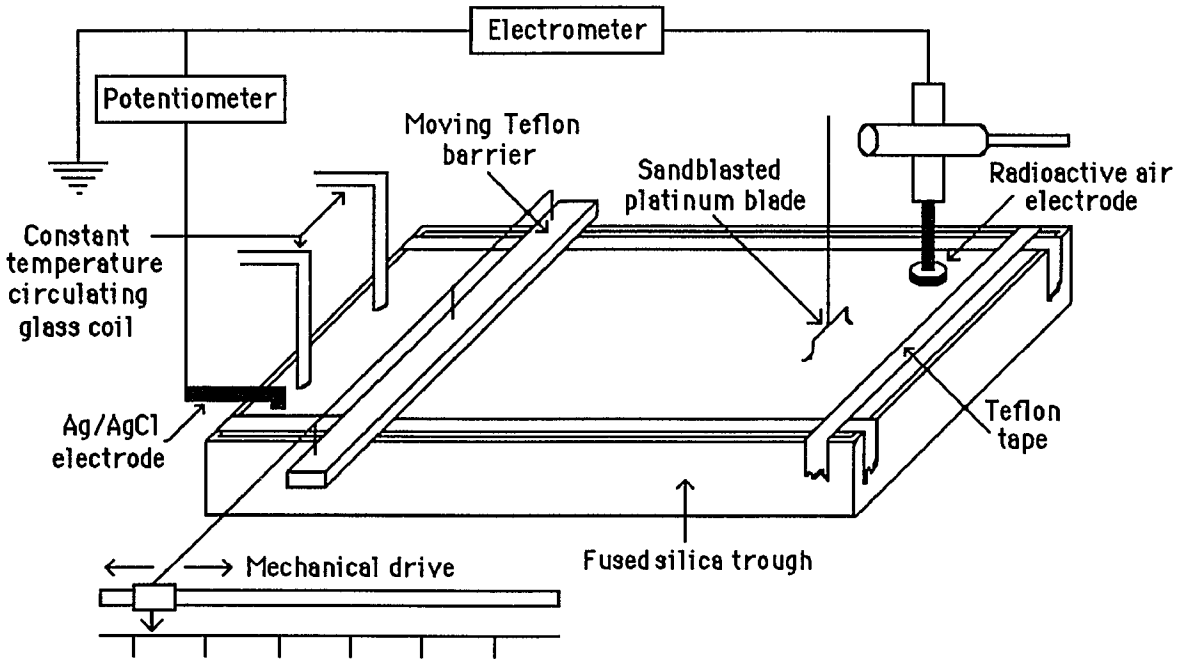

Figure II-14: experimental apparatus for measuring surface pressure and surface potential isotherms (within a Faraday cage)

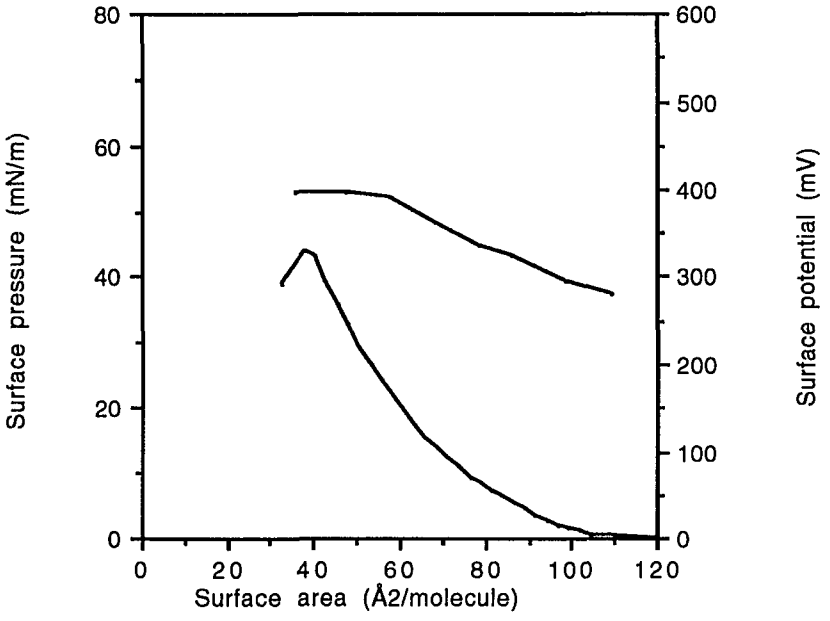

Figure II-15a: surface pressure and surface potential isotherms of commercial EYP on saline at pH 6.8 and 25°C

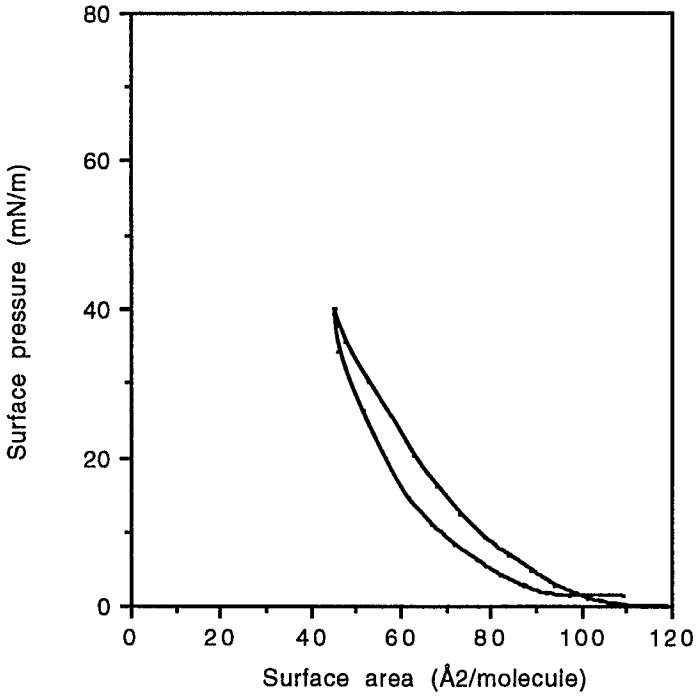

Figure II-15b: surface pressure isotherms (compression/decompression) of commercial EYP on saline at pH 6.8 and 25°C

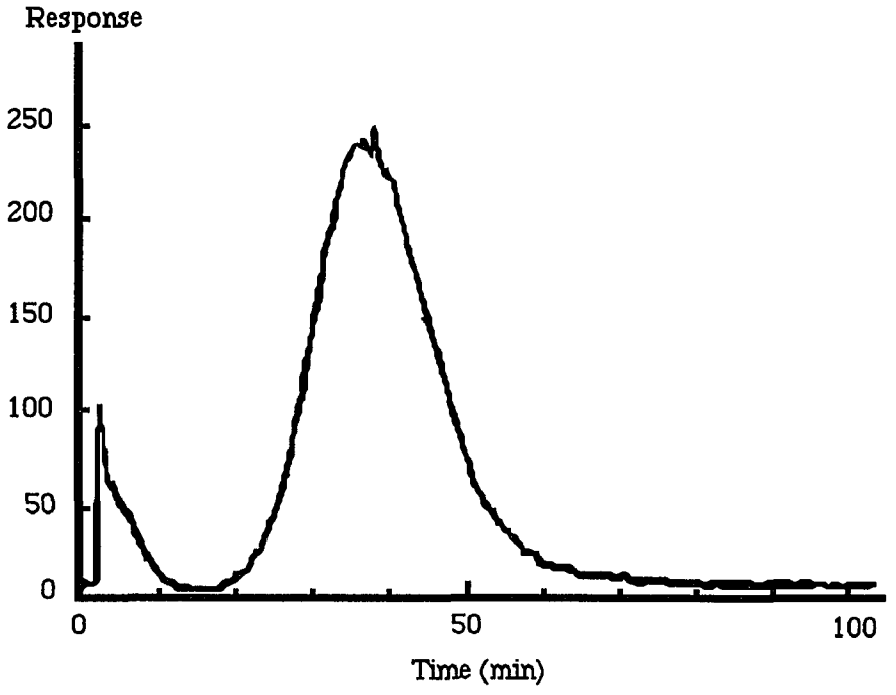

Figure II-16: sedimentation field flow fractionation fractogram of a 52% v/v (100% w/v) perflubron/EYP/saline emulsion

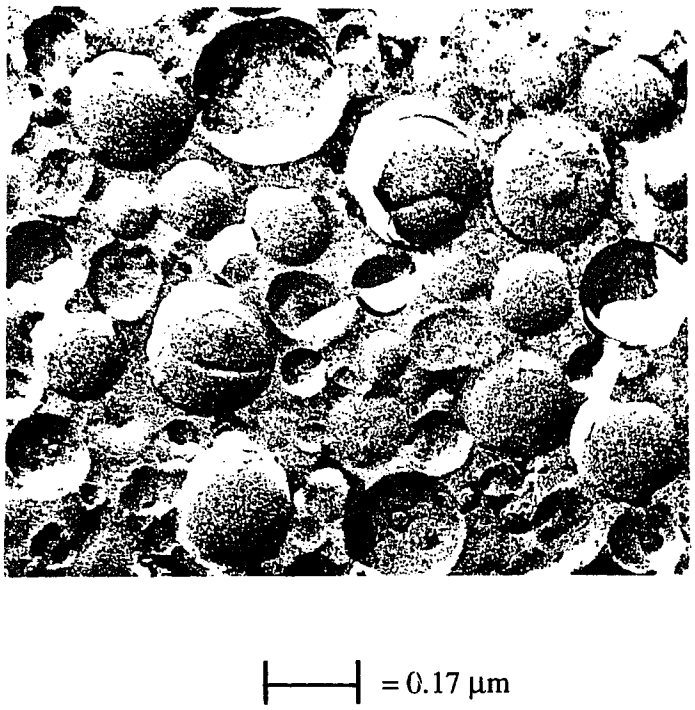

Figure II-17: transmission electron micrograph of a 52% v/v (100% w/v) perflubron/EYP/saline emulsion

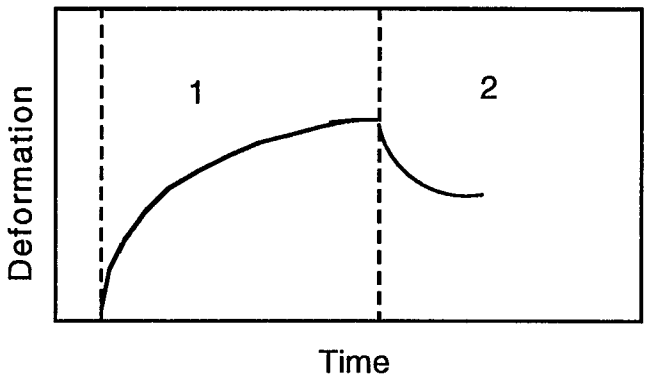

1: Creep under constant stress
2: Recovery after removal of stress

Figure II-18: creep and recovery curve for typical viscoelastic fluid [70.c]

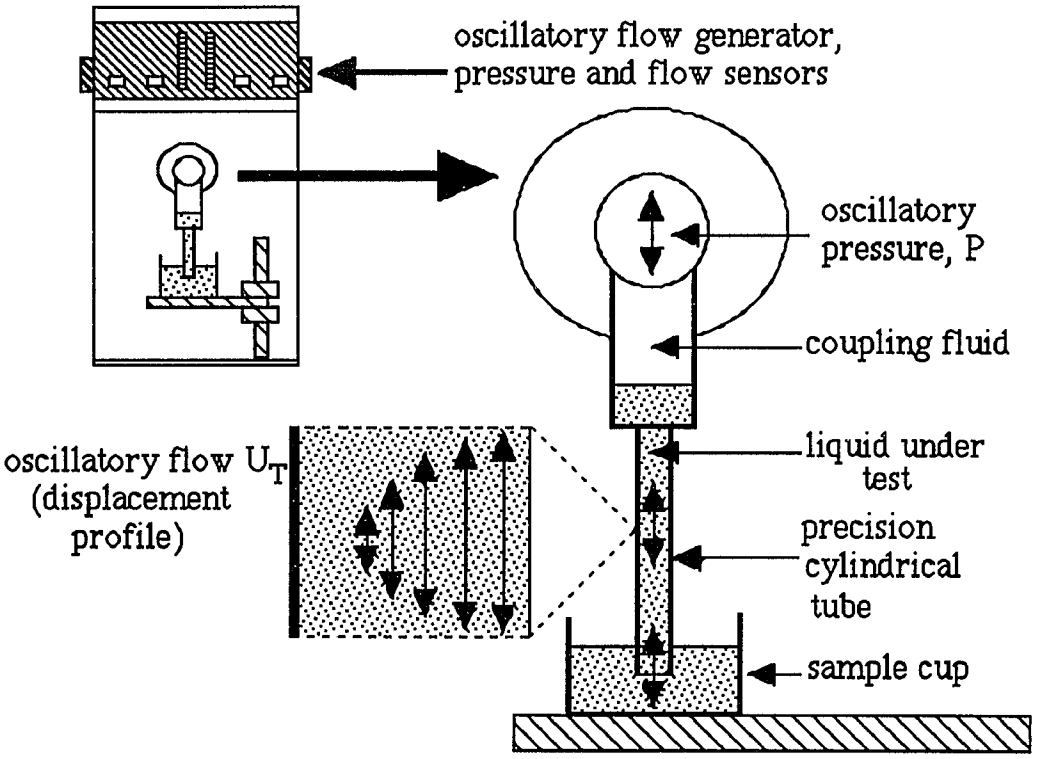

Figure II-19: "Vilastic 3" apparatus
(Vilastic Scientific, Inc., Bedford Hills, NY)

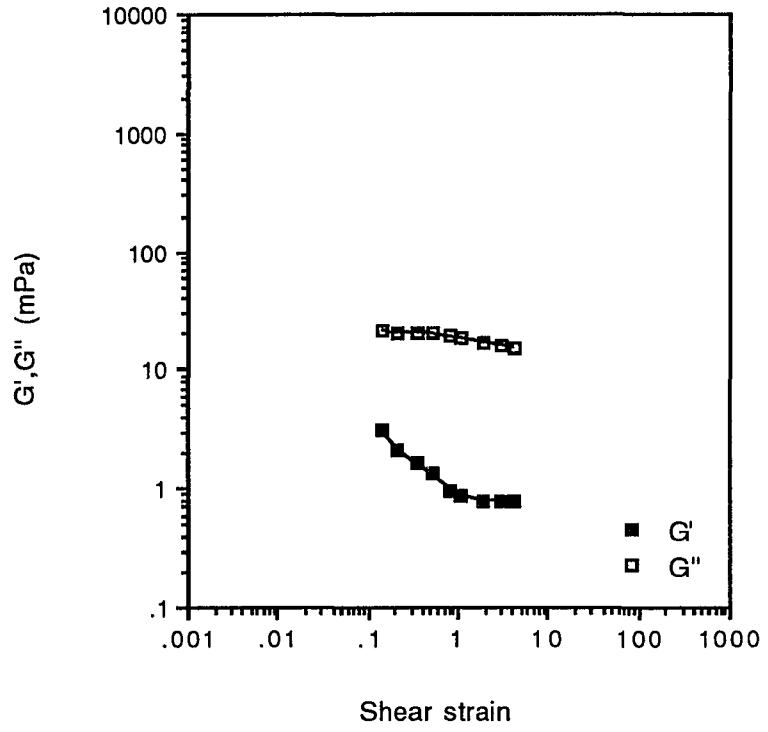

Figure II-20: viscous and elastic moduli (G", G') versus shear strain for a perflubron/EYP/saline emulsion

CHAPTER III

STABILITY STUDY

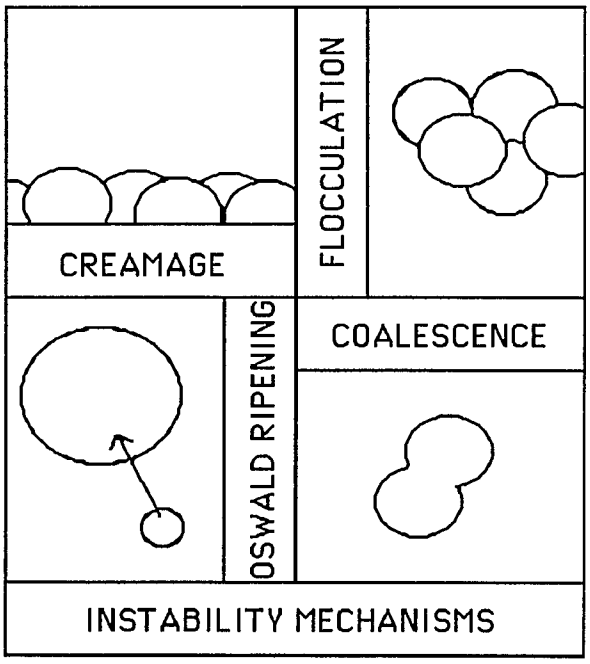

III. STABILITY STUDY

Stability is one of those words that take on a full meaning only when they are placed in a certain context. Let us agree that stability is the conservation of a certain characteristic for a certain period of time. My purpose in this chapter is (a) to define, in the context of emulsion science, the different characteristics that are commonly observed when one wishes to study stability, (b) to decide what I mean by stability in the case of perflubron/EYP/saline emulsions and how I intend to study it, and finally (c) to give the results of this stability study.

III.1. STABILITY

There are four major phenomena through which an emulsion can experience instability: creamage (upward or downward sedimentation of the dispersed phase droplets due to a difference in density between the continuous phase and the dispersed phase), flocculation (formation of a gel-like network linking a certain number of dispersed phase droplets due to bonding between the surfactant molecules covering the droplets), coalescence (fusion of droplets leading eventually to phase separation), and Oswald ripening (increase in size of the larger droplets at the expense of the smaller ones, as a result of the Kelvin effect). Of course, these phenomena are usually not independent of one another, but I will treat them independently for clarity and simplicity.

III.1.a. Creamage

Creamage, or upward or downward sedimentation, is the result of the effect of gravity. The flow rate of sedimentation, F_S, is given by:

(1) $$F_S = cA\frac{dx}{dt}$$

where c is the particle concentration

A is the area crossed by the particles in a time dt

The driving force acting on a particle of mass m and specific volume ν in a liquid of density ρ can be expressed (with g as the local acceleration due to gravity) as

(2) $$m(1-\nu\rho)g$$

From Equation 2 it appears that if the density of the dispersed particle ($\rho_2=1/\nu$) is less than ρ, the driving force will be opposite to gravity (upward sedimentation), and if the density is greater than ρ, the driving force will be in the same direction as gravity (downward sedimentation). The liquid medium, or continuous phase, offers a resistance to the flow of the particles that is, in a first approximation, proportional to the velocity of the sedimenting particles. The coefficient of proportionality is f, the so-called frictional coefficient of the particle for a given continuous phase. When the driving force on the particle and the resistance of the continuous phase are equal, we have:

(3) $$m(1-v\rho)g = f\frac{dx}{dt}$$

In the case of spherical particles (which is the case for the perflubron/EYP/saline emulsions), and provided (1) the motion of the particles is slow, (2) the system is diluted, and (3) the particle dimensions are large compared with the molecules constituting the continuous phase, f is given by Stokes' law:

(4) $$f = 6\pi\eta a$$

where η is the viscosity of the continuous phase

a is the radius of the spherical particles

π is Archimedes' constant

Combining Equations 3 and 4, we have the following expression for the velocity of the sedimenting particles:

(5) $$\frac{dx}{dt} = \frac{2a^2(\rho_2 - \rho)g}{9\eta}$$

And combining Equations 1 and 5, we find the flow rate of the particle subjected to gravity to be:

(6) $$F_s = \frac{2a^2(\rho_2 - \rho)g}{9\eta} Ac$$

In addition to the effect of gravity, the particles are subjected to Brownian (or thermal) motion. As a result, they are continually moving in

all directions and experiencing random collisions. Fick's first law of diffusion states that the particle will preferably go from a region of high concentration to a region of low concentration; the flow rate of diffusion (F_d) is:

(7) $$F_d = -DA\frac{dc}{dx}$$

where D is the diffusion coefficient

$\frac{dc}{dx}$ is the concentration gradient along the x axis

Combining Stokes' law (4) and Einstein's law, which relates the diffusion coefficient and the frictional coefficient according to Equation 8, allows us to derive an expression for the diffusion coefficient (9).

(8) $$Df = kT$$

where k is the Boltzmann constant

T is the absolute temperature

(9) $$D = \frac{kT}{6\Pi\eta a}$$

Combining Equations 7 and 9, we have

(10) $$F_d = -\frac{kT}{6\Pi\eta a}A\frac{dc}{dx}$$

If one wishes to slow down the sedimentation, one must decrease the sedimentation rate and increase the diffusion rate. Therefore, stability with respect to sedimentation will be increased by:

(1) a temperature increase, since it increases the diffusion rate;

(2) a decrease in particle size, since it increases the diffusion rate and decreases the sedimentation rate;

(3) a low difference in density between the dispersed particles and the continuous phase, since it decreases the sedimentation rate; and

(4) an increase in the continuous phase viscosity, since, even though it decreases the diffusion rate, it decreases the sedimentation rate to a larger extent.

Of course, the solution adopted to stabilize the emulsion with respect to sedimentation in a given situation will be dependent upon the constraints related to the specific use intended for the emulsion (e.g., an injectable emulsion cannot be more viscous than blood).

III.1.b. Flocculation

So far, we have not considered interactions between particles or droplets as possible causes of instability. As we have seen in Chapter III.1.a, Brownian motion is responsible for particle (droplet) encounters, and flocculation (aggregation) will occur if interactions take place during these encounters. Since the principal cause of flocculation is the van der Waals-London attractive forces between the droplets, any repulsive forces opposing these attractive forces will enhance stability with respect to

flocculation; these repulsive forces include the electrostatic repulsive forces between similarly charged droplets and hydration forces.

Van der Waals-London forces between dispersed particles

The van der Waals forces represent all the attractive forces, other than chemical bonds, between atoms. They are generally very weak, but because they can be seen as additive at first approximation, their summation over all the atoms in the volume under consideration is large and has a long effective range. These forces can be divided into three kinds of forces:

(1) the dipole orientation, or Keesom, forces;

(2) the induction, or Debye, forces; and

(3) the dispersion, or London, forces.

In the cases of the dipole orientation and induction forces, the dipole of each molecule (whether it is a permanent dipole for both molecules, or a permanent and an induced dipole as in the case of the Debye forces) orients itself in such a way that, on average, attraction occurs. In the case of the London forces, the forces result from a charge fluctuation in the molecule associated with the motion of electrons that creates a time-dependent dipole moment, and a phase difference in the fluctuating dipoles results in mutual attraction.

Hamaker derived the equation for the dispersion energy in vacuum for two particles of radii a_1 and a_2, containing q atoms per cm^3 each, of polarizability α_0 and frequency ν_0 [1]:

(1) $$V_D = \int_{v_1} dv_1 \int_{v_2} dv_2 \frac{q^2\beta}{r^6}$$

where v_1 and v_2 are the particle volumes

r is the interparticle distance

β is the London constant, $\beta = \frac{3}{4} h\nu_0 \alpha_0^2$

After integration, if we consider the particles to have the same radius a, where this radius is much larger than d, the minimum distance between the particles, the dispersion energy can be expressed very simply, as follows:

(2) $$V_D = -\frac{Aa}{12d}$$

where A is the van der Waals-Hamaker constant

$A = \beta \Pi^2 q^2$

In practice, particles are not in vacuum but dispersed in a continuous phase. Hamaker, considering that the dispersion forces are additive, adapted Equation 2, defining an overall van der Waals-Hamaker constant A*:

(3) $$A^* = \left(\sqrt{A_1} - \sqrt{A_0}\right)^2$$

where A_1 is the van der Waals-Hamaker constant for the particles

A2 is the van der Waals-Hamaker constant for the continuous phase

Equation 2 can then be written as:

(4) $$V_D = -\frac{A^* a}{12d}$$

The situation gets even more complicated when the spherical particle is surrounded by an adsorbed layer of a third substance (e.g., a surfactant layer, as is the case for the perflubron/EYP/saline emulsions). Vold made a similar analysis, attributing a van der Waals-Hamaker constant to the third substance [2]. The expression for the dispersion energy can be simplified greatly if the van der Waals-Hamaker constants for the oil and the lipophilic part of the surfactant layer are considered to be equal (a very legitimate assumption). We then have, with d being the thickness of the lipophilic part of the surfactant layer (see Figure III-1):

(5) $$V_D = -\frac{A^*(a+\delta)}{12(d-2\delta)}$$

Repulsive electrostatic forces between dispersed particles

Electrostatic repulsion occurs when two particles of like charge approach each other. In the case of an emulsion with an ionic surfactant, it

is not possible to calculate these repulsive forces through the direct application of the Coulomb law, because, since the droplets are surrounded by counterions and co-ions, the overall structure (droplet and diffuse double layer; see Figure III-2) can be considered neutral. Repulsive forces will occur only when the double layers interpenetrate. These electrical repulsive forces were calculated by Derjaguin and Landau [3] and by Verwey and Overbeek [4]. I refer the reader to the works of Gouy [5], Chapman [6], Stern [7], and Whitney and Grahame [8] for a complete treatment of the electrical diffuse double layer (see Figure 2 for the potential drop as a function of the distance from the interface), and I will briefly discuss the interaction energy of spherical droplets, with which we are concerned in the case of emulsions.

The repulsive energy of spherical particles of radius a at a minimum distance can be calculated by [3, 4]:

(6) $$V_{el} = \frac{a}{z^2} f(\psi_0, \kappa d)$$

where
- z is the valency of the counterion
- ψ_0 is the potential at the surface of the droplet
- κ is the Debye-Hückel parameter, which represents the thickness of the double layer ($1/\kappa$)
- d is the interparticle distance
- f is a function of κ and d

Levine obtained a very complicated solution for the electrostatic repulsive energy by series-expanding $V_{el}(d)$ [9]. As a good approximation

for large interparticle distances, we may retain the first term of the series [10]:

$$(7) \qquad V_{el} = \frac{8k^2T^2\varepsilon a e^{-\kappa d}}{e^2z^2}\left[\frac{\exp\left(\frac{ze\psi_0}{2kT}\right)-1}{\exp\left(\frac{ze\psi_0}{2kT}\right)+1}\right]^2$$

where k is the Boltzmann constant

T is the absolute temperature

e is the elementary charge

ε is the dielectric constant in the bulk of the solution

A further approximation is obtained when y_0 is low and the radius a is large in comparison with the thickness of the diffuse double layer [3]:

$$(8) \qquad V_{el} = \frac{\varepsilon a \psi_0^2}{2}\ln\left(1+e^{-\kappa d}\right)$$

Superposition of electrostatic and van der Waals interaction forces

The tendency for a system to flocculate depends on the relative magnitude of the attractive forces and of the repulsive forces, in other words, on the sign and the magnitude of the sum of the van der Waals attractive energy V_D and the electrostatic repulsive energy V_{el}. Let us call the total interaction energy V:

(9) $$V = V_D + V_{el}$$

This theory is refered to as the DOV theory after Derjaguin, Overbeek, and Verwey. We have seen, in Equation 2, that V_D decreases as a function of 1/d, while from Equation 8 we conclude that V_{el} decreases exponentially with d. It is clear, then, that the attractive forces are predominant at large and at very small interparticle distances, while the electrostatic forces dominate for medium interparticle distances. Figure III-3 shows the typical shapes of a curve plotting total potential energy of interaction versus interparticle distance. For the same value of the van der Waals-Hamaker constant (approximately $5x10^{-13}$ erg for an oil-in-water emulsion), curve V_2 (which corresponds to a large surface potential) shows a repulsive energy maximum that predominates over the van der Waals attraction energy: the system will not flocculate provided the energy maximum is large compared to the thermal energy kT. At low surface potential (curve V_1), the total potential energy of interaction does not exhibit a maximum large enough compared to the attractive force potential: the system flocculates. At larger interparticle distances, a total potential energy of interaction minimum may occur (secondary minimum), and if this minimum is deeper than kT, a loose, easily reversible flocculation phenomenon is possible. The different factors that influence the shape of these curves, and therefore the tendency of a system to flocculate, are:

(1) the electrolyte concentration and valence that affect the electrical diffuse double layer: the smaller the electrolyte concentration and the valence of the counterions, the larger the interaction potential maximum. It is sometimes possible to determine the critical flocculation concentration above which the system flocculates.

(2) the value of the van der Waals-Hamaker constant: the larger the van der Waals-Hamaker constant, the larger the attractive force potential and therefore the higher the risk of flocculation. The nature of the surfactant layer and of the immediate surrounding of the droplets is crucial in preventing flocculation (e.g., the hydration of the surface and the organization of the water molecule layers can be very successful in preventing flocculation).

(3) the magnitude of the potential of the diffuse layer: the larger the electrical surface potential, the larger the repulsion potential and thus the larger the total interaction potential maximum.

III.1.c. Coalescence

Coalescence is a term comprising all the phenomena that lead to direct contact between the dispersed phase contents of two droplets. This direct contact entails the contact and subsequent rupture of the surfactant layers surrounding the dispersed phase droplets. Therefore, a necessary condition for droplet coalescence is that the barrier that prevented flocculation be overcome: the droplets must approach each other for the surfactant layers to fuse together. In particular, the electrostatic forces must be overcome and the surface must be free of its water of hydration at the point of contact. Once the two surfaces are close enough for contact to occur, different mechanisms can lead to surfactant layer fusion. Among these we may mention the so-called adhesion-condensation mechanism [11] and the stalk mechanism [12]. In the adhesion-condensation mechanism, the dehydration of the surfaces leads to crystallization of the surfactant molecules, which in turn leads to the decrease in surface area. Associated

with the decrease in surface area is an elastic stress causing disruption of the monolayers, which allows the fusion of the two droplets. In the stalk mechanism, bulging defects on the surface of each droplet can close one upon another either directly or through a micelle or a liposome. Regardless of the mechanism, certain characteristics of the interfacial surfactant film will promote droplet coalescence:

(1) when the fusion is initiated by membrane fusogens, the membrane must be charged [13]; hydrostatic pressure by itself can make neutral droplets fuse [14].

(2) since the film must be in its liquid state [15], the fusion of two droplets will occur at a temperature above the phase transition temperature of the surfactant layer surrounding them. As a consequence, it is sometimes possible to limit coalescence by storing the emulsions at low temperature or by adding to the interface a minor compound that will increase the transition temperature of the film. (Disagreeing, Papahadjopoulos believes that the the film is unstable at the boundary between liquid and crystalline phases and that fusion will occur at these weak points of the surfaces of the droplets [16].)

(3) the geometrical characteristics of the surfactant layer are crucial: a large curvature for the film, and thus a large droplet, is often thought to promote fusion between droplets [17].

III.1.d. Oswald ripening

Oswald ripening is a process of gradual growth of the larger droplets at the expense of smaller ones by means of molecular diffusion. This theory, first developed by Lifshitz and Slezov [18] and Wagner [19], is

based on the Kelvin effect [20] whereby the solubility of a substance dispersed as spherical droplets increases as droplet size decreases:

(1) $$C_{(a)} \approx C_{(\infty)}\left(1+\frac{2\gamma V_m}{RTa}\right)$$

where:
- γ is the interfacial free energy
- V_m is the molar volume of the dispersed phase
- $C_{(a)}$ is the solubility when the substance is dispersed as spherical droplets of radius a
- $C_{(\infty)}$ is the bulk solubility (infinite radius)
- R is the universal gas constant
- T is the absolute temperature

This model is based upon the following assumptions:

(1) the dispersed phase droplets are spherical and fixed in space, and the volume fraction of the dispersed phase tends to zero (very diluted systems);

(2) the dispersed phase concentration in the continuous phase is constant except in the very near vicinity of the surface of the droplet (inhomogeneities of the concentration distribution in space caused by diffusion are neglected); and

(3) the mass transfer is limited by the molecular diffusion of the dispersed phase in the continuous phase.

The Lifshitz-Slezov-Wagner (LSW) theory predicts the kinetics for droplet growth via molecular diffusion, in the case of a single component system, as follows:

$$\omega = \frac{d(a)^3}{dt} = \frac{8\gamma V_m C_{(a)} D}{9RT} \quad (2)$$

This theory made it possible to confirm that the cube of the droplet radius increases linearly with time [21]. Several questions arise when one looks at the perflubron in saline emulsions that are under consideration: first, assumption (1) above does not hold (the system is very concentrated and the droplets are not fixed in space but subjected to Brownian motion), and second, even if we consider that Equation 2 is valid, it seems that the phenomenon can quickly reach a limit. The rate of radius growth over time is governed by, among other factors, the interfacial free energy between the saline and the oil phase. As the droplet size decreases, since the phospholipids are water-insoluble, the phospholipid film will be compressed and the interfacial free energy will decrease according to the compression isotherm exhibited in Figure II-15a, going from very small values (below 1 mN/m; see Chapter II.4.a) to (probably) near zero or negative values if the surface pressures exceed 43 mN/m. As a result, the rate of radius growth should rapidly approach zero, and the Oswald ripening should stop. In the LSW theory, the phenomenon stops when the smaller droplets totally disappear--a highly unlikely event, it would seem, when the surfactant is insoluble in the continuous phase (in the systems under consideration, phospholipids are dispersed as vesicles): even if the driving force is so large that the small droplet can flatten enough for the

two sides to touch and form a bilayer, that bilayer will be too small to curl and form a vesicle. Nonetheless, the phenomenon was observed in the case of fluorocarbon in saline emulsions [21, 22]. Weers et al. [23] proposed a solution to this problem consisting of the addition of a second dispersed phase component that is insoluble in saline (perfluorodecyl bromide, PFDB). The stabilizing effect of adding a second dispersed phase component was first proposed by Higuchi and Misra [24] and was applied to perfluorocarbon emulsions by Davis [22]. In effect, the smaller droplets impoverish themselves in perflubron due to the Kelvin effect, and as a result the concentration of PFDB in the droplets increases, due to its insolubility. According to Raoult's law, there will be a flux of perflubron from the larger droplets towards the smaller ones to restore a constant chemical potential for PFDB in all droplets, large or small. Droplet growth stops when the concentration effect balances the Kelvin effect. The kinetic of growth is governed by the following equation [25]:

(3)
$$\omega_{ab} = \frac{1}{\frac{\phi_a}{\omega_a} + \frac{\phi_b}{\omega_b}}$$

where:

ω_{ab} is the growth rate for the two fluorocarbon emulsion

ϕ_a is the volume fraction of fluorocarbon a

ϕ_b is the volume fraction of fluorocarbon b

ω_a is the individual emulsion growth rate according to Equation 2 for fluorocarbon a

ω_b is the individual emulsion growth rate according to Equation 2 for perfluorocarbon b

Weers et al.'s experimental study is quite spectacular, representing a great improvement in our understanding of the stability of the emulsion with respect to the increase in particle size, but a more in-depth study is necessary to address the problem of the peculiarities of EYP that do not fit the theory [21].

The subject of the next subchapter is to determine, in the context of an injectable perflubron/EYP/saline emulsion, what we will call a stable emulsion and how we will assess its stability.

III.2. STABILITY ASSESSMENT

Before presenting techniques to assess stability, we must define, in the context of an injectable perflubron in saline emulsion, what we mean by stability. One of the key criteria for injectability is that the emulsion not separate into its oil and aqueous phases, as perflubron would cause a lethal oil embolus. The first priority, therefore, is to avoid coalescence. As we saw in the previous chapter, regardless of the mechanism by which emulsion droplets fuse, an essential prerequisite for coalescence is that the surfaces of the droplets approach each other very closely. As a result, it is crucial to prevent flocculation and to limit creamage (the droplets concentrated at the bottom of the vial are very closely packed). Note that flocculation is not necessarily followed by coalescence, especially when it is a very weak, easily reversible, flocculation (of the type corresponding to the secondary minimum); flocculation is still to be avoided, however, as flocs (1) increase the viscosity of the emulsion (the viscosity must be

compatible with the viscosity of human blood), (2) can be too big to circulate through blood capillaries (and can thus cause emboli), and (3) can trigger the immune response faster, thus diminishing the efficacy of the emulsion as a respiratory gas carrier. Oswald ripening is a phenomenon that occurs very rapidly, and its study requires specific pieces of equipment unfortunately unavailable during the course of my research. For that reason, and also because additional theoretical work on the contribution of the phospholipidic interface needs to be done, I will not consider Oswald ripening in this dissertation. Particular attention will accordingly be paid to stability with respect to creamage, flocculation, and coalescence. Without a time frame, however, stability is still a meaningless word: from a purely clinical standpoint, the emulsion must be stable for at least six hours once injected, but from an industrial standpoint (cost effectiveness, production, storage) stability for more than a year is desirable. Stability will be assessed both through direct observation and through measurement of particle size and viscoelastic parameters.

III.2.a. Direct observation

Two phenomena are easily detectable through direct observation: creamage and phase separation. When creamage has occurred, most of the perflubron-filled droplets are at the bottom of the vial in a thick gel-like white layer (the density of perflubron is almost double the density of the saline), leaving on top a clearer white solution that contains most of the empty vesicles. A vigorous shaking of the vial returns the emulsion to its original state (a milky fluid solution) provided no coalescence or flocculation has occurred. If coalescence occurred to such an extent that

phase separation took place, the dense transparent perflubron is easily recognizable at the bottom of the flask; the supernatant is a fluid non-homogeneous phase that contains the saline, perflubron-filled droplets of all sizes, phospholipids vesicles, and (probably) phospholipid film bilayers of all sizes formed by the droplets now empty of perflubron. It is difficult to appreciate flocculation through observation alone: if the degree of flocculation is small, it is simply not detectable. As the flocs get bigger, the milky solution becomes less homogeneous and more viscous, but a limited coalescence (increase in particle size without phase separation) would yield an emulsion with the same visual aspect. If the solution returns to its original state after shaking, flocculation had definitely occurred; but failure to return to the original state is not conclusive either way, as the flocs present might be very strong and difficult to break by shaking alone. Therefore, although direct observation is still a good way of getting a quick impression, and in certain cases of obtaining a definitive answer, additional investigative techniques must be used in order to determine the degree of stability of the emulsions .

III.2.b. Particle size measurement

Particle size is determined using photon correlation spectroscopy (PCS; see Chapter II.4.b). The emulsions are highly concentrated and must be diluted up to 2,000-fold prior to investigation. For a system that does not flocculate, the result of the measurement will be the same whether the emulsion sample is diluted with pure saline (which contains salts; see Chapter 11.2.b) or with distilled deionized water. In the case of a system that flocculates, a larger particle size will be found, since the instrument

cannot discriminate between a floc and a single droplet and will therefore give the size of a floc. Thus, when the particle size of a system is larger than the particle size for the reference emulsion (250 nm), it is difficult to tell whether the system is made of large droplets (resulting from coalescence) or of flocs. To decide this question, a second experiment is run using the same system but this time diluted in distilled deionized water: we have seen in Chapter III.1.b. that the concentration in electrolytes could markedly affect the electrical double layer surrounding the droplets, and that the smaller this concentration, the larger the interaction potential maximum and thus the larger the barrier against flocculation (in other words, the dilution with deionized water pushes the system below the critical flocculation concentration). Therefore, for a given system, if the results from particle size measurement are the same whether the system is diluted with saline or with deionized water, the system is not flocculated and a large particle size could be the result of coalescence. If a smaller particle size is found when the system is diluted with deionized water, the system flocculated and floc size was measured when the system was diluted in saline. This technique is particularly useful for discriminating between flocculation and coalescence when the particle size of a system increases with time, but it is a very intrusive technique (the system is diluted up to 2,000-fold). Viscoelastic parameters measurement in oscillatory flow gives a very good insight into the state of the emulsion without being intrusive (the emulsion is used without prior preparation).

III.2.c. Viscoelasticity

The technique for measuring the viscosity and elasticity (or rather the viscous and elastic moduli) was described in Chapter II.4.c, and typical

viscous and elastic moduli versus shear strain curves were given for the reference emulsion (perflubron/EYP/saline, Figure II-20). The characteristics of both curves can be drastically affected by flocculation. The magnitude of the viscous modulus is much larger than that of the reference emulsion, first, because the flocs, larger than the droplets they are made of, impair the flow of the emulsion, and second, because the flocs can deform, align to the flow, and break resulting in a shear thinning effect (the magnitude of the viscous modulus decreases as the shear strain increases). The elastic modulus versus shear strain curve follows the same pattern (large magnitudes and shear thinning effect) due to the fact that flocs can store more energy in the weak bonds between droplets (a single droplet is small and requires large pressures to deform and thus to store energy), with the decrease in the elastic modulus being due to a gradual breakage of the flocs (the smaller the floc, the less energy it can store) along with a deformation of the flocs as the shear strain increases (the more deformed the floc, the lower its capacity to deform and thus to store energy).

The three ways to assess emulsion stability described above will be used according to what kind of stability is sought; whenever possible, analyses from different techniques will be correlated.

III.3. CORRELATION BETWEEN EYP COMPOSITION AND EMULSION STABILITY

As mentioned in Chapter II.2.c, EYP are a complex mixture of phospholipidic and non-phospholipidic compounds with various degrees of saturation, charge, and surface activity. In addition, EYP composition varies tremendously from one supplier to another and even, for one supplier, from one batch to another. As expected, it has been observed that not all batches of EYP yield stable emulsions. Since we are not considering Oswald ripening as a cause of instability, the nature of the interface (i.e., the composition of the surfactant layer surrounding the oil droplet and the nature of the continuous phase that is part of the interface) is the prime parameter that should be studied and correlated with the stability of the resulting emulsion. We have seen in Chapter II.4 that EYP could be characterized through the surface isotherm technique, which allows such parameters as the packing of the film, its compressibility (the elasticity and reversibility of the compression), and its surface potential to be assessed. The object of my investigation was to correlate the properties of various films of EYP to the stability of the emulsion. Different batches of EYP were analyzed in parallel with respect to their composition [26]. Unfortunately, all batches of EYP studied gave the same isotherms (comparable to the isotherms displayed in Figures II-15a and II-15b): (a) a reversible surface compression up to a collapse of the film at a pressure between 40 and 45 mN/m, (b) comparable compressibilities (no EYP yielded a very condensed or a very expanded film), and (c) a surface potential that lies between 300 and 400 mV for a fully organized film. Similarly, all batches of EYP had about the same composition in both major and minor ingredients. The conclusion of this study is that

instability with respect to flocculation and/or coalescence results not from a poorly organized film (it is clear that all the EYP tested yielded well-organized films but not necessarily flocculation-stable emulsions), but rather from the interaction between two interfacial films, and that some minor components of EYP that do not destabilize the packing of the film can prevent or promote flocculation and/or coalescence. In all composition analysis, one can only identify and detect what is suspected, which may explain why a similar composition was found for all the batches of EYP; it is possible that the composition of certain batches of EYP would differ in levels of an ingredient not measured, and that these levels would correlate with the stability of the resulting system. As mentioned by Davis et al. [27], "it will be difficult to predict the stabilizing capacity of a given lecithin [EYP] sample from a knowledge of its major and minor components." Still, the question remains: what minor ingredient(s) present in EYP prevent(s) flocculation and/or coalescence?

Working on a model for EYP is a more simple and efficient way to answer this question, since EYP are very complex, EYP composition is not thoroughly defined, and EYP are sensitive to oxidation. A logical model for EYP is a pure phospholipid species that is not sensitive to oxidation. As we saw in Chapter II.2.c, the major component of EYP is phosphatidylcholine; therefore, my model for EYP in the study described below is a fully hydrogenated (and thus not sensitive to oxidation) phosphatidylcholine whose trade name is Phospholipon 90H (PL90H).

III.4. HYDROGENATED PHOSPHATIDYLCHOLINE AS A MODEL FOR EGG YOLK PHOSPHOLIPIDS

III.4.a. Composition

The hydrogenated phosphatidylcholine (Phospholipon 90H, PL90H) was purchased from American Lecithin Company (Danbury, CT) and was used with no further purification. Its composition as determined by the supplier is as follows:

93 ± 3% Phosphatidylcholine	86% stearyl (18:0)
	14% palmitoyl (16:0)

max. 4% Lysophosphatidylcholine

It is important to notice that due to the lack of double bonds and minor ingredients, the phase transition temperature (PTT) of PL90H is much higher than that of EYP [28, 29]; more precisely, the PTT for PL90H as determined by differential scanning calorimetry is 52°C. This fact will have to be taken into consideration in the emulsification process, as the dispersion of the phospholipids in saline must take place above the PTT [30]. The fact that PL90H is not oxidizable allows the emulsification process to take place under air atmosphere all the way through, which compensates for the constraint on temperature (the mechanical work provided by the Ultra-Turrax and the microfluidizer was enough to keep the system above the PTT, 52°C).

III.4.b. Surface properties of PL90H

Pure hydrogenated phosphatidylcholine has already been shown to reduce dramatically the perflubron/saline interfacial free energy (see Chapter II.4.a), and it is thus a good candidate to play the part of the surfactant in perflubron in saline emulsions. We have seen as well that reducing interfacial free energy between the dispersed phase and the continuous phase was not sufficient to make a surface active component the "ideal" surfactant for a particular system: the surfactant molecules must also organize themselves in a film capable of insuring stability. In a first analysis, the quality of the film can be investigated through the monolayer technique (see Chapter II.4.a). Figure III-4a shows surface pressure and surface potential isotherms of PL90H on saline at room temperature. The film was below the phase transition temperature throughout the measurement. The surface compression isotherm shows characteristics very similar to those of a film of a straight-chain fatty acid: the film is very condensed and the cohesion between molecules very strong. Due to the higher purity, along with an absence of kinks in the fatty acid chains of the phospholipids, the collapse pressure of the film reaches a high value, viz., 67 mN/m. The compression of the film is reversible (Figure III-4b), and the surface potential reaches values as high as 500 mV when the film is fully compressed. All these characteristics are proof of a very well packed, well organized film that can stand high lateral pressures without breaking. As developed in Chapter II.4.a, a very condensed film is the mark of a very strong cohesion between molecules that can cause islands of well-organized molecules to be in equilibrium with molecules in the gaseous state when the film is stretched, and the border between these two states can be the site for weak points (where leakage of dispersed phase

and/or coalescence through fusion of the surfactant layers of two droplets may occur). It is often preferable to have more expanded films, and we will see how the addition of a second surfactant species to PL90H can solve this problem.

The next step is actually to make the perflubron in saline emulsion using PL90H as the surfactant, and to characterize its stability with respect to creamage, flocculation, and coalescence according to the methods described in Chapter III.2.

III.4.c. Stability study of perflubron/PL90H/saline emulsions

The emulsion was prepared using the standard method described in Chapter II.3 (the initial dispersion of PL90H was performed at 55°C, however). Direct observation showed a rapid settling of a thick, gel-like, white phase characteristic of a flocculated system. This conclusion was supported by particle size analysis (PCS) and viscoelastic parameter measurements (Vilastic 3):

(a) the particle size was on average 1 mm when the system was diluted in saline, while it dropped to 300 nm when the system was diluted in distilled water.

(b) Figure III-5 shows the G', G" versus shear strain curves for the perflubron/PL90H/saline system. Two things are to be noticed. First, the magnitude of both G' and G" is considerably higher for this system than for the reference perflubron/EYP/saline system seen in Figure II-20 (2,000 to 10 mPa and 3 to 0.8 mPa, respectively, for G' and 2,000 to 90 mPa and 20 to 5 mPa, respectively, for G"), which is proof of a flocculated system:

the more flocs and the bigger the flocs, the more viscous the system and the more energy it can store (within the interdroplet bonds). Second, the magnitude of both G' and G" decreases tremendously as the shear strain is increased, which can be explained by the fact that the flocs, gradually broken down as the strain gets higher, get smaller and therefore can store less energy (G' decreases), while causing less disturbance to the flow of the emulsion (G" decreases). It is important to notice that regardless of the flocculation of the system, such high values for the elastic and viscous moduli make it unsuitable for intravenous injection. The system eventually coalesces, as evidenced by the perflubron's separation and migration to the bottom of the vial.

It is clear from the previous observation that the fact that PL90H provides a well-structured film at the interface between perflubron and saline is not enough for it to yield a stable emulsion. As we have seen previously, flocculation can be prevented if the electrostatic repulsive forces are large enough and/or if the van der Waals attractive forces are small enough for the droplets not to come too close to one another. The object of the next subchapter is to identify a way to modify the perflubron/PL90H/saline emulsions to prevent flocculation and therefore achieve a good model for perflubron/EYP/saline emulsions.

III.4.d. A model for perflubron/EYP/saline emulsions

First, an evaluation of the electrostatic repulsive forces was done through measurement of the zeta potential of the perflubron/PL90H/saline system. The zeta potential of the emulsion particles was measured by

microelectrophoresis using the ZetaSizer 3 operating in the cross-beam mode at 25°C with samples diluted 500-2,000-fold and contained in a 4 mm-diameter AZ4 cell. The zeta potential of the system under consideration is almost zero (3 ± 7 mV), as was to be expected from the nature and the geometry of PL90H at the interface. It has been shown [31, 32] that the phosphatidylcholine head group is almost parallel to the surface of the droplet. As a result, the positive and negative charges of the zwitterionic molecules (phosphatidylcholine is a zwitterion at pHs higher than 3) cancel each other to yield a zero net charge at the surface of the droplet. A similar result was found by Washington et al. [33], who investigated soya oil/dipalmitoylphosphatidylcholine (DPPC)/water emulsions and found a zeta potential of -1 mV. The systems studied by Washington et al. were used for parenteral nutrition and were the object of intensive investigation. It was shown, in particular, that flocculation could be prevented by the addition of a negatively charged surfactant to the pure primary zwitterionic surfactant DPPC. This negatively charged surfactant disturbs the array of negative and positive charges of DPPC that yielded a zero net charge at the surface of the droplets, and yields a net negative zeta potential that in turn, through the increase in electrostatic repulsive forces, prevents flocculation [34, 35, 36, 37, 38, 39]. To check this theory two emulsions of perflubron in saline were prepared using PL90H as a primary surfactant and doping it with a negatively charged surfactant (cholesterol hemisuccinate, CHS) or with a positively charged surfactant (stearylamine, SA). First, the effect of SA and CHS on the film of PL90H was investigated through surface isotherm measurement (Figures III-6a,b and III-7a,b): both films still show a high collapse pressure, high surface potential throughout the compression, and reversible compression. The

PL90H film is therefore not destabilized by the addition of CHS or SA, and still provides a good structure at the perflubron/saline interface. The zeta potentials of the resulting emulsions were found to be comparable in magnitude but, of course, opposite in sign:

CHS system: perflubron/PL90H:CHS (9:1, mol:mol)/saline: -14 ± 6 mV

SA system: perflubron/PL90H:SA (9:1, mol:mol)/saline: $+17 \pm 7$ mV

The emulsions showed dramatic difference in terms of stability. Direct observation of the SA system showed settling of a viscous phase at the bottom of the vial characteristic of a flocculated system, and flocculation was confirmed by particle size measurements (600 nm when the system is diluted in saline and 330 nm when it is diluted in water) and viscoelasticity measurements (see Figure III-8: the magnitude of both G' and G" is higher than for the reference system, while decreasing with increasing shear strain). The magnitude of the flocculation is not as large as that of the pure PL90H system, however (less settling, smaller flocs, and lower magnitude for G' and G"). The CHS system showed much better results in terms of stability: only a very small amount of (easily reversible) settling was observable (comparable to what occurred in the reference system), the particle size was the same (300 nm) regardless of the diluting medium, and the viscoelasticity parameters were those of a non-flocculated system (see Figure III-9: the value of G" is constant with increasing shear strain and its magnitude is comparable to that of the reference system, while G' is below noise level). The CHS and SA systems have zeta potentials of comparable magnitude but show different degrees of stability: a negatively charged interface prevents flocculation more efficiently than a positively charged one (using dicetylphosphate (DCP), a negatively charged surfactant, instead of CHS yielded an emulsion that did

not flocculate either). Electrostatic repulsion forces alone could not justify this observation. Washington [40] reached the same conclusions, and mentioned the effect of "hydration forces" on the stability of fat emulsions. We have seen in Chapter III.1.b that flocculation could be prevented both through an increase in the electrostatic repulsive forces and through a decrease in the van der Waals attractive forces. In particular, the more the surface is hydrated, the smaller the van der Waals-Hamaker constant and the smaller the attractive force potential between two droplets. We have seen as well that a charged interface is surrounded by a diffuse double layer, a positively charged interface being surrounded by negative counterions and a negatively charged interface by positive counterions. That positive counterions can be more hydrated than negative counterions explains why a negative interface is more efficient in preventing flocculation. Stability with respect to flocculation is provided by a combination of both electrostatic and hydration repulsive forces: although a negatively charged and a positively charged interface yield zeta potentials with the same order of magnitude but opposite signs (and therefore the same electrostatic repulsive forces), the hydration shell provided by the positive counterions surrounding the negatively charged interface is larger, and therefore will prevent flocculation better than the hydration shell provided by the negative counterions surrounding the positively charged interface. That hydration forces can participate in preventing flocculation was confirmed by preparing an emulsion where electrostatic repulsion forces are minimal (using PL90H alone, which yields a near-zero zeta potential) both in water and in a saccharide solution. (Various researchers have studied the effect of saccharides on emulsion stability [41, 42, 43]. In particular, Hauser et al. [44, 45] showed that the sugar can probably be

adsorbed on the head group of the phospholipids (hydrogen bonding) and therefore play the part of the water of hydration (in any event, saccharide molecules can be very hydrated themselves).) As expected, perflubron/PL90H/water emulsions flocculate immediately as evidenced by a large thick gel-like phase at the bottom of the vial. The effect of sucrose in the second emulsion was to limit flocculation significantly: some settling, easily reversible, was observed, the particle size was slightly larger when the emulsion was diluted in the sucrose solution than when it was diluted in water (450nm and 300 nm respectively), and the viscoelastic parameters of the emulsion were very comparable to those of the perflubron/EYP/saline emulsion (see Figure III-10: low magnitude for G' and G", and a decrease in G' and G" as the shear strain increases).

III.5. CONCLUSIONS

Flocculation resulting from attractive forces can be prevented by the combined effects of electrostatic and hydration repulsive forces. Systems prepared with PL90H and a negatively charged additive (such as CHS) and/or an additive capable of providing a strong hydration shell around the emulsion droplet, provided that these additives yield a mixed film with PL90H but do not affect the film's molecular packing, offer a convenient model for understanding EYP systems. It is now possible to propose an explanation of why the perflubron/EYP/saline system is stable with respect to flocculation and coalescence.

EYP have a balanced composition: (a) the major components (phosphatidylcholine, phosphatidylethanolamine, cholesterol) provide a well-organized structure at the perflubron/saline interface, one capable of

standing stress without losing its integrity; and (b) some minor components prevent flocculation (a necessary first step for emulsion coalescence), both by providing electrostatic repulsive forces combined with a hydration layer, as we have seen above (i.e., acidic phospholipids such as phosphatidylserine and phosphatidylglycerol), and by providing a strong hydration shell directly (i.e., phosphatidylinositol, whose saccharide head group, inositol, can be highly hydrated) [46, 47, 48]. The difference in terms of stability between EYP systems and saturated phosphatidylcholine systems has been investigated quantitatively [49]: it has been shown that the hydration repulsive forces decay exponentially with separation between bilayers and that the decay constant for liquid-crystalline EYP was larger than that for the gel-state DPPC (respectively 1.7Å and 1.4Å)

Unfortunately, having the "right" formulation, one yielding an injectable emulsion that does not flocculate and does not coalesce over a period of more than a year, is not enough to make the emulsion a success. Once injected into the blood stream of a (human) patient, the emulsion is in a totally new environment. In particular, it was noticed that the density of the liver and the spleen of the patient increased tremendously a few hours after the injection: the droplets of the emulsion are being recognized as invaders by the immune system and stored in the spleen and the liver, where they are rapidly attacked and destroyed by macrophages. The success of the emulsion as a respiratory gas carrier depends upon its residence time in the circulatory system. The next step, after the physico-chemistry of the emulsion on the shelf is understood, is to investigate how the emulsion interacts with the (human) blood, and to learn how to prevent

the droplets from being recognized by the immune system and thus how to increase the residence time. This will be the subject of the next chapter.

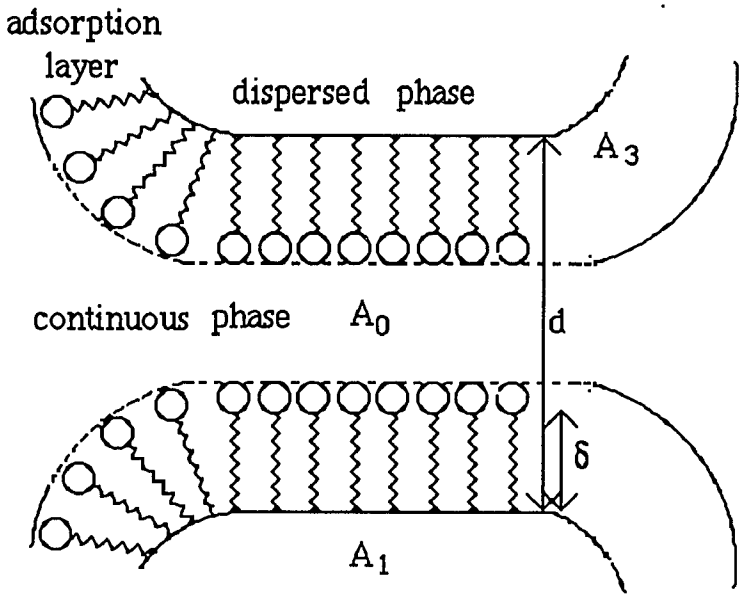

Figure III-1: schematic diagram of the dispersion interaction of plate-shaped particles with oriented adsorption layers in an aqueous solution (after [50])

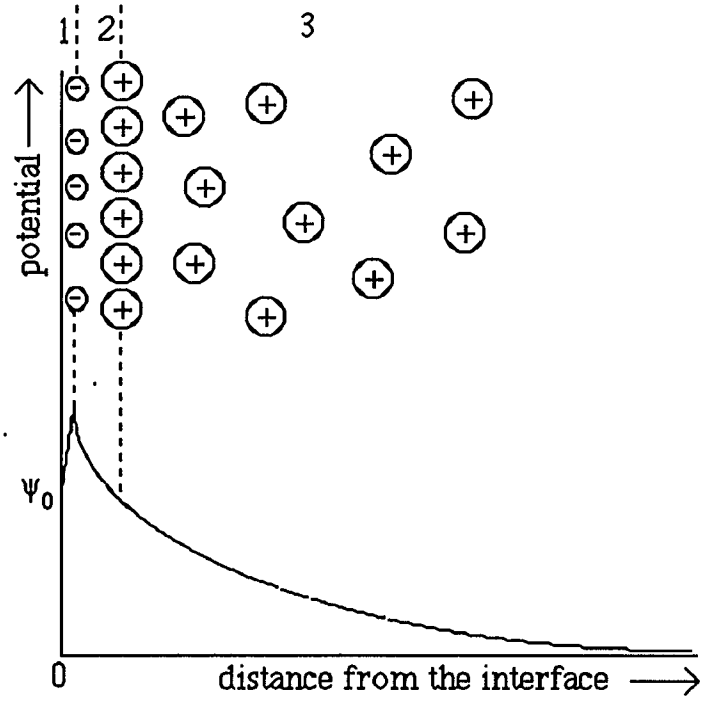

1 = specifically adsorbed dehydrated ions (inner Helmholtz layer)
2 = outer Helmholtz or Stern layer
3 = diffuse electrical double layer

Figure III-2: the electrical diffuse double layer

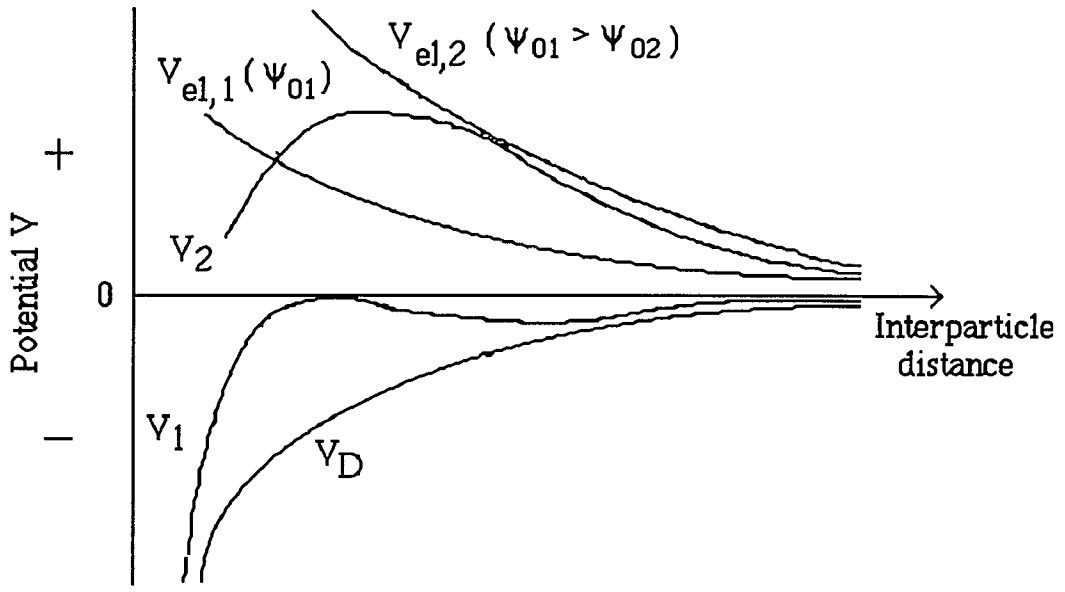

Figure III-3: potential energy of interaction versus interparticle distances

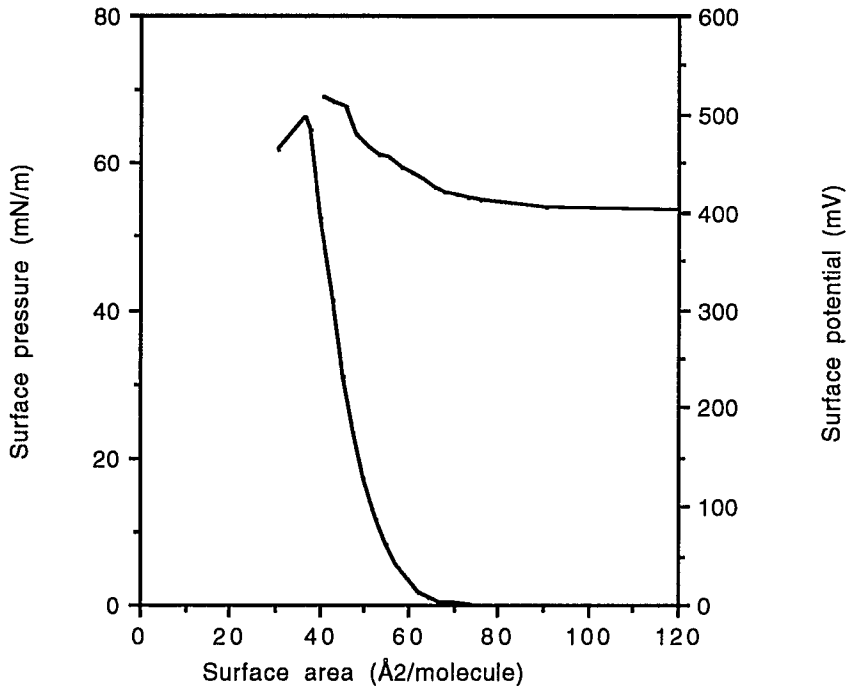

Figure III-4a: surface pressure and surface potential isotherms of PL90H on saline at pH 6.8 and 25°C

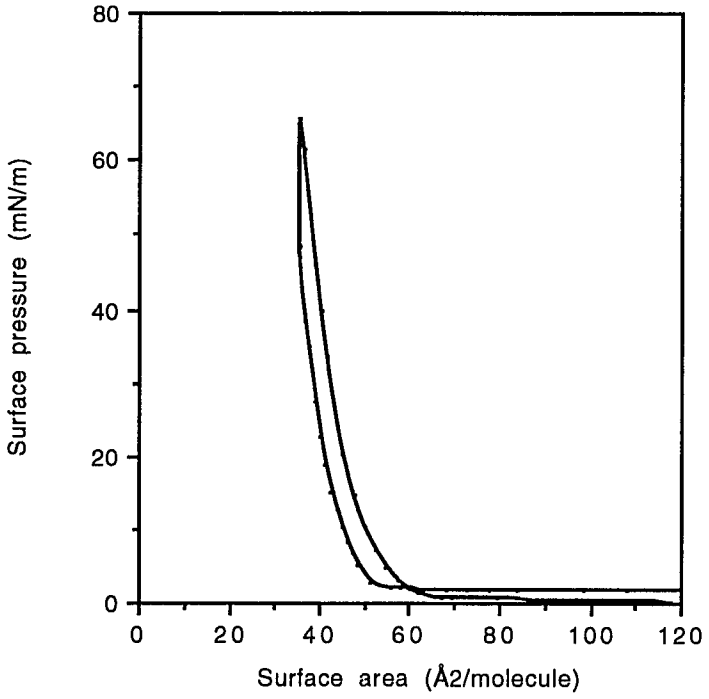

Figure III-4b: surface pressure isotherms (compression/decompression) of PL90H on saline at pH 6.8 and 25°C

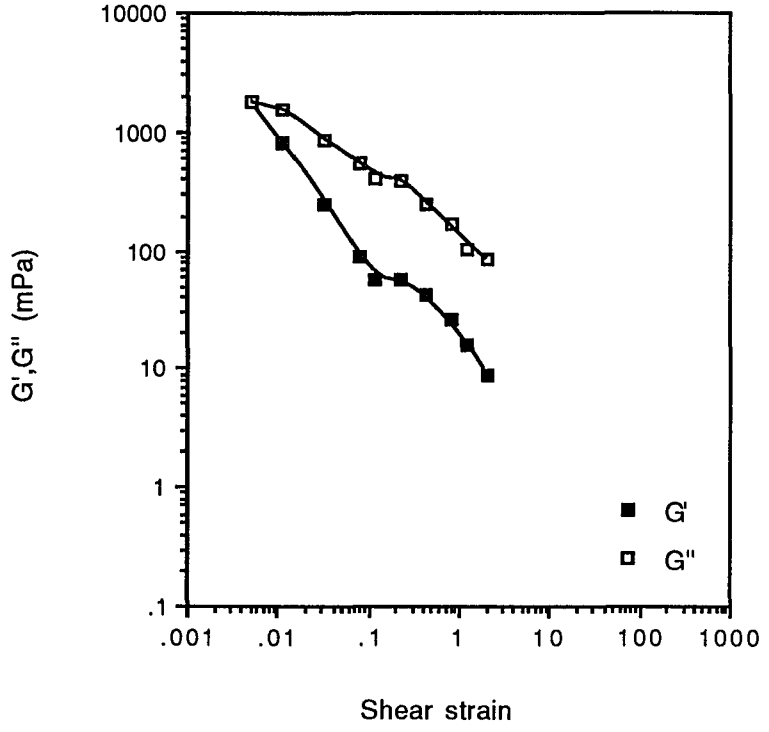

Figure III-5: viscous and elastic moduli (G", G') versus shear strain for a perflubron/PL90H/saline emulsion

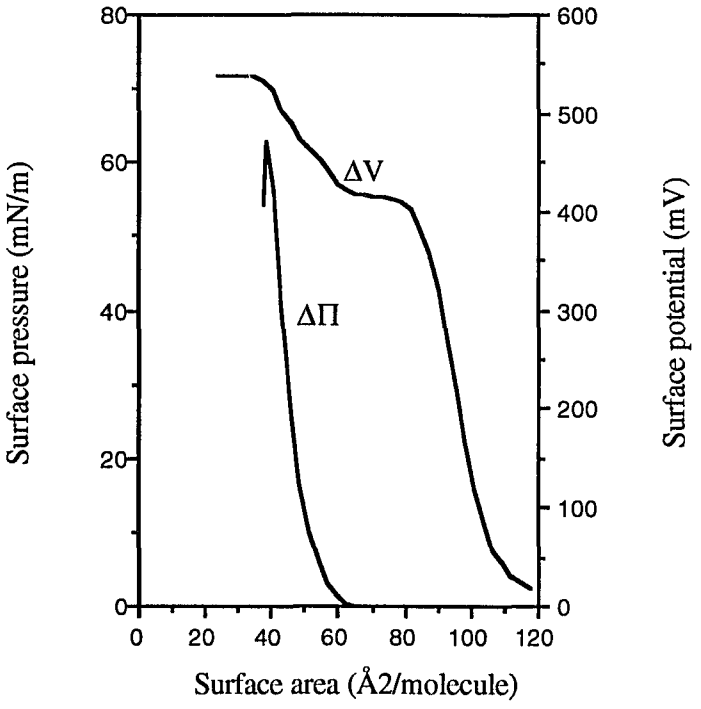

Figure III-6a: surface pressure and surface potential isotherms of PL90H:CHS (9:1 mol:mol) on saline at pH 6.8 and 25°C

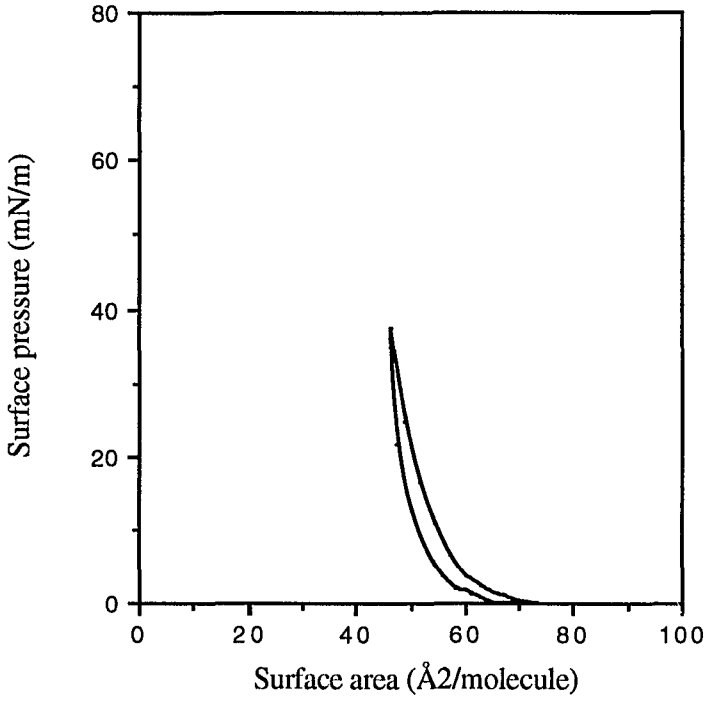

Figure III-6b: surface pressure isotherms (compression/decompression) of PL90H:CHS (9:1 mol:mol) on saline at pH 6.8 and 25°C

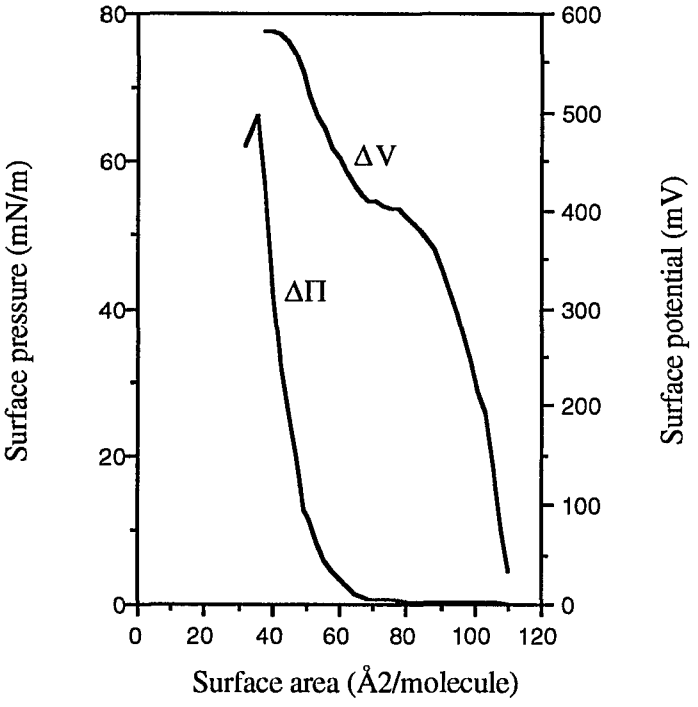

Figure III-7a: surface pressure and surface potential isotherms of PL90H:SA (9:1 mol:mol) on saline at pH 6.8 and 25°C

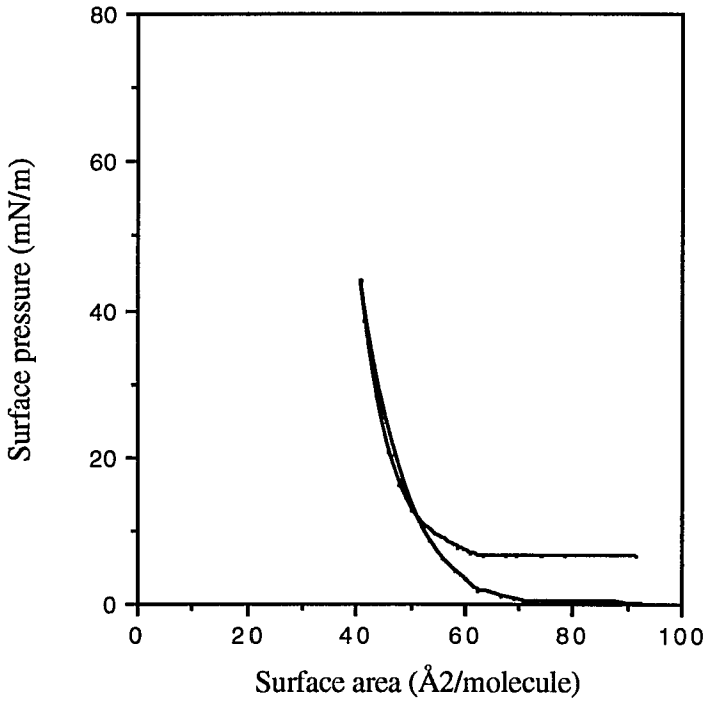

Figure III-7b: surface pressure isotherms (compression/decompression) of PL90H:SA (9:1 mol:mol) on saline at pH 6.8 and 25°C

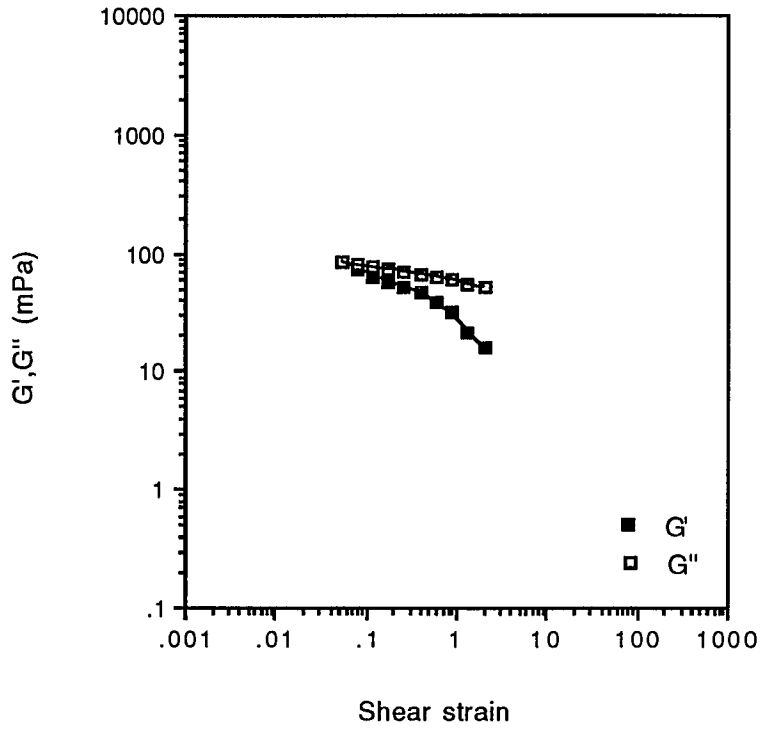

Figure III-8: viscous and elastic moduli (G", G') versus shear strain for a perflubron/PL90H:SA (9:1 mol:mol)/saline emulsion

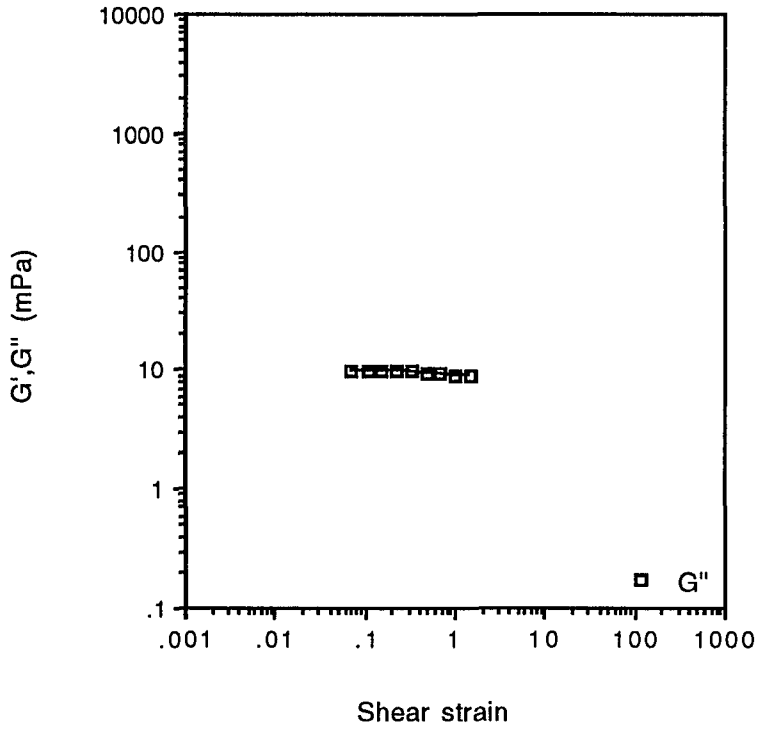

Figure III-9: viscous and elastic moduli (G", G') versus shear strain for a perflubron/PL90H:CHS (9:1 mol:mol)/saline emulsion

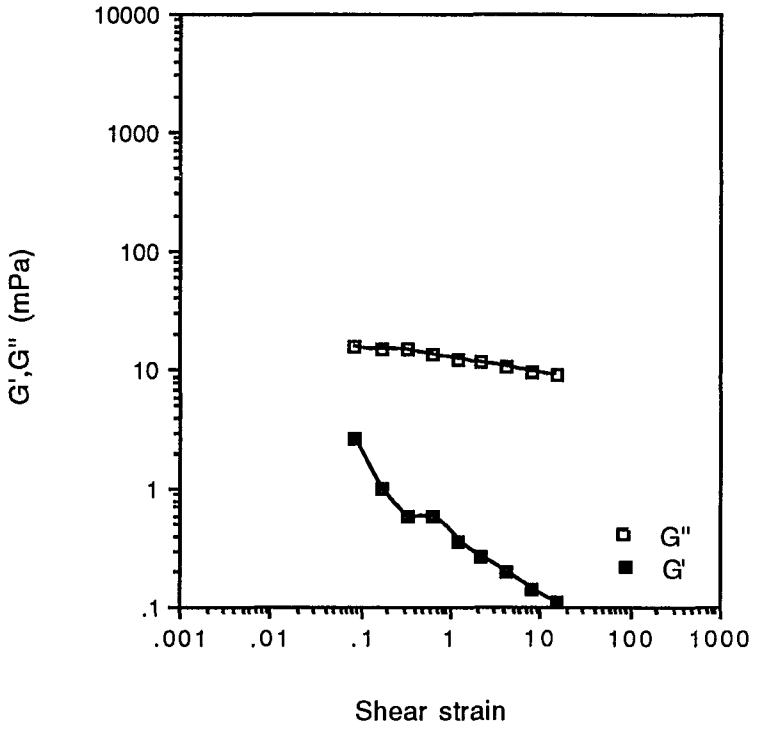

Figure III-10: viscous and elastic moduli (G", G') versus shear strain for a perflubron/PL90H/9.5% sucrose solution emulsion

CHAPTER IV

EMULSIONS WITH INCREASED RESIDENCE TIME IN THE CIRCULATORY SYSTEM

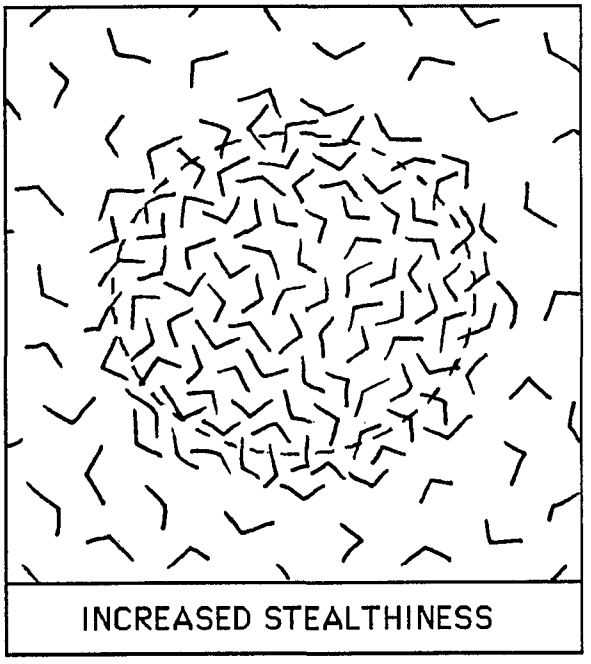

IV. EMULSIONS WITH INCREASED RESIDENCE TIME IN THE CIRCULATORY SYSTEM

IV.1. THE PROBLEM

As stated in the previous chapter, the efficacy of a respiratory gas carrier depends not only on the volume of gases that can be transported (this should be enough to oxygenate the vital tissues and to clear them of carbon dioxide) but on the residence time in the circulatory system as well. Perflubron/EYP/saline emulsions are cleared from the circulatory system in five to six hours. This is the result of a rapid uptake into the reticuloendothelial system, which is made of mononuclear phagocytes located principally in the liver (Kupffer cells) and the spleen (fixed macrophages) [1]. Injection in human patients yielded an increased density of both the liver and the spleen due to storage of the emulsion droplets (the density of perflubron is 1.93 g/ml). Ultimately, the droplets will be digested by the macrophages and the perflubron exhaled through the lungs. It was originally argued that the residence time in the circulatory system was a matter of droplet size: the smaller the droplets, the less likely they are to be stuck in the spleen and the liver, and Rosano and Gerbacia [2] first suggested preparing microemulsions of PFC (the particle size is smaller than 100Å). To make microemulsions requires high concentrations of a surfactant with specific properties (EYP cannot yield microemulsions, for example); the biocompatibility of such a surfactant has not yet been proven. The issue of efficacy was also raised, since microemulsions have low dispersed phase (PFC) concentration . Since then, the issue of particle size has been reconsidered, since even small liposomes are stored in the liver and spleen [1]. Other factors seem to play an important part in the

tendency of a system to follow this scenario (clearance from the circulatory system and storage in liver and spleen): (a) the composition of the surfactant layer (the closer it is to the composition of the red blood cell membrane, the longer the residence time [1]); (b) its rigidity (the more rigid, the longer the residence time [3, 4, 5, 6, 7]); (c) the packing of the surfactant molecules at the interface (a tight packing interferes with the interactions between the surface of the droplet and the surface proteins of macrophages; these surface proteins play a central role in the binding of the droplets to the macrophages [8]); (d) the charge of the interface (a negatively charged interface increases the residence time [1, 9]); and (e) the hydrophilicity of the surface of the droplets (the more hydrophilic the surface of the droplets, the longer the residence time [10, 11]).

The approach chosen to increase the residence time in the circulatory system was not to try to mimic exactly the composition of the red blood cell bilayer (very complex and varied) or to make the binding between the target cells (macrophages) and the emulsion droplets difficult, but to "hide" the emulsion droplets from the target cells. It is possible to increase the "stealthiness" of the emulsion droplets by making it possible for the droplets to be surrounded by a thick layer of hydrated molecules: the droplet surface will be buried under the water layer and the target cells will be unable to distinguish between the water molecules of the plasma and the water molecules surrounding the droplets. For that it is necessary to include in the formulation of the interface a molecule that will not disturb the packing of the PL90H or EYP film, that will provide a strong shell of hydration, and that will be injectable. We will see in the next chapter that ethoxylated cholesterol meets all three criteria.

IV.2. ETHOXYLATED CHOLESTEROL (CnEO)

As stated before, the molecule that will bear the highly hydrated group must be compatible with the phospholipids of the already existing surfactant layer. A polyoxyethylene group is an injectable compound (nonionic, therefore nonhemolytic) that can be highly hydrated (depending on the number of oxyethylene groups). Unfortunately, it is not compatible with the phospholipid layer, and adsorption alone will reduce the efficacy of the molecule once the emulsion is injected (the adsorbed molecules might desorb and lose their capacity to hydrate the droplet surface once the emulsion is diluted in the blood stream). Cholesterol is a molecule known for its compatibility with phospholipids: it is a natural constituent of biological membranes and, in the case of EYP, it is known to increase the rigidity of the membrane (at 37°C, the human body temperature, EYP are in the gel phase), which is one of the key factors increasing residence time in the circulatory system. The idea is to bond the polyoxyethylene group to the cholesterol molecule so that the hydrated molecule will be well anchored in the surfactant layer of the droplet. The resulting molecule is polyoxyethylene cholesteryl ether, or ethoxylated cholesterol (CnEO, $C_{27}H_{45}(OCH_2CH_2)_nOH$ (n = 5, 20), see Figure V-1). CnEO was synthesized by Croda Inc. (North American Technical Center, Edison, NJ) and used with no further purification.

These compounds have been shown to be nonhemolytic [12] and, when used alone, to form efficient rigid nonphospholipid liposomes, usable as drug delivery systems [13]. Surface isotherm measurements show that they do not disturb the packing of the PL90H and EYP films (Figures IV-2 and IV-3). Note that the ethoxylated cholesterol expands the film of

PL90H considerably through the combined effects of the cholesterol in the membrane (cholesterol increases the fluidity of a film below its phase transition temperature) and of the bulky, hydrated polar head groups under the surface of the film. The next step is to study the stability of an emulsion of perflubron in saline using a mixture of PL90H and CnEO as a surfactant.

IV.3. STABILITY OF PERFLUBRON/PL90H-CnEO/SALINE EMULSIONS

Four systems were prepared, with the following formulations:

1: perflubron/PL90H:C20EO (9:1, mol:mol)/saline

2: perflubron/PL90H:C5EO (9:1, mol:mol)/saline

3: perflubron/PL90H:CHS:C20EO (18:1:1, mol:mol:mol)/saline

4: perflubron/PL90H:CHS:C20EO (8:1:1, mol:mol:mol)/saline

Direct observation showed viscous systems at room temperature for all formulations under investigation. No separation of a viscous gel-like phase at the bottom of the vial was visible, however. Analysis of the particle size through PCS did not show any flocculation (Figure IV-4): the particle size for all systems was the same (within the error of the experiment) regardless of the dilution medium. It seems that the system is rendered viscous by the polyoxyethylene chains, which, when hydrated, are responsible for steric hindrance that prevents the droplets from flowing against one another. A peculiarity of these long polyethoxylated chains is their degree of hydration with respect to temperature: under a critical temperature (the cloud point), the chains are highly hydrated, and above the cloud point, they are dehydrated [14]. (Some other authors argue that

it is a question, not of hydration/dehydration, but rather of orientation of the water molecules on the polyethoxylated chains.) Regardless of the molecular explanation, the steric hindrance is maximum below the cloud point and minimum above the cloud point. It was shown that the cloud point for the polyoxyethylene chains was around 40°C for a wide range of chain lengths (5- and 20-ethoxylated groups fall within that range). The viscoelastic parameters of two systems (perflubron/ PL90H:CHS:C5EO (18:1:1) / saline and perflubron / PL90H:CHS:C20EO (18:1:1) / saline) were studied below and above the cloud point (Figures IV-5, IV-6). For both systems, below the cloud point the viscous modulus G" and the elastic modulus G' decrease as the shear strain increases and the magnitudes of G' and G" are much larger than for the reference perflubron/EYP/saline system. We have seen that this could be evidence of flocculation, but measurement of the particle sizes below cloud point showed that the system was not flocculated. The large viscous and elastic moduli below the cloud point are probably due to a deployment and interdigitation of the ethoxylated chains creating a gel-like viscous three-dimensional network capable of storing energy (Figure IV-7: very little free water between the droplets, with no facilitating effect on the flow of the droplets). As the strain is increased, the long ethoxylated chains align themselves with the flow, which results in a lowering of both G' and G". Above the cloud point, the viscous modulus, although still large, is constant as the shear strain increases, and no or very little elastic modulus is detectable: the ethoxylated chains, whether these are dehydrated or the water molecules are flattened, can be flat on the surface of the droplet and do not form the gel-like three-dimensional network that impairs the flow of the droplets and allows some elastic energy to be stored. The fact that, even above the

cloud point, the system is still very viscous (and thus not suitable for intravenous injection) is probably due to the fact that the system is very concentrated--which suggests that the concentration in CnEO should be adjusted. It should be observed that trials have been made at Alliance Pharmaceutical Corp. using EYP instead of PL90H (Alliance's facilities permit work under nitrogen) and that the viscosity of the resulting system was very acceptable for injection. The Alliance researchers, using the sedimentation field flow fractionation technique, also showed that the CnEO was well mixed with the EYP and that there were not two kinds of perflubron-filled droplets, one with EYP as a surfactant and one with CnEO, but one (we have seen that CnEO alone is capable of forming rigid vesicles).

IV.4. CONCLUSIONS

The results presented above are very promising, and it seems that the addition of CnEO to EYP permits the preparation of very stable systems. The toxicity of these systems is being studied, and there is great hope not only that these systems will be injectable (preliminary tests were positive) but that they will have a longer residence time in the circulatory system.

In addition, the fact that the viscosity of the emulsion is a function of temperature could help solve a shipment problem: it has been noticed that the shaking experienced during shipment of the emulsions could promote coalescence. Shipping the emulsions at a temperature below the cloud point, where the system is very viscous, could prevent the droplets from bumping into one another and therefore prevent coalescence.

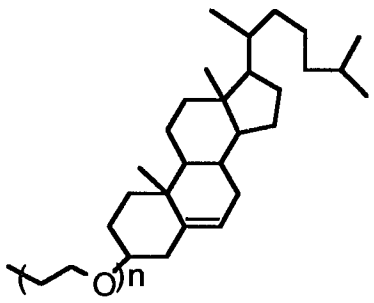

$C_{27}H_{45}(OCH_2CH_2)_nOH$ (n = 5, 20)

Figure IV-1: structure and formula of cholesterol ethoxylated (CnEO)

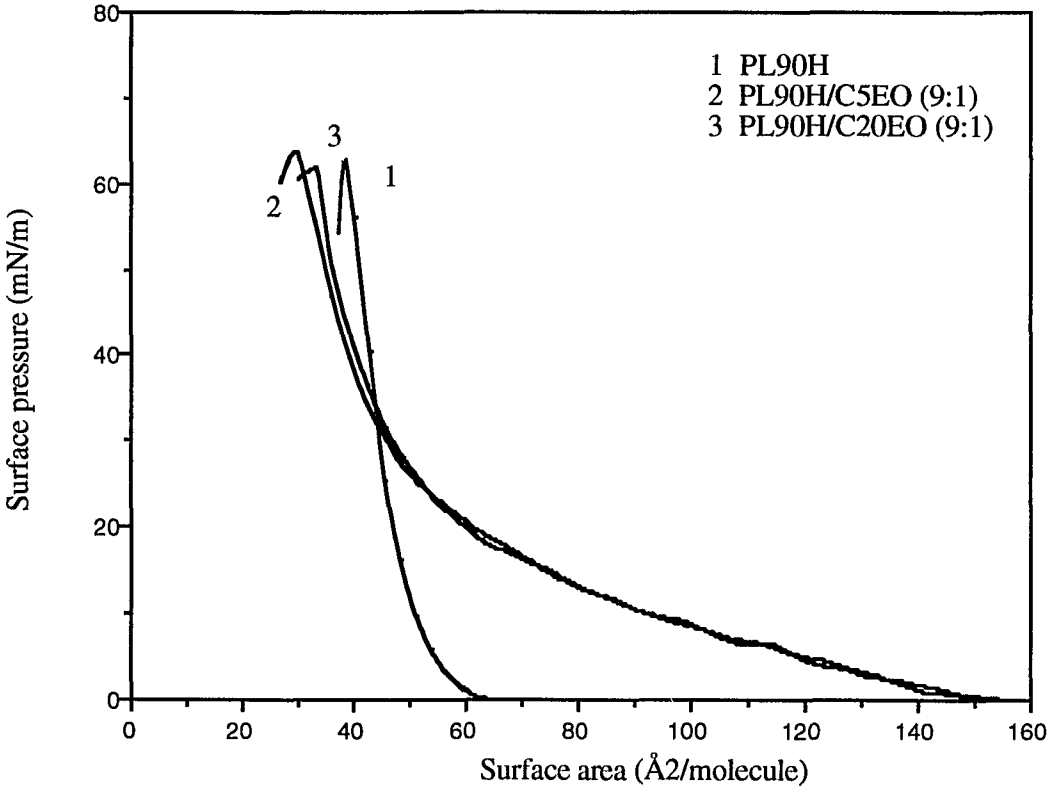

Figure IV-2: surface pressure isotherms for two PL90H/CnEO mixtures on saline at pH 6.8 and 25°C

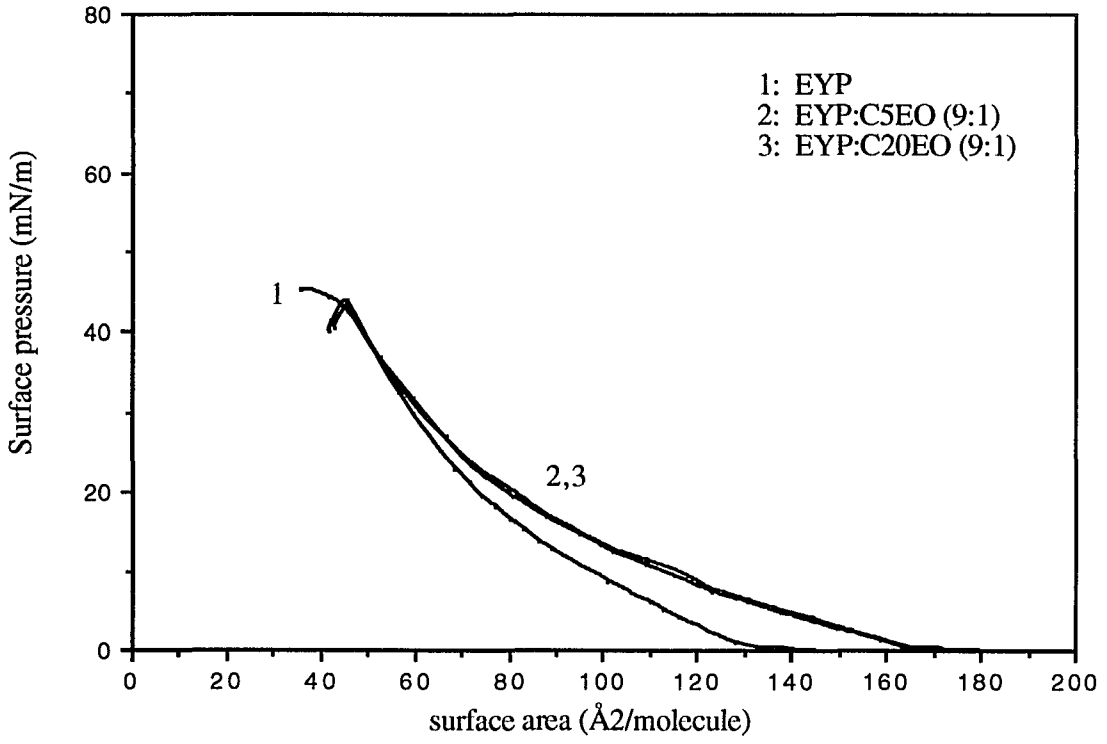

Figure IV-3: surface pressure isotherms for two EYP/CnEO mixtures on saline at pH 6.8 and 25°C

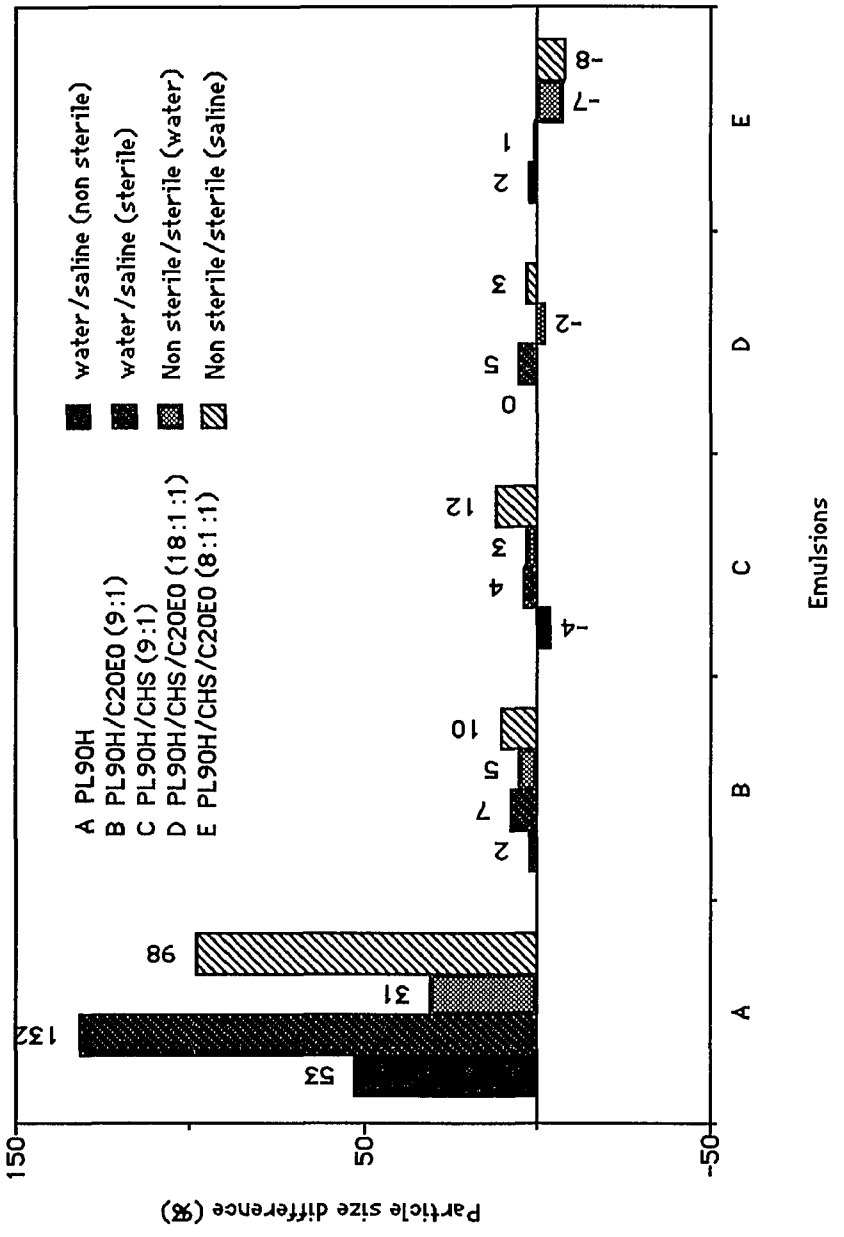

Figure IV-4: particle size difference for emulsions diluted in water or in saline and sterile or nonsterile (at 25°C)

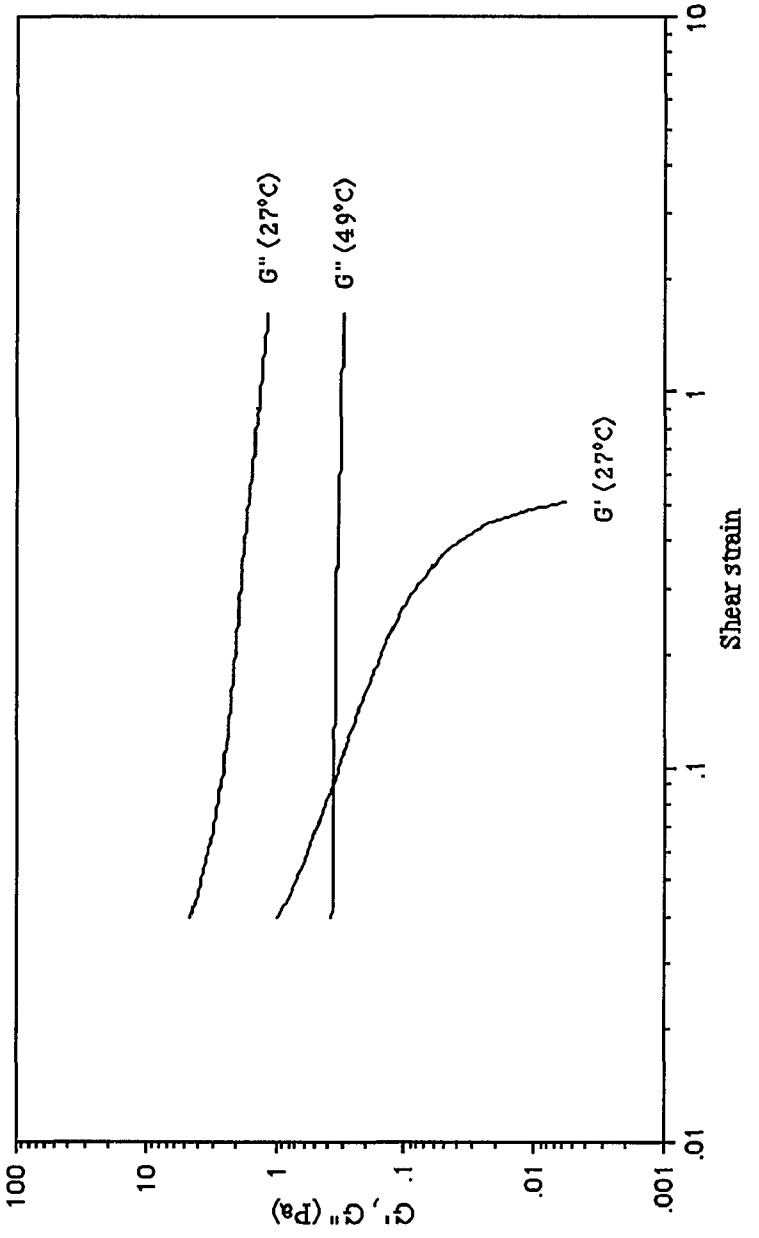

Figure IV-5: viscous and elastic moduli (G", G') versus shear strain for a perflubron/PL90H:C5EO (9:1 mol:mol)/saline emulsion below and above the cloud point

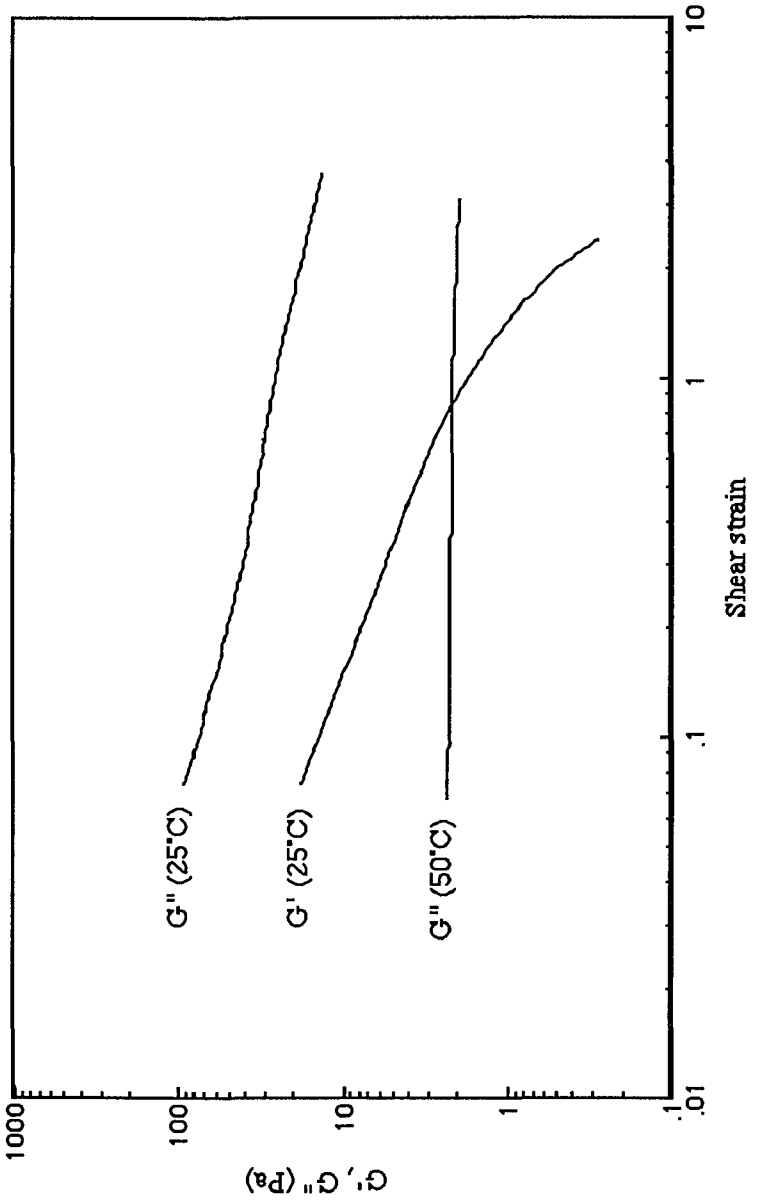

Figure IV-6: viscous and elastic moduli (G", G') versus shear strain for a perflubron/PL90H:C20EO (9:1 mol:mol)/saline emulsion below and above the cloud point

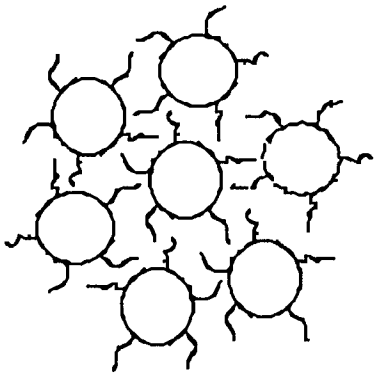

Below the cloud point:
The polyoxyethylene chains are highly hydrated

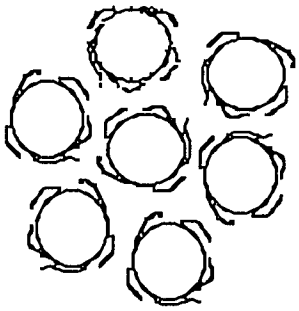

Above the cloud point:
The polyoxyethylene chains are less hydrated

Figure IV-7: arrangement of the ethoxylated chains below and above the cloud point

CHAPTER V

A MODEL OF MICRO- AND FINE EMULSION FORMATION

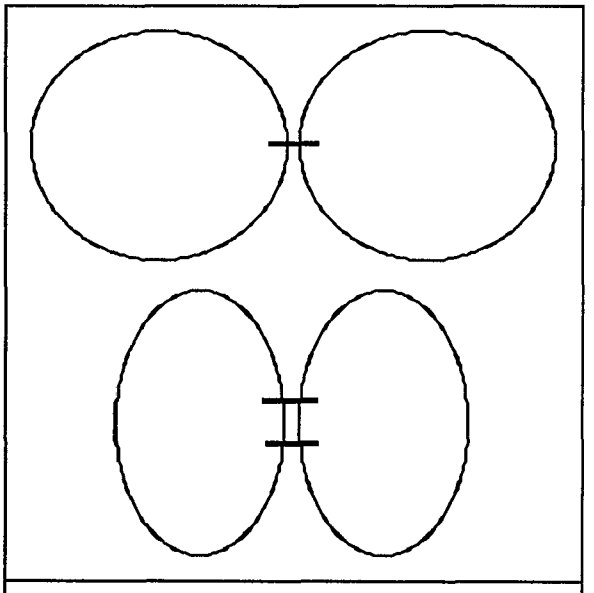

LAPLACE PRESSURE EFFECT

V. A MODEL OF MICRO- AND FINE EMULSION FORMATION

V.1. INTRODUCTION

V.1.a. Characteristics common to micro- and fine emulsions

Our emulsion systems all involve three or more components: a hydrophobic component ("oil"), a hydrophilic component ("water"), and one or more surfactants. The mathematical model of emulsion formation developed in this dissertation takes into consideration the following characteristics common to micro- and fine emulsions:

1. The surfactant or surfactants are required (a) to reduce the interfacial free energy and facilitate the formation of the interface, and (b) to provide an interfacial film capable of ensuring dispersion stability.

2. Lowering of the interfacial free energy is beneficial during emulsion formation, but, at equilibrium, the interfacial free energy cannot be lower than a certain critical value if we are to obtain the curling of the interface that gives rise to the droplets.

3. The decrease in droplet size that accompanies the increase in the number of surfactant molecules required is limited to a value R_0, the natural radius of curvature of the interface.

4. During the preparation of the dispersion, as we increase the volume of the dispersed phase, we pass from a monodispersed system (with low dispersed phase volume) to a polydispersed system (with a dispersed phase volume larger than a limiting volume beyond which, in the case of

microemulsion systems, percolation occurs [1, 2, 3]) and finally, at even higher dispersed phase volumes, to phase separation, phase inversion, or equilibrium with the excess dispersed phase.

V.1.b. Importance of interface rigidity

Rosano [4] developed a formula for calculating the amount of surfactant needed to emulsify a certain volume V of dispersed phase. Assuming that all the surfactant molecules end up at the interface, we have

$$R = \frac{3V}{n\sigma} \qquad (1)$$

where

R = radius of a droplet [nm]
V = volume of the dispersed phase [nm^3]
n = number of surfactant molecules
σ = cross-sectional area of a surfactant molecule [nm^2/molecule]

But experimental results [5] show that, above a certain concentration of surfactant molecules, rather than a smooth transition to smaller particle sizes, we observe a phenomenon of creamage due to reversible flocculation by free surfactant. The maximum value of n before creamage occurs, plugged into Equation 1, yields the value R_0, the natural radius of curvature of the interface. This value, R_0, represents the particular radius of curvature at which (in the absence of other forces acting on the system) the structure of a given surfactant molecule and the three-dimensional structure of the interface together result in steric constraints that prevent

the adsorption of additional surfactant molecules at the interface [6]. The excess surfactant molecules then form micelles in the solvent phase that may foster the instability of the emulsion [5].

It is thus important to develop a model taking into account not only the interfacial free energy but also a term relative to the three-dimensional structure of the interface, namely K_R, the rigidity of the interface.

V.2. PREVIOUS MODEL AND ITS LIMITATIONS

V.2.a. The Chan-Rosano model

In a recent paper, Chan and Rosano [7] developed a mathematical model for the formation of oil-in-water microemulsions, one based on the various components of the difference in total free energy of the system, G, before and after emulsification.

We have

$$G = NG_T$$

where

G_T = total free energy of formation of a droplet
N = total number of droplets

Then,

(2) $$G_T = G_{SH} + G_A + G_B + G_I$$

where

G_T = total free energy of formation of a droplet [J]

G_{SH} = free energy of formation of the interfacial sheath structure [J]

G_A = work required to expand the interface [J]

G_B = interfacial bending energy [J]

G_I = free energy of interaction between droplets [J]

Working out these different terms of free energy, Rosano et al. found:

$$G_T = -\varepsilon\frac{4}{3}\Pi R^3\Delta G_M + 4\Pi R^2\left[\gamma_I + \frac{K_R}{2}\left(\frac{1}{R}-\frac{1}{R_0}\right)^2\right] \quad (3)$$
$$+16\Pi^2 K_R\left(\frac{R-R_{min}}{R_{min}}\right)^2\left(\frac{R-R_{max}}{R_{max}}\right)^2$$

where

ΔG_M is the free energy of formation of the interfacial sheath structure, in joules per cubic meter of interface. We consider that the interface is an ideal mixture of octane and dodecane (50:50 mole:mole). The free energy of mixing is then calculated to be 9 x 10^6 J/m^3.

ε is a correction factor representing the fraction volume of the interface relative to the total volume of the droplet. If we assume that, for microemulsions (R_0 = 9nm), the thickness of the interface represents 60% of the radius of the droplet, the volume of the interface will be the total volume of the droplet, corrected by ε = 0.94.

R is the radius of the microemulsion droplets [nm]

γ_I is the interfacial free energy [N/m]

R_0 is the natural radius of curvature of the interface [m]

K_R is the rigidity constant of the interfacial sheath [J]

R_{min} is the radius of the smallest droplet that can be found in a stable emulsion, for a given value of the rigidity constant K_R [m]

R_{max} is the radius of the largest droplet that can be found in a stable emulsion, for a given value of the rigidity constant K_R [m]

Our determination of K_R, R_{min}, and R_{max} is based on a separate consideration of G_{TS}, the total free energy per droplet assuming no droplet interaction--which means omitting G_I from G_T . If we plot G_{TS} versus R at various K_R for a given set of R_0, ΔG_M, and γ_I (see Figure V-1), we can make the following observations:

1. K_R can only vary between two limits, K_{Rmin}, under which the curves exhibit no minimum (the energy decreases asymptotically and the system is not stable), and K_{Rmax}, above which the maximum of the curve is so highly positive that only a narrow window of possible radii remains, in contrast to the commonly observed polydispersity.

2. For a satisfactory value of K_R we are very unlikely to observe droplets of radii smaller than the radius corresponding to the first optimum of the curve (minimum) or larger than the radius corresponding to the second optimum of the curve (maximum). This last observation leads us to identify these two optima as R_{min} and R_{max}, respectively.

G_{TS} was a satisfactory approach to the free energy of formation of a droplet until the phenomenon of percolation was observed [2]. At that point, it was necessary to consider a term relative to the energy cost of the fusion between two droplets--namely G_I. As just noted, the radii of the smallest and the largest droplets that can interact are respectively R_{min} and R_{max}. The interaction between two droplets of radii R_1 and R_2 involves only work against the deformation of the interface occurring when the droplets coalesce. G_I is then approximated by the product of the rigidity constant of the interface K_R and the product of the relative increases in surface area when the droplets fuse. An exact if tedious way to compute this energy contribution would be to consider all the possible two-droplet encounters resulting in a droplet of radius R, and to average the energy contributions over all such encounters. Instead, we approximate this value by considering that this average can be expressed as the energy contribution of the encounter between the most probable droplet (droplet of radius R_{min}, heavily represented because it corresponds to the minimum in total free energy) and the least probable one (droplet of radius R_{max}, poorly represented because it corresponds to the maximum in total free energy). Comparison of Figures V-2 and V-3 reveals that G_I leads to a model that accounts for the experimental results related to polydispersity [8]. For given values of G_{SH}, γ_I, R_0, and K_R, the total energy of the system exhibits two minima, having comparable magnitudes and radii R_a and R_b, where R_b ranges in value from $1.8R_a$ to $2.2R_a$. So, for a particular set of parameters, the system will have two possible stable states, one with droplets of radius R_a and one with droplets of radius R_b, coexisting in the emulsion.

V.2.b. Limits of the model at low interfacial free energy

If we now consider that, for given values of G_{SH}, γ_I, and R_0, K_R varies slightly from one droplet to another due to different molecular configurations (the rigidity of the interface is related to its structure), we find that the system exhibits not two but a whole set of energy minima covering a range of radii, accounting for the experimentally observed polydispersity [8] (Figure V-2).

Keeping the rigidity K_R constant but varying the interfacial free energy γ_I between values as low as 0.01 mN/m and as high as 5 mN/m (Figure V-3), we observe (according to the Chan-Rosano model) that, whatever the interfacial free energy, the system exhibits two energy minima (comparable in magnitude and radius), which account for polydispersity and stability. But very low interfacial free energies have been experimentally proven to be detrimental to the stability of the microemulsion (type I to II or II to III transition [9,10]). As mentioned by Friberg et al. [11], a low interfacial free energy results in a low Laplace pressure ($P = 2\gamma/R$), and it is reasonable to conclude that the droplets, unable to maintain a regular spherical geometry, will have a tendency to flatten and thus to increase their surface of contact (Figure V-4b). The resulting coalescence of pairs of droplets leads to droplets whose Laplace pressure is half as great, since the radius is doubled during the coalescence and $P = 2\gamma/R$. It is easy to imagine that all of the droplets will coalesce rapidly, with a resultant phase separation, or formation of a bicontinuous phase: the emulsion is unstable. The same reasoning applies at high interfacial free energies, when the Laplace pressure is sufficiently high that the surface of contact between two droplets is too small to allow fusion

between them, resulting in a system that, if stable, does not experience percolation (Figure V-4a). Intermediate Laplace pressure values will characterize a system that is still stable above the percolation threshold, where coalescence is possible due to a high probability of encounters between droplets, but limited due to a moderate area of surface contact. Such a system breaks down upon further increase of the emulsified phase because of the greater probability of encounters of "doubled droplets" (resulting from the percolation of two droplets). The resultant low Laplace pressure leads rapidly to phase separation, as explained above (Figure V-5b).

V.3. IMPROVEMENT OF THE MODEL

Since the probability of interaction between two droplets, which depends on the Laplace pressure, is responsible for the stability of the emulsion, it seems reasonable to weight the fourth term of Equation 2, i.e., G_I, by a dimensionless factor reflecting the effect of the surfactant layer on the Laplace pressure. This factor is the ratio of the Laplace pressure (arising from the difference between pressures inside and outside the droplet) that is applied on the droplet in the presence of the surfactant film to that applied on it in the absence of surfactant. We call this factor L_p.

$$L_P = \frac{2\gamma_I / R}{2\gamma_{I,0} / R} = \frac{\gamma_I}{\gamma_{I,0}} \qquad (4)$$

where

γ_I = interfacial free energy of the interface with surfactant layer [N/m]

$\gamma_{I,0}$ = interfacial free energy of the bare interface [N/m]

Equation 2 can now be written

$$G_T = G_{SH} + G_A + G_B + L_p G_I, \tag{5}$$

and Equation 3 becomes

$$G_T = -\varepsilon \frac{4}{3} \Pi R^3 \Delta G_M + 4\Pi R^2 \left[\gamma_I + \frac{K_R}{2} \left(\frac{1}{R} - \frac{1}{R_0} \right)^2 \right] + 16\Pi^2 K_R \frac{\gamma_I}{\gamma_{I,0}} \left(\frac{R - R_{min}}{R_{min}} \right)^2 \left(\frac{R - R_{max}}{R_{max}} \right)^2 \tag{6}$$

If we analyze Figure V-5, which corresponds to the plot of Equation 6 for various values of interfacial free energies, we conclude that:

(1) At low interfacial free energy (0.01 mN/m), the total free energy exhibits two minima, but the second minimum occurs at a radius far greater than the radius corresponding to the first minimum (4,000 nm as against 13.6 nm) and at a free energy far smaller than the free energy of the first minimum (-6×10^{-7} J as against -0.4×10^{-17} J). The only physical significance of such a curve is that the system will be entirely in a state corresponding to the second minimum, and the radius value is too great to be realized physically in a droplet. The end result is thus a phase separation or a bicontinuous phase.

(2) At high interfacial free energy (10 mN/m), the radii are of physically realizable magnitude (13.6 nm and 32 nm), but the first minimum is much lower than the second, and the system will be entirely in a state corresponding to the first minimum. Note that, when R_0 = 9 nm, the second minimum rapidly becomes positive for relatively low values of the interfacial free energy (>2.5 mN/m) and the system is not stable for the corresponding value of the radius.

(3) At intermediate interfacial free energy (1.5 to 2 mN/m), both the radii and the magnitude of the total free energies at the minima are comparable; the system is stable and displays percolation, which accounts for the experimentally observed polydispersity.

Our latest model was developed using experimental data relative to microemulsions (R_0 = 9 nm). When a fine emulsion is considered (R_0 = 90 nm), the volume of a 4 nm thick interface represents 16% of the volume of a droplet. Provided the cohesion of the interface is high enough, the surfactant sheath will resolve into 90 nm droplets at a larger value of the rigidity constant than in the case of 9 nm droplets. It is interesting to note that, if we increase both the rigidity of the interface and the free energy of formation of the interface (which accounts for the cohesion of the resulting interface), the conclusions listed above remain valid for a fine emulsion, as shown in Figure V-6.

V.4. CONCLUSIONS

This model has the merit of being based on physico-chemical properties common to micro- and fine emulsions. The crucial system-determining roles played by two experimentally measurable properties [12]--interfacial free energy and rigidity of the interface--lead us to believe that further work, taking into account the effect of interparticle forces (Van der Waals, hydration, and electrostatic forces) along these lines will facilitate prediction of emulsion stability based on these properties.

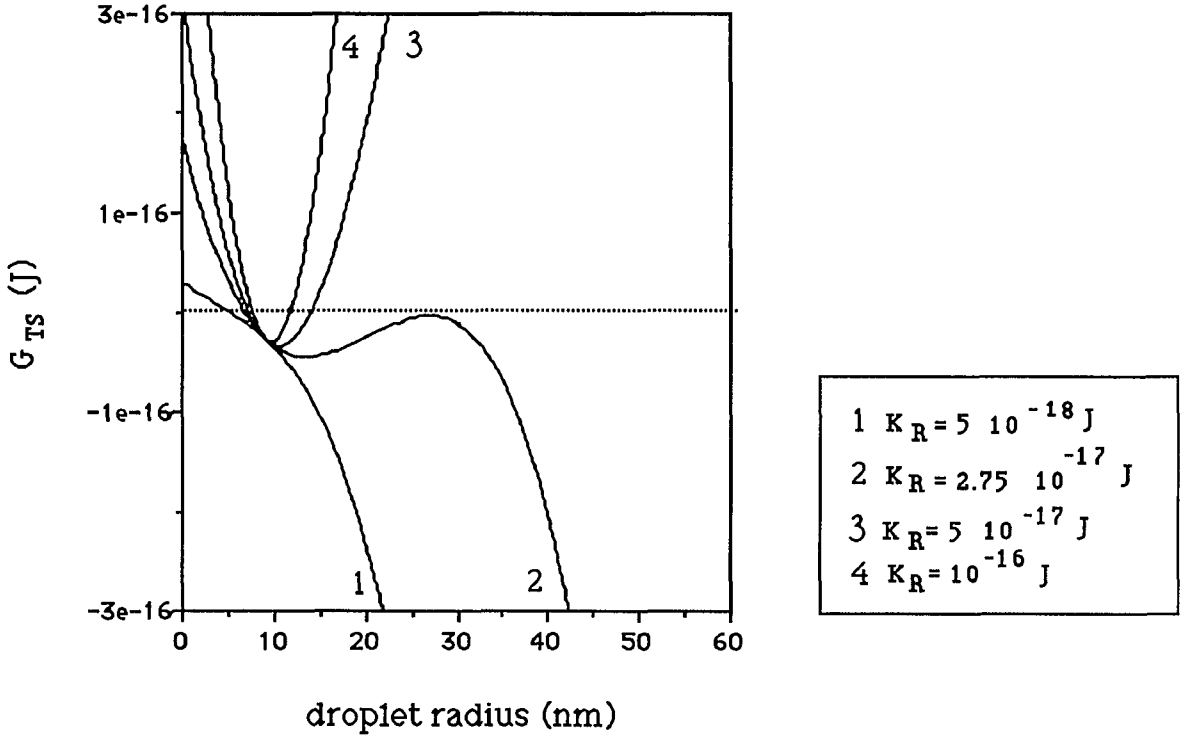

Figure V-1: G_{TS} vs droplet radius for various values of the rigidity constant ($G_{TS} = G_{SH} + G_A + G_B$, $R_0 = 9$ nm, $\Delta G_M = 9 \times 10^6$ J/m^3, $\varepsilon = 0.94$, $\gamma_I = 0.1 \times 10^{-3}$ N/m)

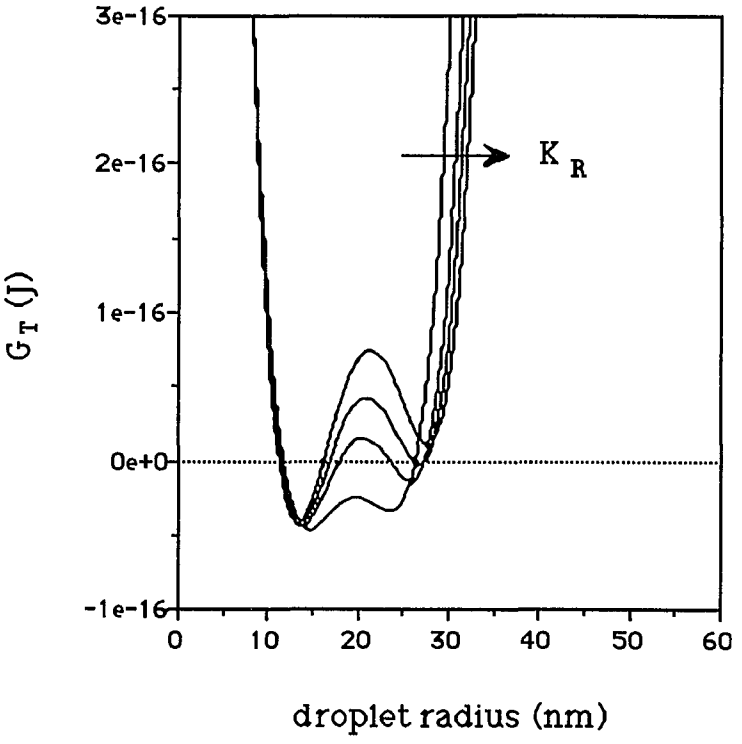

Figure V-2: G_T vs droplet radius for various values of the rigidity constant, K_R increases from 2.6 x 10^{-17} to 2.8 x 10^{-17} J ($G_T = G_{SH} + G_A + G_B + G_I$, R_0 = 9 nm, $\Delta G_M = 9 \times 10^6$ J/m^3, ε = 0.94, $\gamma_I = 0.1 \times 10^{-3}$ N/m)

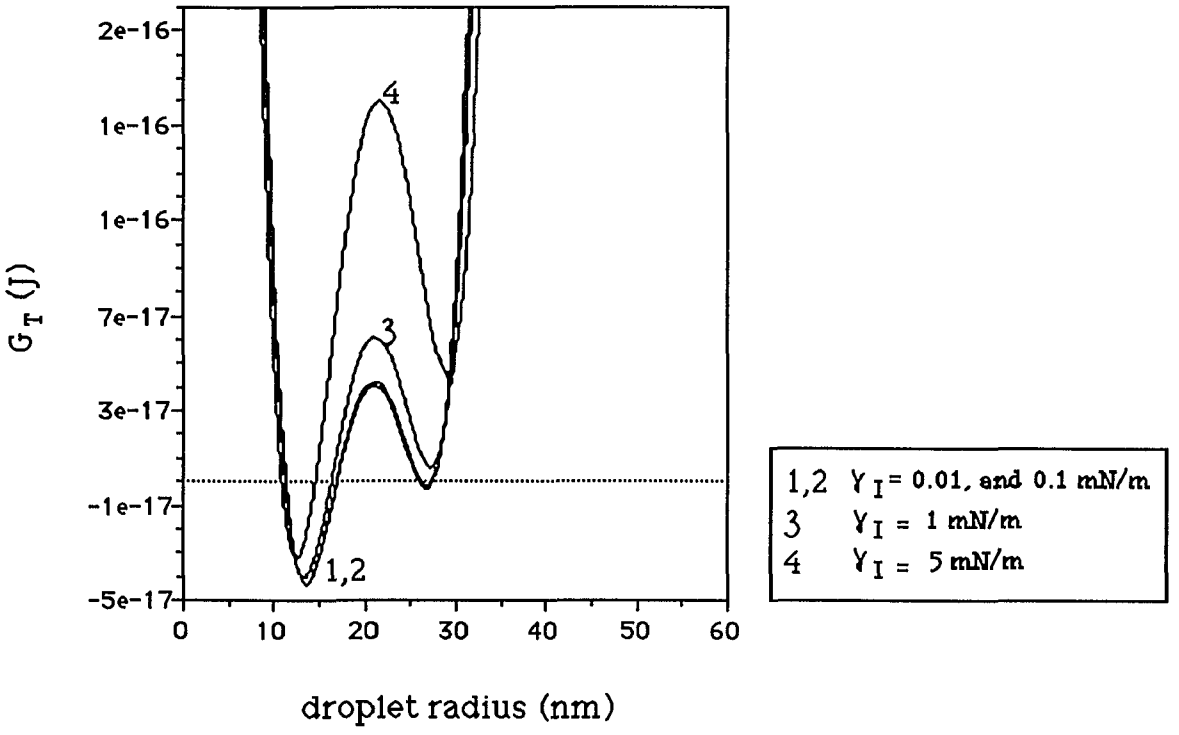

Figure V-3: G_T vs droplet radius for various values of γ_I ($G_T = G_{SH} + G_A + G_B + G_I$, $R_0 = 9$ nm, $\Delta G_M = 9 \times 10^6$ J/m^3, $\varepsilon = 0.94$, $K_R = 2.75 \times 10^{-17}$ J)

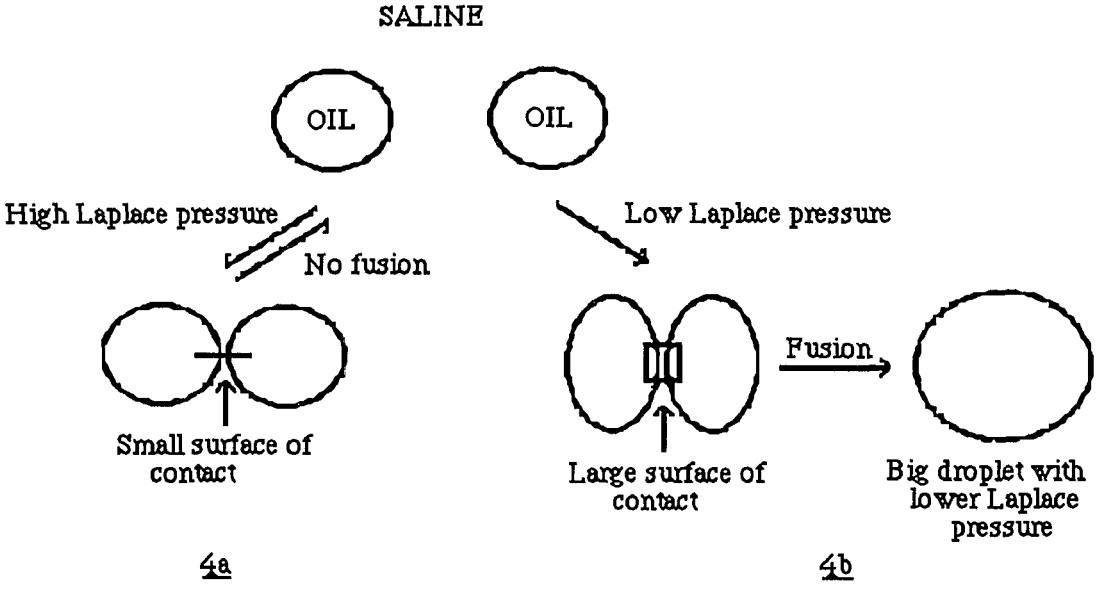

Figure V-4: Effect of the Laplace pressure on the probability of fusion of two droplets

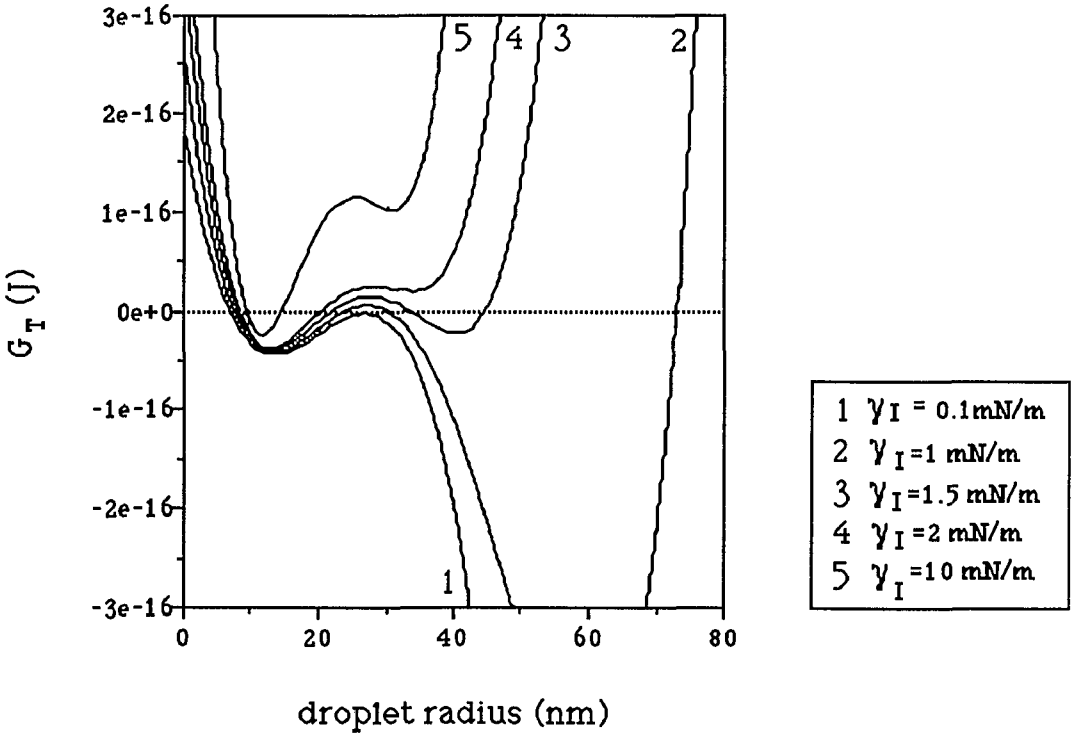

Figure V-5: G_T vs droplet radius for various values of γ_I ($G_T = G_{SH} + G_A + G_B + L_p G_I$, R_0 = 9 nm, $\Delta G_M = 9 \times 10^6$ J/m^3, $\varepsilon = 0.94$, $K_R = 2.75 \times 10^{-17}$ J)

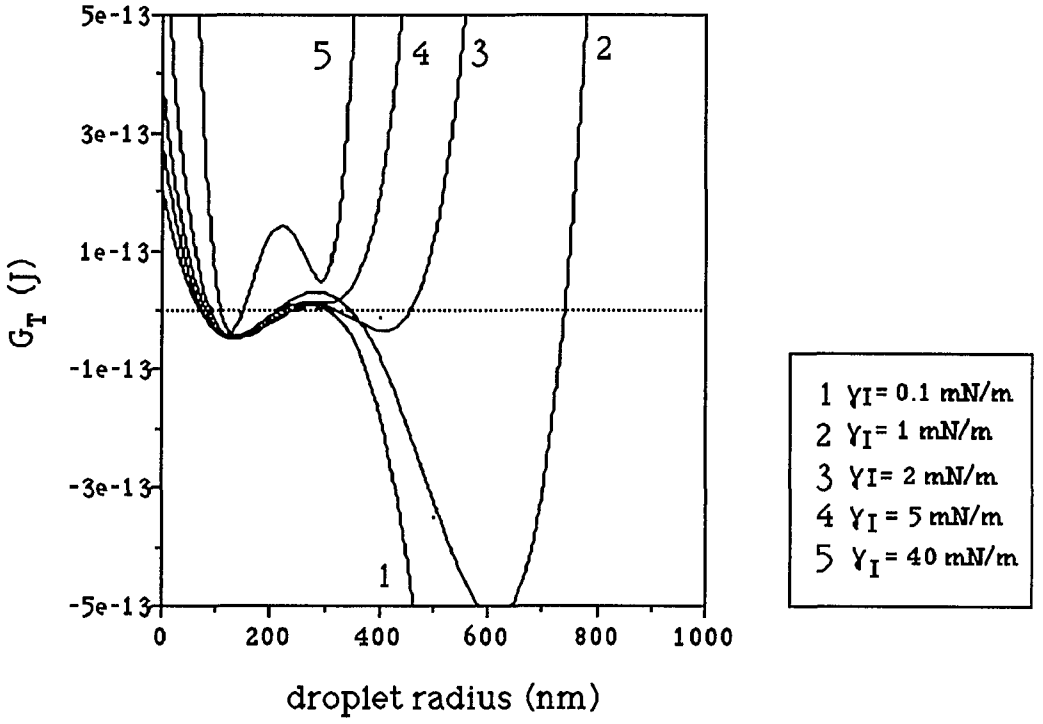

Figure V-6: G_T vs droplet radius for various values of γ_I ($G_T = G_{SH} + G_A + G_B + L_p G_I$, R_0 = 90 nm, ΔG_M = 5.8 x 10^7 J/m^3, ε = 0.16, K_R = 3 x 10^{-14} J)

CHAPTER VI

CONCLUSIONS AND PERSPECTIVES

VI. CONCLUSIONS AND PERSPECTIVES

The emulsion systems that were the subject of this dissertation are composed of (a) oil droplets stabilized by an interfacial phospholipid monolayer of egg yolk phospholipids (EYP) and (b) perflubron-free phospholipid vesicles. These systems have numerous biomedical applications, principally due to the capacity of perflubron (a perfluorocarbon) to dissolve oxygen. Provided a good batch of EYP is used and the emulsion is prepared under nitrogen atmosphere, the perflubron/EYP/saline emulsions are stable for years. Why are these systems stable for such an extended period of time? The part played by EYP in the stability of the emulsions seems to be crucial (not all batches of EYP yield stable emulsions). The study of the interface of the perflubron/EYP/saline emulsions through surface isotherm measurements correlated with EYP composition and resulting emulsion stability was inconclusive, due to the fact that EYP are a very complex mixture of phospholipidic and nonphospholipidic compounds, to the high sensitivity of EYP to oxidation, and to the fact that no two batches of EYP are identical in composition. An alternative emulsifier was subsequently substituted for the overly oxidizable and overly complex EYP, namely Phospholipon 90H (PL90H, a hydrogenated phosphatidylcholine). The stability of the emulsions with respect to flocculation and coalescence was assessed by direct observation, particle size measurements (photon correlation spectroscopy), and viscoelastic measurements in oscillatory flow (Penkem Vilastic 3). The resulting perflubron/PL90H/saline emulsion was very unstable, as evidenced by a rapid and substantial flocculation followed by a phase separation. It was found that instability could be prevented provided

that the virtually uncharged PL90H interface (PL90H is a zwitterionic emulsifier that yields a near zero zeta potential) was doped with a negatively charged additive and/or with an additive providing a hydration shell, both having the effect of keeping the perflubron-filled droplets from approaching one another. These results were extended to EYP and the part played by the EYP different constituents in the stability of perflubron/EYP/saline emulsions. EYP have a balanced composition: (a) the major components (phosphatidylcholine, phosphatidylethanolamine, and cholesterol) provide a well-organized structure at the perflubron/saline interface, capable of standing stress without losing its integrity; and (b) some minor components prevent flocculation (a necessary first step for emulsion coalescence) by providing electrostatic repulsive forces combined with a hydration layer (i.e., acidic phospholipids such as phosphatidylserine and phosphatidylglycerol) and/or by providing a strong hydration shell directly (i.e., phosphatidylinositol, whose saccharide head group, inositol, can be highly hydrated). Recently, the residence time of the emulsions in the circulatory system, and thus their efficiency, raised concerns: injections of the perflubron/EYP/saline emulsions in human patients showed that liver and spleen densities increased rapidly after injection (after five to six hours) due to storage of the perflubron-filled droplets in these organs. It was suggested that the droplets were recognized by the immune system as invaders and stored in the liver and the spleen, where they were digested by macrophages. An additive made of a cholesteryl moiety that is well anchored in the phospholipidic interface and of a long, highly hydrated moiety that wraps the droplet with a thick layer of water molecules (namely ethoxylated cholesterol, CnEO) not only yields a stable system but, in addition, is believed to be able to increase the "stealthiness"

of the droplets (i.e., their invisibility to the immune system). Injection trials of perflubron/EYP-CnEO/saline emulsions are currently being performed to test their innocuousness and their residence time in the blood stream.

On a theoretical level, a mathematical model for the formation of micro- and fine emulsions was developed. This model places the emphasis on the interface of the droplets of the emulsion. The interface is seen not as a virtual line but rather as a three-dimensional structure whose physical properties are the key elements in the formation of the emulsion. The rigidity of the interface and the interfacial free energy of the system--both measurable physical entities--are found to play particularly important roles.

The perspectives opened by this work are twofold. First, on a theoretical level, it follows from the experimental part described above that the model should be extended to take into account the effects of the electrical and hydration repulsive forces on the long-term stability (the model, as it stands now, concentrates on the formation and the immediate stability of the emulsion). Second, on an experimental level, the results of the injection trials will tell us if CnEO is an acceptable additive from both safety and efficiency standpoints (is the residence time of the emulsion in the circulation system significantly increased?). Although perflubron/EYP/saline emulsions are very close to winning acceptance by the FDA, the formulation can still be improved. In particular, a primary surfactant, simpler and therefore more controllable than the complex and oxidation-sensitive EYP, would help to predict and master emulsion stability. As mentioned in the introduction, perflubron and emulsions of

perflubron already have a wide array of applications, and new ones are being developed even as I write this conclusion. In addition, the results reported here will also have broader relevance for the entire family of fluorochemicals, whose wide range of potential biomedical applications are currently the object of extensive investigation.

REFERENCES

1 . D. L. Melchior, J. M. Steim. Prog. S
Sci. 13:211 (1979).

2 . J. F. Nagle and H. L. Scott. Phys. T

3 . D. L. Melchior, J. M. Steim. Biochi
466:148 (1977).

4 . F. Wunderlich, W. Kreutz, P. Mahle
Heppeler. Biochemistry. 17:2005 (1978

5 . A. F. Esser and K. A. Souza. Proc.
71:4111 (1974).

CHAPTER I

1. L.C. Clark and F. Gollan. Science. 152:1755 (1966).

2. H.A. Sloviter and T. Kamimoto. Nature. 216:458 (1967).

3. R.P. Geyer. N. Engl. J. Med. 289:1077 (1973).

4. T. Mitsuno, H. Ohyanagi, and R. Naito. Ann. Surg. 195:60 (1982).

5. B. Naunyn. Arch. Anat. Physiol. Wiss. Med. [n.v.]:4 (1868).

6. L.C. Sheffield and J.R. DeLoach. Biotechnology and Applied Research. 14(3):249 (1991).

7. G.P. Biro. Can. Med. Assoc. J. 129:237 (1983).

8. S.R. Snyder and J.A. Walder. Biotechnol. Ser. 19 (Biotechnol. Blood):101 (1991).

9. L.R. Segal, A.L. Rosen, S.S. Gould, H.S. Segal, and G.S. Moss. Chemtech. 21(Feb.):116 (1991).

10. L. Dayton. New Scientist. Jun. 3:42 (1989).

11. M. Mobed, T. Nishiya, and T.M.S. Chang. Biomat., Art. Cells & Immob. Biotech. 20(1):53 (1992).

12. R. Pool. Science. 250 (Dec.):1655 (1990).

13. E. Tsuchida and E. Hasegawa. Artif. Organs Today. 1(1):23 (1991).

14. K.C. Lowe. Adv. Mater. 3(2):87 (1991).

15. S.S. Davis and P. Hansrani. J. Pharm. and Physiol. [n.v.:n.p.] (1979).

CHAPTER II

1. W.D. Bancroft. J. Phys. Chem. 17:54 (1913).

2. W.C. Griffin. J. Soc. Cosmetic Chemists. 1:311 (1949).

3. W.C. Griffin. J. Soc. Cosmetic Chemists. 5:4 (1954).

4. Davies. Proc. 2nd Internat. Congr. Surface Activity. 1:47 (1957).

5. H.M. Princen, M.P. Aronson, and J.C. Moser. J. Colloid Interface Sci. 75(1):246 (1980).

6. K. Shinoda and H. Saito. J. Colloid Interface Sci. 30(2):2258 (1969).

7. K. Shinoda and H. Sagitani. J. Colloid Interface Sci. 64(10):68 (1978).

8. K.C. Lowe. Adv. Mater. 3(2):87 (1991).

9. D.D. Dixon and D.C. Holland. Fed. Proc. 34(6):1444 (May 1975).

10. J.G. Riess. Artif. Organs. 8(1):44 (1984).

11. J.G. Riess and M. Leblanc, in Blood Substitutes: Preparation, Physiology and Medical Applications (K.C. Lowe, ed.), Ellis Horwood, Chichester, England, 1988, p. 94.

12. H. Meinert, R. Fackler, A. Knoblich, J. Mader, P. Reuter, and W. Rohlke. Biomat., Art. Cells & Immob. Biotech. 20(1):95 (1992).

13. K. Yokoyama, C. Fukaya, Y. Tsuda, T. Suyama, R. Naito, K. Yamanouchi, and K.V. Scherer. Screening of new perfluorochemicals as candidates for use in fluorochemical emulsion blood substitutes - structures and biological properties [abstract]. Symposium on organofluorine compounds in medicine and biology, Amer. Chem. Soc. Natl. Meeting, Las Vegas, March 1982.

14. J.W. Sargent and R.J. Seffl. Fed. Proc. 29(5):1699 (1970).

15. N. Kossovky and D. Millett. MRS Bulletin. Sept.:78 (1991).

16. K.C. Lowe. Comp. Biochem. Physiol. 87(A):825 (1987).

17. N.S. Faithfull. Anaesthesia. 42:234 (1987).

18. Y. Kuroda, T. Kawamura, Y. Suzuki, H. Fajiwara, K. Yamamoto, and Y. Saitoh. Transplantation. 46:457 (1988).

19. R. Xiong, R.A. Zhang, H.F. Chen, W.Y. Huang, C.P. Lao, and W.T. Cao. Chin. J. Surg. 19:213 (1981).

20. A.T. King, B.J. Mulligan, and K.C.Lowe. Biotechnology. 7:1037 (1989).

21. L.K. Ju, J.F. Lee, and W. B. Armiger. Biotechnol. Prog. 7:323 (1991).

22. R.F. Mattrey. Am. J. Radiol. 152:247 (1988).

23. D.M. Long, D.C. Long, R.F. Mattrey, R.A. Long, A.R. Burgan, W.C. Herrick, and D.F. Shellhamer, in Blood Substitutes (T.M.S. Chang and R.P. Geyer, eds.), Marcel Dekker, New York, 1989, pp. 411-420.

24. S.S. Habif, Preparation and Characterization of Perfluorocarbon Emulsions for Biomedical Applications, Ph.D. diss., City University of New York, 1994, (a): pp. 3-20; (b): pp. 32-33

25. H. Wittcoff, The Phosphatides, Reinhold Publishing Corporation, New York, 1951, pp. 3-25.

26. G. Cevc and D. March, Phospholipid Bilayers, Physical Principles and Model, John Wiley & Sons, New York, 1987, pp. 1-28.

27. J. Folch, M. Lees, and G. H. Sloane Stanley. J. Biol. Chem. 226:497 (1957).

28. B. Ramesh, A. V. Prabhudesai, and C. V. Viswanathan. JAOCS. 55:501 (1978).

29. M. A. Wells and D. J. Hanahan, in Methods in Enzymology, Academic Press, New York, 1969, Vol. 14, pp. 179-181.

30. B. Ramesh, S. S. Adkar, A. V. Prabhudesai, and C. V. Viswanathan. JAOCS. 56 (May):585 (1979).

31. M. Schneider, Lucas Meyer GmbH & Co., D-2000 Hamburg 28, West Germany [n. d.].

32. J. F. Nagle. Ann. Rev. Phys. Chem. 31:157 (1980).

33. K. Larsson and I. Lundström, [n.t.], [n.p.], 1974, chapter 4, [n.pp.].

34. D. L. Melchior and J. M. Steim. Prog. Surface and Membr. Sci. 13:211 (1979).

35. J. F. Nagle and H. L. Scott. Phys. Today. 31:38 (1978).

36. D. L. Melchior and J. M. Steim. Biochim. Biophys. Acta. 466:148 (1977).

37. F. Wunderlich, W. Kreutz, P. Mahler, A. Ronai, and G. Heppeler. Biochemistry. 17:2005 (1978).

38. A. F. Esser and K. A. Souza. Proc. Natl. Acad. Sci. USA. 71:4111 (1974).

39. G. Cevc. Biochemistry. 30:7186 (1991).

40. A. Tardieu, V. Luzzati, and F.C. Reman. J. Mol. Bio. 75:711 (1973).

41. M. C. Phillips, R. M. Williams, and D. Chapman. Chem. Phys. Lipids. 3:234 (1969).

42. B. P. Gaber, P. Yager, and W. L. Peticolas. Biophys. J. 24:677 (1978).

43. G. Cevc. Biochemistry. 26:6305 (1987).

44. D. M. Small. Journal of Lipid Research. 8:551 (1967).

45. Private communication (Alliance Pharmaceutical Corp.).

46. W. van Nieuwenhuyzen. J.A.O.C.S. Oct:886 (1981).

47. K. Colbow, O. Avramovic-Zikic, and S. Wessel. J. Colloid Interface Sci. 82(1):233 (1981).

48. M.-P. Krafft, J.-P. Rolland, and J.G. Riess. J. Phys. Chem. 95:5673 (1991).

49. T. Hajri, J. Ferezou, and C. Lutton. Biochim. Biophys. Acta. 1047:121 (1990).

50. S.H. Untracht. Biochim. Biophys. Acta. 711:176 (1982).

51. J.T. Davies and E.K. Rideal, Interfacial Phenomena, Academic Press, New York, 1961, (a) pp. 44-46; (b) pp. 360-361.

52. J.H. Schulman, in Cytology and Cell Physiology, [n.p.], 1942, pp. 119-149.

53. Plutarch's Moralia, translated by Lionel Pearson and F. H. Sandbach. XV volumes. Cambridge: Harvard University Press, 1965.

54. See, e.g., The Complete Works of Benjamin Franklin (J. Bigelow, ed.), G. P. Putnam's Sons, New York, 1887, Vol. V, p. 253.

55. F. A. Pockels. Nature. 43:437 (1891).

56. Lord Rayleigh. Phil. Mag. 48:610 (1899).

57. W. Hardy. Proc. Roy. Soc. (London) A86:610 (1912) and A88:303 (1913).

58. I. Langmuir. J. Amer. Chem. Soc. 38:2221 (1916) and 39:1848 (1917).

59. H.L. Rosano, H. Schiff, and J. H. Schulman. J. Phys. Chem. 66:1928 (1962).

60. J.H. Schulman and J.B. Montagne. Ann. NY Acad. Sci. 92:366 (1961).

61. G.L. Gaines, Jr., Insoluble Monolayers at Liquid-Gas Interfaces, Interscience Publishers, New York, 1966, pp. 17-20.

62. W.D. Harkins and E.K. Fisher. J. Chem. Phys. 68:852 (1933).

63. J.H. Schulman and E.K. Rideal. Proc. Roy. Soc. (London). A130:259 (1931).

64. J.H. Schulman and E.K. Rideal. Proc. Roy. Soc. (London). A130:[n.pp.] (1931).

65. S. McLaughlin. Annu. Rev. Biophys. Chem. 18(36):113 (1989) and publications cited therein.

66. J.H. Schulman. Cytology and Cell Physiology. [n.v.]:119 (1942).

67. A.P. Christodoulou and H.L. Rosano. Adv. Chem. Ser. 84:210 (1968).

68. K.D. Caldwell and J. Li. J. Interface Sci. 132(1):256 (1989).

69. T. Tarara, L. Trevino, and T.J. Pelura. Private communication. (1991).

70. D.J. Shaw, Introduction to Colloid and Surface Chemistry (third edition), Butterworths & Co., Boston, 1980, (a) pp. 213-231; (b) p. 60; (c) p. 227.

71. J.B.A.F. Smeulders, C. Blom, and J. Mellema. Physical Review A. 42(6):3483 (1990).

72. G.B. Thurston. Microvascular Research. 9:145 (1975).

73. G.B. Thurston. J. Acoust. Soc. Am. 32(2):210 (1960).

74. G.B. Thurston. Biorheology. 13:191 (1976).

75. J.R. Womersley. Amer. J. Physiol. 127:553(1955).

76. G.B. Thurston. Microvascular research. 11:133 (1976).

77. G.B. Thurston. J. Rheology. 23(6):703 (1979).

78. G.B. Thurston. Proc. IX Intl. Congress on Rheology, Mexico, 1984, pp. 197-202.

79. G.B. Thurston. Biorheology. 10:375 (1973).

80. G.B. Thurston. Biorheology. 12:341 (1975).

81. G.B. Thurston. Biorheology. 24:297 (1987).

82. G.B. Thurston. Biorheology. 16:149 (1979).

83. G.B. Thurston. Biorheology. 15:239 (1978).

84. D. Burtner, T. Pelura, T. Tarara, and L. Trevino, Bound/Unbound Egg Yolk Phospholipids, private communication, Alliance Pharmaceutical Corp., San Diego, CA, October 1990.

85. Lucas Meyer GmbH & Co., Lecithin, Properties and Applications, information brochure, D-2000 Hamburg 28, West Germany [n. d.].

86. M. Kates and P. S. Sastry. Methods Enzymol. 14:197 (1969).

87. F. Tomioka and T. Kaneda. Chemical Abstracts. 86:1542 (1977).

88. P. L. Julian; U.S. Pat. 2,629,662 (1953).

89. R. D. Cole; U.S. Pat. 2,907,777 (1957).

90. A. Hermetter and F. Paltauf. Chem. Phys. Lipids. 28:111 (1981).

91. P. Bergell; U.S. Pat. 803,541 (1905)

92. D.A. Cadenhead, Structures and Properties of Cell Membranes, CRC Press, New York, 1985, pp. 21-62.

CHAPTER III

1. H.C. Hamaker. Physica (Utrecht). 4:1058 (1937).

2. M.J. Vold. J. Colloid Sci. 16:1 (1961).

3. B.V. Derjaguin and L.D. Landau. Acta Physicochim. URSS. 14:633 (1941).

4. E.J. Verwey and J.Th.G. Overbeek, Theory of the Stability of Lyophobic Colloids, Elsevier, Amsterdam, 1948.

5. G. Gouy. J. Phys. Radium. 59:418 (1910). Ann. Phys. 7:129 (1917).

6. D.L. Chapman. Phil. Mag. 25:475 (1913).

7. O.Z. Stern. Elektrochem. 30:508 (1924).

8. R.B. Whitney and D.C. Grahame. J. Chem. Phys. 9:827 (1941); D.C. Grahame. Z. Elektrochem., Ber. Bunsenges Phys. Chem. 62:264 (1958).

9. S. Levine. Discuss. Faraday Soc. 18:202 (1954).

10. H. Reerink and J.Th.G. Overbeek. Discuss. Faraday Soc. 18:74 (1954).

11. M.M. Kozlov and V.S. Markin. Gen. Physiol. Biophys. 5:379 (1984).

12. V.S. Markin, M.M. Kozlov, and V.L. Borovjagin. Gen. Physiol. Biophys. 5:361 (1984).

13. D. Papahadjopoulos, G. Poste, B.E. Schaeffer, and W.J. Wail. Biochim. Biophys. Acta. 352:10 (1974).

14. E. Neher. Biochim. Biophys. Acta. 373:327 (1974).

15. W. Breisblatt and S. Ohki. J. Membrane Biol. 23:385 (1975).

16. D. Papahadjopoulos in Membrane Fusion (G. Poste and G.L. Nicolson, eds.) Elsevier-North-Holland Biomedical Press, New York, 1978, pp. 765-790.

17. A. Portis, C. Newton, W. Pangborn, and D. Papahadjopoulos. Biochemistry. 18: 780 (1979).

18. I.M. Lifshitz and V.V. Slezof. Sov. Phys. JETP. 35:331 (1959).

19. C. Wagner. Z. Electrochem. 35:581 (1961).

20. W. Thomson (Lord Kelvin). Proc. Roy. Soc. (Edinburgh). 7:63 (1871).

21. A.L. Kabalnov and E.D. Shchukin. Advances in Colloid and Interface Sciences. 38:69 (1992).

22. S.S. Davis, H.P. Round, and T.S. Purewall. J. Colloid Interface Sci. 80:508 (1981).

23. J.G. Weers, Y. Ni, T.E. Tarara, T.J. Pelura, and R.A. Arlauskas. Proc. 205th ACS Natl. Mtg. (Denver, March 1993) [forthcoming].

24. W.I. Higuchi and J.Misra. J. Pharm. Sci. 51:459 (1962).

25. A.S. Kabalnov, A.V. Pertsov, and E.D. Shchukin. Colloids and Surfaces. 24:19 (1987).

26. D. Burtner, T. Pelura, T. Tarara, and L. Trevino, Bound/Unbound Egg Yolk Phospholipids, private communication, Alliance Pharmaceutical Corp., San Diego, CA, October 1990.

27. S.S. Davis and P. Hansrani. J. Pharm. and Physiol. [n.v.:n.p.] (1979).

28. G. Cevc. Biochemistry. 26:6305 (1987).

29. G. Cevc. Biochemistry. 30:7186 (1991).

30. J.M. Pasternacki-Surian, R.L. Schnaare, and E.T. Sugita. Pharm. Res. 9(3):406 (1992).

31. J. Seelig, P.M. MacDonald, and P.G. Scherer. Biochemistry. 26(24):7535 (1987).

32. P.G. Scherer and J. Seelig. Biochemistry. 28:7720 (1989).

33. C. Washington, A. Chawla, N. Christy, and S.S. Davis. Int. J. Pharm. 54:191 (1989).

34. C. Washington. Int. J. Pharm. 66:1 (1990).

35. C. Washington and S.S. Davis. Int. J. Pharm. 39:33 (1987).

36. J.T. Rubino. J. Parenter. Sci. Technol. 44(4):210 (1990).

37. B. Stampa, J.-S. Lucks, B. W. Müller, and R.H. Müller. J. Colloid Interface Sci. 143(1):188 (1991).

38. S.S. Davis, in Phospholipids: Biochem., Pharm.,Anal. Consid., [Proc. Int. Colloq. Lecithin, 5th meeting, 1989] (I. Hanin and G. Pepeu, eds.), Plenum Press, New York, 1990, pp. 69-82.

39. O.L. Johnson, C. Washington, S.S. Davis, and K. Schaupp. Int. J. Pharm. 53:237 (1989).

40. C. Washington. Int. J. Pharm. 64:67 (1990).

41. J.H. Crowe, M.A. Whittam, D. Chapman, and L.M. Crowe. Biochim. Biophys. Acta. 769:151 (1984).

42. L.M. Crowe and J.H. Crowe. Biochim. Biophys. Acta. 1064:267 (1991).

43. C. Washington, A. Athersuch, and D.J. Kynoch. Int. J. Pharm. 64:217 (1990).

44. G. Strauss, P. Schurtenberger, and H. Hauser. Biochim. Biophys. Acta. 858:169 (1986).

45. H. Hauser and G. Strauss, in Biotechnological Applications of Lipid Microstructures [Proceedings of the workshop on the technological applications of phospholipid bilayers, vesicles, and thin films, Tenerife, Canary Islands, 1986] (B.P. Gaber, J.M. Schnur, and D. Chapman, eds.), Plenum Press, New York, 1988, pp. 71-80.

46. A.C. Cowley, N.L. Fuller, R.P. Rand, and V.A. Parsegian. Biochemistry. 17(15) (1978).

47. T.J. McIntosh, A.D. Magid, and S.A. Simon. Biophys. J. 57:1187 (1990).

48. T.J. McIntosh, A.D. Magid, and S.A. Simon. Biochemistry. 26:7325 (1987).

49. T.J. McIntosh and S.A. Simon. Biochemistry. 25:4058 (1986).

50. H. Sonntag and K. Strenge, Coagulation and Stability of Disperse Systems, Halsted Press, Jerusalem, 1972, pp. 4-80.

CHAPTER IV

1. T.M. Allen, C. Hansen, and J. Rutledge. Biochim. Biophys. Acta. 981:27 (1989).

2. H.L. Rosano and W.E. Gerbacia; U.S. Patent 3,778,381 (1973).

3. T.M. Allen. Biochim. Biophys. Acta. 640:385 (1981).

4. A. Gabizon and D. Papahadjopoulos. Proc. Natl. Acad. Sci. USA. 85:6949 (1988).

5. J. D. Morisett, R.L. Jackson, and A.M. Gotto. Biochim. Biophys. Acta. 472:93 (1977).

6. G.L. Scherphof, J. Damen, and J. Wilschut, in Liposome Technology (G. Gregoridis, ed.), CRC Press, Boca Raton, 1984, Vol.III. pp. 205-224.

7. F. Bonté and R.L. Juliano. Chem. Phys. Lipids. 40:359 (1986).

8. H.H. Spanjer, M. van Galen, F.H. Roerink, J. Regts, and G.L. Scherphof. Biochim. Biophys. Acta. 863:224 (1986).

9. F.J. Sharon and C.W.M. Grant. Biochim. Biophys. Acta. 507:280 (1978).

10. L. Illum, I.M. Hunneyball, and S.S. Davis. Int. J. Pharm. 29:53 (1978).

11. C.H. Wynn. Biochem. J. 240:921 (1986).

12. K. Miyajima, T. Baba, and M. Nakagaki. Colloid and Polymer Science. 267:201 (1989).

13. K.R. Patel, M.P. Li, J.R. Schuh, and J.D. Baldeschwieler. Biochim. Biophys. Acta. 797:20 (1984).

14. K. Miyajima, T. Lee, and M. Nakagaki. Chem. Pharm. Bull. 32:3670 (1984).

CHAPTER V

1. A. M. Cazabat, D. Langevin, J. Meunier, and A. Pouchelon. J. Phys. Lett. 43:L89 (1982).

2. K. E. Bennett, J. C. Hatfield, C. W. Macosko, and L. E. Scriven, in Microemulsions (I.D. Robb, ed.), Plenum Press, New York, 1982, pp. 65-75.

3. J.L. Cavallo and H.L. Rosano. J. Phys. Chem. 90:6817 (1986).

4. H.L. Rosano. J. Soc. Cosmet. Chem. 25:609 (1974).

5. M.P. Aronson. Colloids and Surfaces. 58:195 (1991).

6. P.G. De Gennes and C. Taupin. J. Phys. Chem. 86(13):2294 (1982).

7. S.Y. Chan and H.L. Rosano. Dispersion Science and Technology. 9(5,6):523 (1988-89).

8. S.A. Safran, G.S. Grest, and A.L.R. Bug, in Microemulsion Systems (H.L. Rosano and M. Clause, eds.), Marcel Dekker, New York, 1987, Chapter 14, pp. 235-243.

9. H. Saito and K. Shinoda. J. Colloid Interface Sci. 32:647 (1970).

10. R.L. Reed and R.N. Healy, in Improved Oil Recovery by Surfactant and Polymer Flooding (D.O. Shah and R.S. Schechter, eds.), Academic Press, New York, 1977.

11. S.E. Friberg and C. Solans. Langmuir. 2(2):121 (1986).

12. J.B.F.A. Smeulders, C. Blom, and J. Mellema. J. Physical Review A. 42:3483 (1990).

13. Wolfram Research, Inc., 1991, "Mathematica Version 2.0," Wolfram Research, Inc., Champaign, IL.